PROPERTIES OF STRETCHED 830 EW AQUIVION®

By

Remington Fischer

Thesis

Submitted to the Faculty of the

Graduate School of Vanderbilt University

in partial fulfillment of the requirements

for the degree of

MASTER OF SCIENCE

in

Chemical Engineering

August, 2012

Nashville, Tennessee

Approved:

Peter N. Pintauro

G. Kane Jennings

TABLE OF CONTENTS

ACKNOWLEDGEMENTS

I would like to thank Naveed Bakh for all his help in completing this research project which would have taken much longer without his numerous invested hours. I also thank the Vanderbilt Chemical Engineering Department which permitted me the opportunity to stay and pursue a Master's Degree after completing the Chemical Engineering undergraduate curriculum. A special thanks to Dr. P. N. Pintauro for his advising and allowing me to work in his lab. Your input has been invaluable during my graduate research.

Many professors have given me guidance and support during my undergraduate and graduate careers here at Vanderbilt, but I especially appreciate the time and investment of Dr. G. Kane Jennings. I am eternally grateful for your guidance both professionally and personally.

Finally, I thank everyone in the Pintauro lab who helped make work more enjoyable and my family for their ever present support.

LIST OF TABLES

Table Page

LIST OF FIGURES

CHAPTER 1

INTRODUCTION

1.1 Motivation

Interest in alternative energy sources has increased as world energy consumption continues to grow and oil reserves shrink. Stimulated by developing economies, the global energy demand is predicted to grow by 30-40% between 2010 and 2040 with oil as the main fuel.[1,2] A substantial portion of that growth is attributed to energy consumption for use in transportation, which even with impressive gains in fuel economy, is expected to rise by 45% over 30 years.[2] The development of Non-OECD (Organization for Economic Cooperation and Development) economies, particularly China, is projected to drastically increase the usage of commercial and personal vehicles.[1-3] Between 2010 and 2040, the global passenger car fleet alone is expected to double, reaching almost 1.7 billion cars.[1-3] All of this growth places additional demand on the current global consumption of 86 million barrels of crude oil per day.[3] Carbon dioxide levels similarly will rise by a predicted 43% through 2035 with the increased oil consumption, causing global warming and air quality concerns.[1] Alternative sources of less polluting energy and impressive gains in fuel economy are pivotal in keeping pace with the growing energy demand and alleviating environmental concerns. Therefore, there are significant efforts to develop alternative energy conversion devices as a replacement for the internal combustion engine, in order to lessen our global dependence on fossil fuels.

1.2 The Fuel Cell

Fuel cells are an energy conversion device with the potential to replace current power generation devices across a variety of applications both portable and stationary (cell phones, lap tops, vehicles, residential power plants, etc.). They provide power by directly converting a fuel's chemical energy into usable electricity (with heat as a by-product).[4-6] Fuel cells produce power with high energy conversion efficiency, little noise, and low maintenance costs.[4,6] Additionally, the wide variety of fuel cells (Phosphoric Acid, Alkaline, Solid Oxide, etc.) provides fuel flexibility with the possible use of non-carbon fuels which will decrease or eliminate the production of harmful greenhouse gases.[4,6] Table 1 lists key characteristics and applications for the five main fuel cell types.

Among the various fuel cell types, proton exchange membrane fuel cells (PEMFCs) are presently the best suited for transportation applications.[4-7] A standard PEMFC is depicted in Figure 1. A PEMFC consists of an anode, an ion exchange membrane, and a cathode. A fuel such as hydrogen or methanol is fed to the anode while an oxidant (typically O_2 from air) is fed to the cathode. The fuel is oxidized at the anode, creating protons and electrons. The ions migrate through the ionically conductive membrane while electrons flow through an external circuit to the cathode where they are consumed in the cathode electrode reaction. At the air cathode, protons, O_2 molecules, and electrons react to form water.[4,8]

Table 1: Comparison of the five most common fuel cell types. Modified from [9].

Fuel Cell Type	***Operating Temperature***	***Efficiency***	***Advantages/ Disadvantages***	***Applications***
Alkaline	90-100°C	60%	Fast cathode reaction leads to high performance. Low cost components. Sensitive to CO_2 in fuel and air. Requires electrolyte management	Military, space
Polymer exchange membrane	50-100°C	35-60%	Solid electrolyte reduces corrosion and electrolyte management. Low operating temperature and quick start-up. Expensive catalyst. Sensitive to fuel impurities.	Backup power, portable power, distributed generation, transportation, specialty vehicles
Phosphoric acid	150-200°C	40%	High temperature enables cogeneration and increased tolerance to fuel impurities. Expensive Pt catalyst. Long start up time and low power densities	Distributed generation
Molten carbonate	600-700°C	45-50%	High efficiency with fuel flexibility. Uses a variety of catalysts. Suitable for cogeneration. High temperature corrosion, long start up time, and low power densities.	Electric utility, distributed generation
Solid oxide	700-1000°C	60%	High efficiency with fuel flexibility. Uses a variety of catalysts. Suitable for cogeneration. High temperature corrosion and long start up time.	Auxiliary power, electric utility, distributed generation

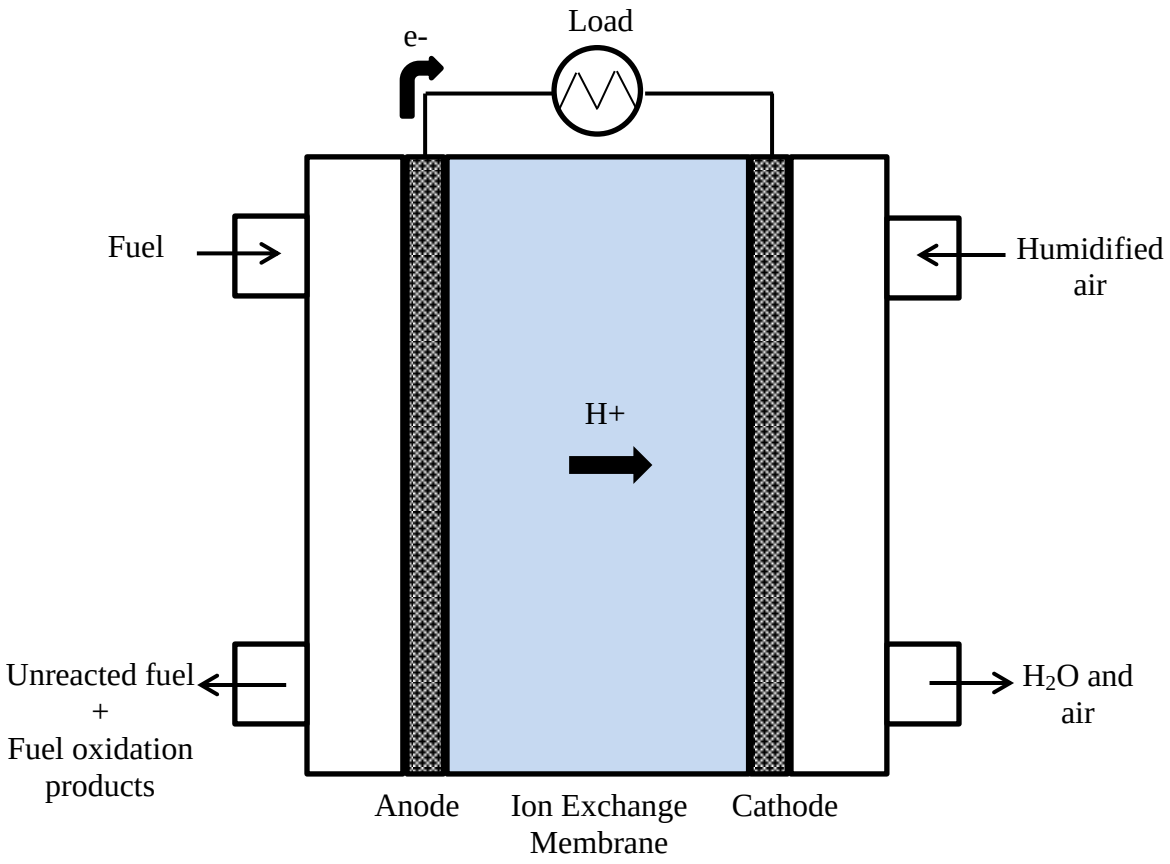

	Direct methanol fuel cell	*Hydrogen fuel cell*
Fuel:	Liquid methanol	Humidified hydrogen gas
Anodic reaction:	$CH_3OH + H_2O \rightarrow CO_2 + 6H^+ + 6e^-$	$H_2 \rightarrow 2H^+ + 2e^-$
Cathodic reaction:	$3/2\ O_2 + 6H^+ + 6e^- \rightarrow 3H_2O$	$2H^+ + ½\ O_2 + 2e^- \rightarrow H_2O$

Figure 1: A diagram of a proton exchange membrane fuel cell with the electrode reactions for a direct methanol fuel cell (DMFC) and a hydrogen fuel cell (HFC).

The two most common PEMFCs are hydrogen fuel cells (HFCs) and direct methanol fuel cells (DMFC), which are both subsets of PEMFCs since they use a solid polymer ionomer membrane to transport protons between the electrodes.[4,6] They differ, however, in their fuel source as HFCs use gaseous hydrogen while DMFCs use an aqueous solution of liquid methanol. Both fuel cell types are under current development since they offer different advantages. Hydrogen fuel cells offer high maximum power conversion efficiency (50%), quick start-up operation, and no greenhouse gas emissions.[6,7] Methanol fuel cells are appealing because they utilize a liquid fuel. Liquid fuels provide higher energy storage densities than a gaseous fuel like H_2. Additionally, fuels cells that use liquid fuels allow for the utilization of our current fuel distribution infrastructure, without the on-board storage issues associated with hydrogen gas.[6,7] Successful commercialization of both HFCs and DMFCs is hindered, however, by the lack of a suitable low cost proton conducting membrane with the requisite performance and durability properties.[4,5]

1.3 The Direct Methanol Fuel Cell Membrane

A key component of a DMFC is the proton exchange membrane which transports protons from the anode to the cathode. This membrane must also act as an electrical insulator to prevent short circuits between electrodes and as a barrier to fuel and air crossover to prevent chemical short circuits. The membrane in a DMFC will always operate in a water-swollen state due to the humidification of the incoming air, the production of water at the cathode, and the presence of water in the liquid anode feed

stream.[4,5,10] The ideal DMFC membrane should have the following properties: high proton conductivity, low methanol permeability, good chemical/thermal stability, zero electronic conductivity, good mechanical strength, and low cost.[4,5,8,10]

DuPont's Nafion® membranes, composed of a perfluorosulfonic acid (PFSA) polymer, have been extensively studied for HFC and DMFC applications.[4,7,10-12] The polytetrafluoro-ethylene (PTFE) backbone provides mechanical integrity, while the sulfonate-terminated side chains promote proton transport (see Figure 2 for the chemical structure of Nafion®).[8,13] The polymer equivalent weight (EW, with units of g dry polymer/mol sulfonate units) or ion exchange capacity (IEC, the inverse of equivalent weight with units of mmol/g) is a measure of the polymer composition. EW (or IEC) is a function of side chain length and the length of backbone repeat units between side chains (the side chain density). Decreasing the side chain length and/or the backbone repeat units between side chains lowers the EW. At a lower EW, a PFSA polymer will often become less crystalline due to shorter CF_2 runs between side chains. The reduction in crystallinity reduces the polymer's mechanical properties and increases water swelling (often accompanied by an increase in methanol permeability). However, the proton conductivity typically increases with decreasing EW due to the increased concentration of charged groups in the polymer. A common issue in the development of fuel cell ionomer membranes is consequently the tradeoff between high proton conductivity (i.e. low EW), low methanol permeability, and acceptable mechanical properties.[8,14] Nafion® 117 with an equivalent weight of 1100 g/mol (an IEC of 0.91 mmol/g) is the current membrane standard for direct methanol fuel cells.

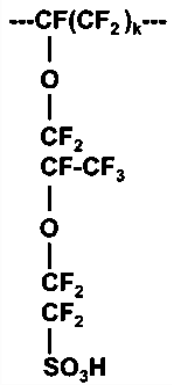

Figure 2: Chemical structure of Nafion® (k=12 for 1100 EW). Image taken from [63]

Nafion® 117 has many desirable fuel cell properties: it exhibits excellent chemical and oxidative stability, it has a high proton conductivity for temperatures ≤80ºC under full humidification conditions, and it has good mechanical properties.[8,10-18] Thus, Nafion® performs well in H_2/air fuel cells at moderate temperatures. It suffers however from high methanol crossover when used in direct methanol fuel cells (DMFCs). Methanol crossover causes fuel loss and a cathodic mixed potential resulting in diminished power output and lower fuel utilization efficiency.[8,10,11] Nafion® does not perform well in fuel cells at operating temperatures >80°C. Higher operating temperatures are desired for an automotive PEMFC to increase the slow fuel oxidation reaction rate, to improve catalyst tolerance to CO poisoning (an intermediate product during methanol electro-oxidation), and to lower the size and complexity of radiators and fans that regulate the fuel cell temperature.[7,8,11,16-20] Nafion® suffers greatly at fuel cell operating temperatures >100°C, where the membrane dehydrates (a common problem of hydrogen fuel cells at high temperature and low feed air humidity) causing a loss in proton conductivity. High temperatures in a DMFC also increase the methanol crossover rate due to greater solvent sorption.[11,15,20] The current challenge for fuel cell engineers is to develop a better

performing DMFC membrane by keeping the proton conductivity high while lowering methanol crossover at both low and high fuel cell operating temperatures.

1.4 Alternative Direct Methanol Fuel Cell Membranes

Researchers have studied a wide variety of polymer materials in an attempt to find a DMFC membrane that performs better than Nafion® (i.e. a membrane that exhibits a lower methanol permeability with the same, or higher, proton conductivity as Nafion®). Some polymers that have been studied include: sulfonated poly(ether ether ketone),[11,21] sulfonated polyimide,[22] and sulfonated polyphosphazene.[23] The microstructure of these polymers can produce more tortuous diffusional pathways, restrict the size of hydrophilic domains, and create dead end pores, which cause a reduction in the methanol permeability.[11] This has been demonstrated in sulfonated poly(ether ether ketone) with its stiffer and less hydrophobic backbone and its less hydrophilic side chains, as compared to Nafion®.[21] These structural differences result in hydrophilic domains that are not well formed, a decrease in membrane swelling (after immersion in methanol solutions), and a lowering in methanol permeability.[21] Figure 3 shows the differences in polymer microstructure between Nafion® and sulfonated polyetherketone.[11]

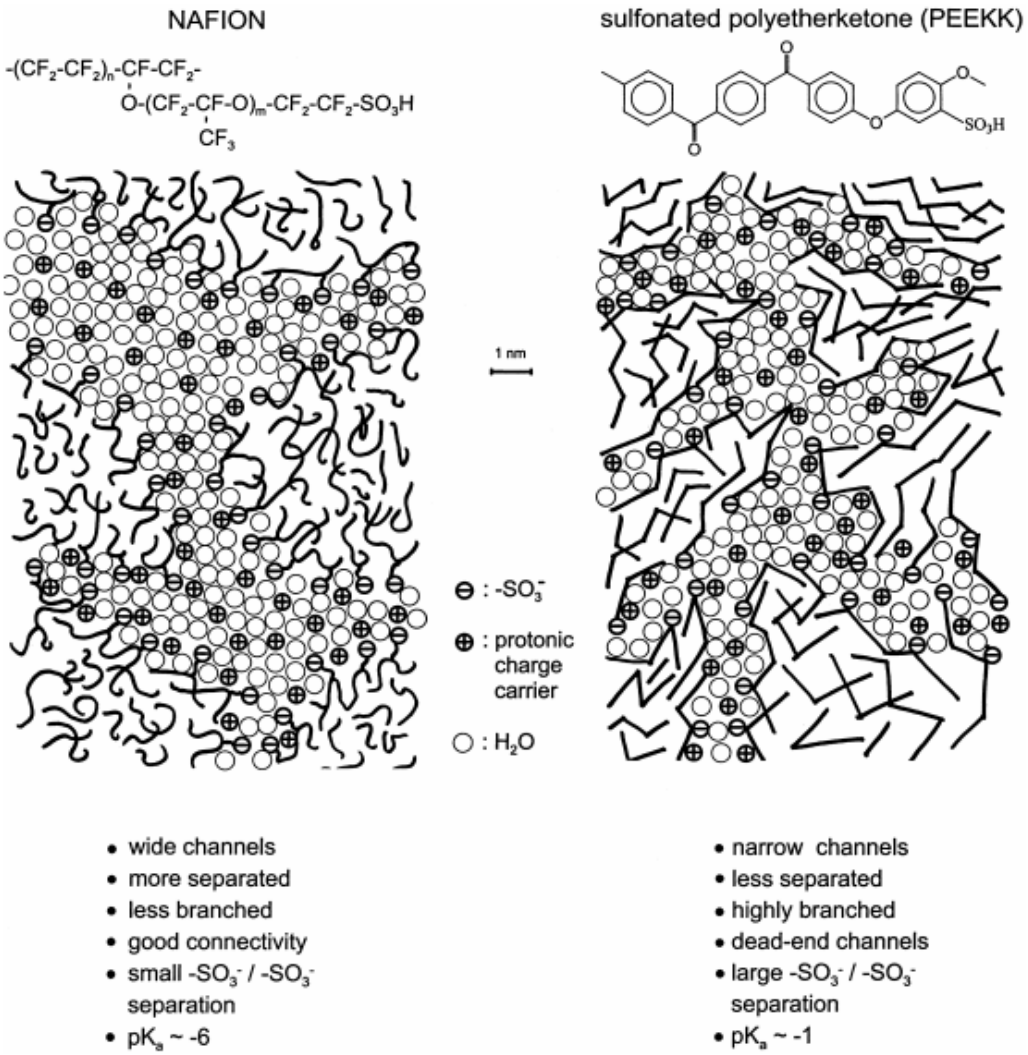

Figure 3: Reported microstructure differences between Nafion® and sulfonated polyetherketone. Image taken from reference [11].

A poly(ether ether ketone) ionomer with a 47% degree of sulfonation (corresponding to an ion exchange capacity of 1.43 mmol/g) had a methanol permeability that was only 3% that of Nafion® 115 (in 1 M methanol at 80°C). Unfortunately there was also a loss in proton conductivity (in water at 80°C); the conductivity was 40% that of Nafion®. The larger reduction in methanol permeability as compared to conductivity

resulted in a selectivity (defined as proton conductivity divided by methanol permeability) that was ~14 times greater than that of Nafion® 115.

Crosslinking the polymer matrix has also been used to reduce membrane swelling and methanol permeability. Crosslinks tie the polymer chains together which increases the rigidity (resistance to swelling) of the polymer network. The effects of crosslinking have been demonstrated in covalently crosslinked sulfonated polyphosphazene.[23] Figure 4 shows the water diffusion coefficient and proton conductivity for Nafion® 117 compared to sulfonated polyphosphazene (POP) with an IEC of 1.40 mmol/g, both crosslinked and uncrosslinked. The increased polymer rigidity was apparent in the reduced water diffusion coefficient (which is often comparable to the methanol diffusion coefficient) after crosslinking. The methanol diffusion coefficient was found to be $1.62*10^{-8}$ cm^2/s (at 30°C, methanol activity=0.80) in crosslinked POP compared to $6.5*10^{-6}$ cm^2/s (at 30°C in 1.0 M methanol) in Nafion® 117.[23] However, the higher resistance towards methanol transport was again accompanied by a loss in proton conductivity (~30% lower than Nafion® 117). A direct comparison in selectivity between Nafion® and crosslinked POP under identical testing conditions was never provided by the authors. Nonetheless, an improvement in selectivity is evident due to the greatly reduced methanol diffusion coefficients in crosslinked POP.

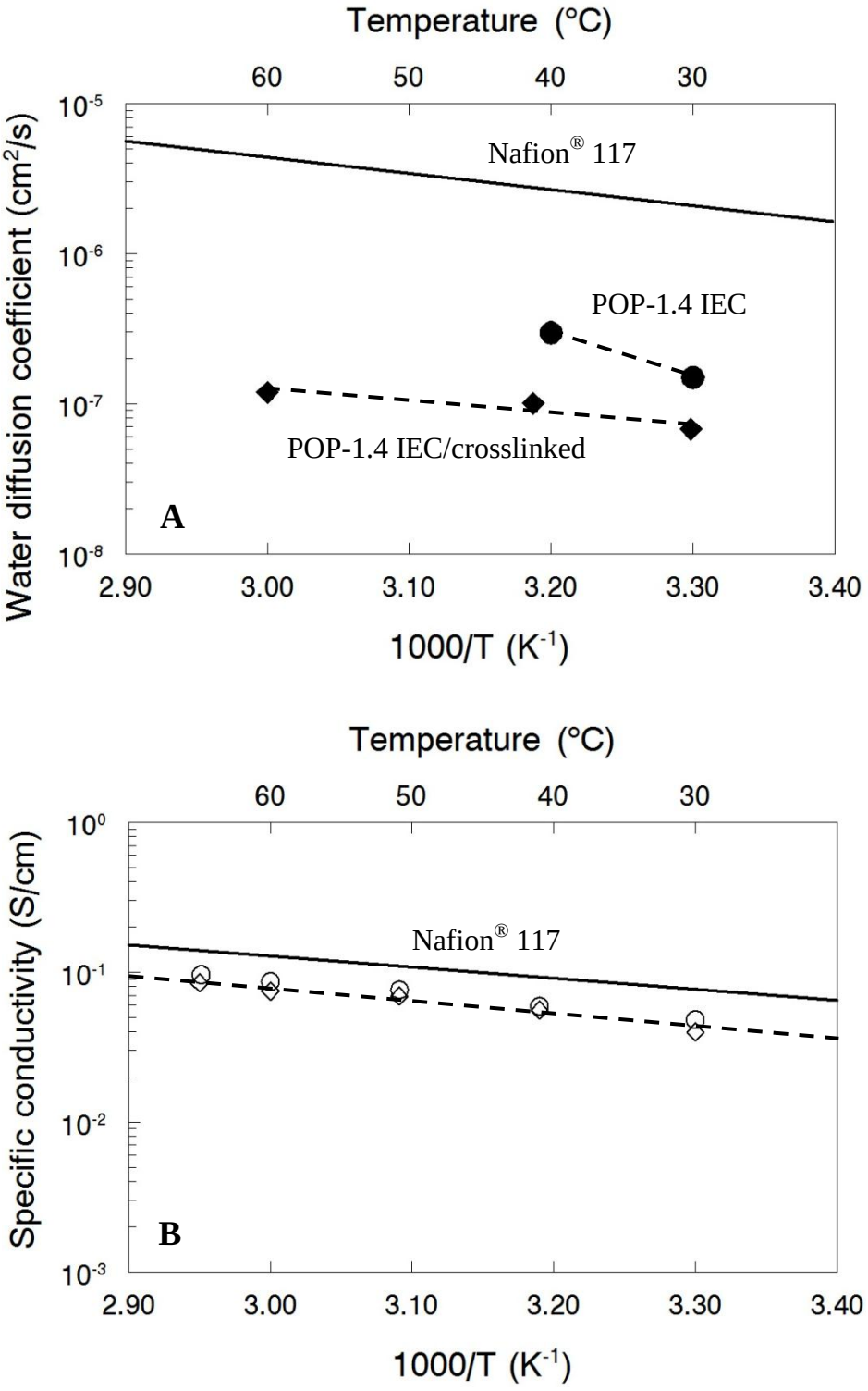

Figure 4: A) Dependence of the water diffusion coefficient on temperature for 1.4 IEC sulfonated polyphosphazene membranes (with and without crosslinking) and Nafion® 117. B) Temperature dependence of the proton conductivity in water for 1.4 IEC sulfonated polyphosphazene membranes, with (◇) and without (○) crosslinking, and Nafion® 117. Plots taken from [23].

Another common approach for DMFC membrane fabrication is to blend Nafion® or another proton conducting polymer such as sulfonated poly(ether ether ketone), with inorganic particle fillers such as silica,[24] silicon dioxide,[25] or acid functionalized zeolite.[26] Similarly, Nafion® has been blended or laminated with a hydrophobic polymer like fluorinated ethylene propylene (Teflon®),[27,28] or poly(vinylidene fluoride).[8,29] These methods are all similar and involve mixing particles or hydrophobic polymers throughout the ionomer matrix in order to reinforce the membrane (control water/methanol swelling) and block methanol transport. Similar to crosslinking however, there was always a loss in proton conductivity when the methanol permeability was lowered. For example, the selectivity (proton conductivity divided by methanol permeability) of a Teflon®/Nafion® blended membrane was enhanced with increasing Teflon® content due to a decline in methanol permeability (see Figure 5A).[27] Because of the added resistance to proton conduction however, it was found that no more than 40 wt% Teflon® should be added to a membrane for use in DMFCs when using a 1.0 M methanol feed. Figure 5B shows the effect of Teflon® wt% on DMFC performance. Higher or lower than 40 wt% Teflon® resulted in lower power output due to excessive proton transport resistance or methanol crossover, respectively. The undesirable reduction in proton conductivity that accompanied the desired decrease in methanol permeability limited the improvement in DMFC power output for the Nafion®/Teflon® blended membranes, as compared to Nafion®.

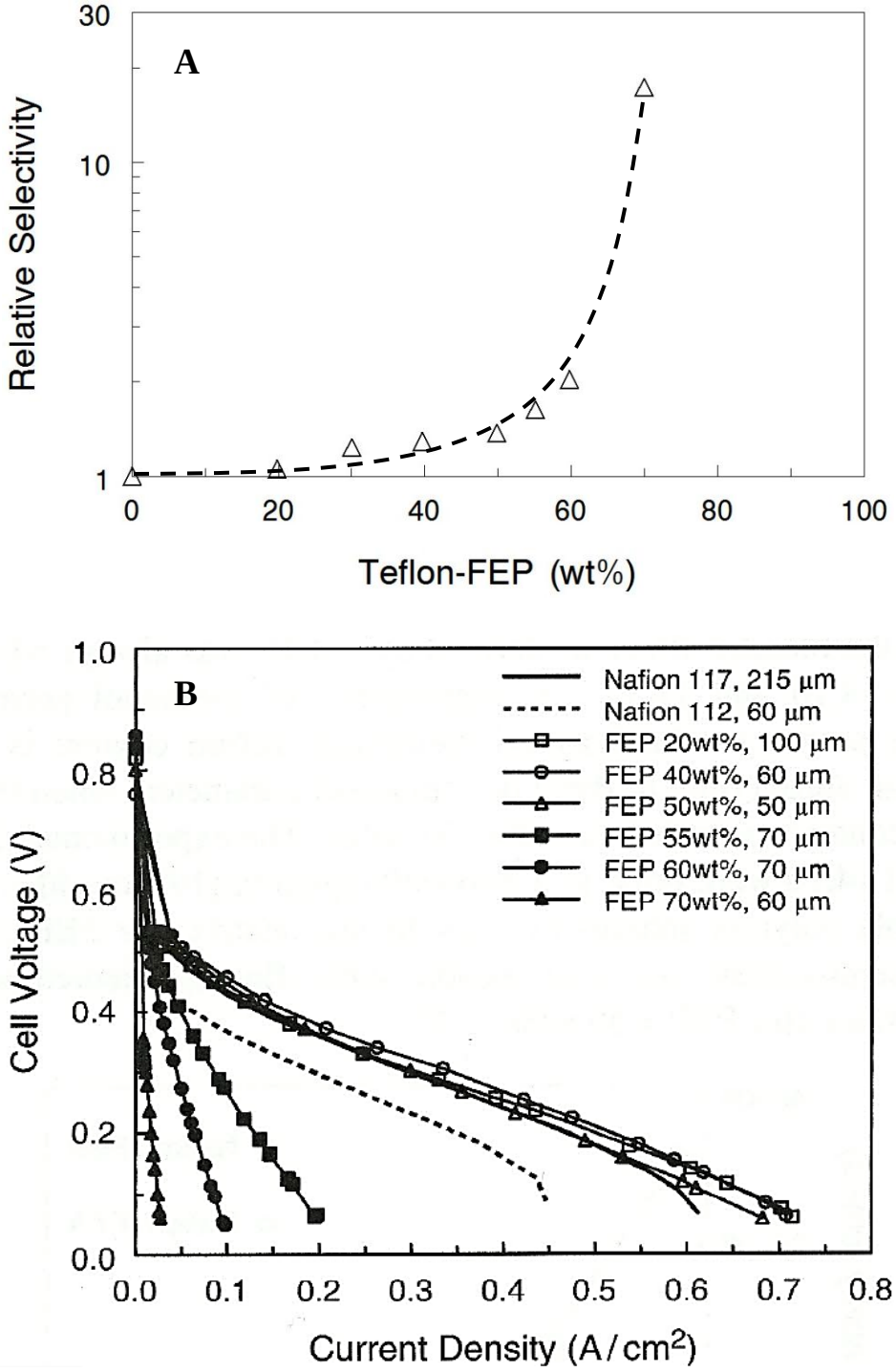

Figure 5: A) Relative selectivity (ratio of membrane selectivity to the selectivity of Nafion® 117) as a function of Teflon-FEP content. Through-plane conductivity at 25°C in water, and methanol permeability at 60°C with 1.0 M methanol. B) Effect of wt% Teflon® on DMFC performance in Teflon®/Nafion® blended membranes. 1.0 M methanol feed and ambient pressure air at 500 sccm. T=60°C. Plots taken from [27].

The focus of all the above studies was to retard trans-membrane methanol permeation without a substantial loss in proton conductivity. As demonstrated in these examples however, there was always a drop in conductivity as compared to Nafion® when the methanol permeability of the membrane was lowered. The improved DMFC performance due to lower methanol crossover was therefore negated by the drop in power output associated with the proton conductivity loss. Table 2 lists the proton conductivity and methanol permeability of various DMFC membranes reported in literature. Figure 6 is a plot of these properties for the same membranes. While there is a decrease in methanol permeability without sacrificing proton conductivity (compared to Nafion®) for some membranes, they frequently suffer from poor adhesion between the catalyst layer and the ionomer due to the lack of an appropriate binder.[30,31] A recent literature review reported that only 40% of DMFC membranes ever get tested in an actual fuel cell due largely to this complication.[30] So although many membranes have been reported as being more selective (proton conductivity divided by methanol permeability) than Nafion® 117, they ultimately did not perform significantly better than Nafion® in a DMFC due to either the binding issues and/or the commonly observed loss in proton conductivity.[30,31] Research therefore continues in the search of a DMFC membrane which provides significant performance improvement over commercial Nafion® without an increase in resistance to proton transport.

Table 2: Wide variety of DMFC membranes and their properties reported in literature. Figure 6 is a plot of these membrane properties. Table adapted from [30].

Proton Exchange Membrane	***Proton Conductivity (S/cm)***	***Methanol Permeability (cm^2/s)($x10^6$)***
Blends of Sulfonated polyphosphazene-polybenzimidazole[32]	0.060[d]	1.300[d]
Crosslinked poly(vinyl alcohol)/poly(acrylic acid)/silica hybrid[33]	0.012[a]	0.210[a]
Nitrile-functional, disulfonated poly(arylene ether sulfone)[34]	0.090[a]	0.870[a]
Sulfonated poly(styrene)/poly(tetrafluoroethylene) composite[35]	0.110[a]	0.670[a]
Sulfonated co-polyimide[36]	0.082[b]	0.480[b]
4-Dodecylbenzene sulfonic acid-doped polyethylene glycol/silica hybrid[37]	0.004[a]	0.020[c]
Sulfonated poly(ethersulfone)-Cardo[38]	0.004[a]	0.210[a]
Sulfonated poly(styrene)[39]	0.050[a]	0.520[a]
IonClad® R-1010[40]	0.080[a]	0.590[a]
Sulfonated polyimide[41]	0.120[b]	0.570[b]
Sulfonated poly(ether ether ketone)[42]	0.070[a]	0.300[a]
Poly(styrene sulfonic acid) grafted onto poly(vinylidene fluoride)[43]	0.120[a]	1.500[a]
Sulfonated poly(styrene-*b*-isobutylene-*b*-styrene) block copolymer[44]	0.019[a]	0.150[a]
Poly(vinyl alcohol)/poly(styrene sulfonic acid-*co*-maleic acid) blend[45]	0.095[a]	0.266[a]
Nafion® 117[46]	0.100[a]	2.60[a]

[a] = at room temperature (20-25°C)
[b]= at 30°C
[c]= at 35°C
[d]= at 60°C

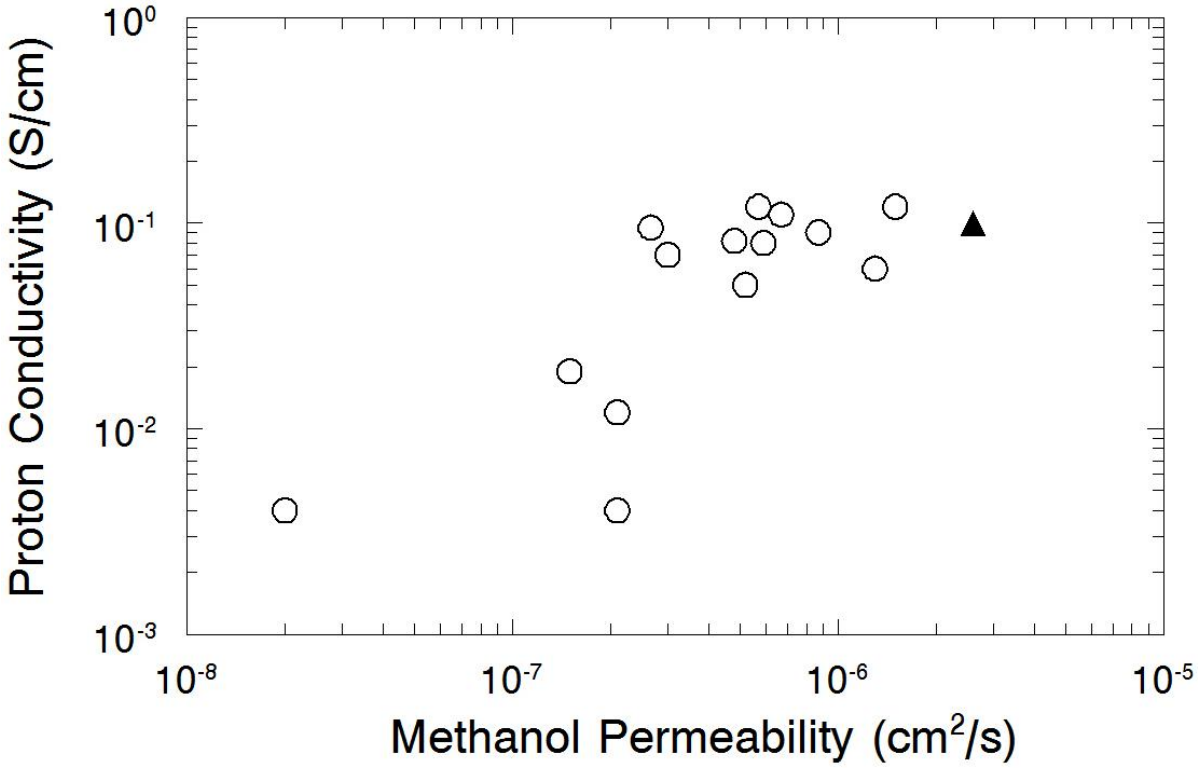

Figure 6: Proton conductivity plotted against methanol permeability for a wide variety of DMFC membranes (○), along with Nafion® 117 (▲). The polymer, proton conductivity, methanol permeability, and tested temperatures are all contained in Table 2.

1.5 Membrane Stretching

Uniaxial and biaxial stretching is a method typically used in the polymer/membrane industry to enhance a membrane's mechanical strength by aligning and orienting polymer chains, causing in most cases an increase in polymer crystallinity.[46-53] The membrane stretching technique has garnered additional attention for the production of DMFC membranes with Nafion® polymer. Pre-stretched recast Nafion® films exhibited a low methanol permeability while maintaining a high proton conductivity.[46-49] These membrane properties are highly desirable for DMFC applications

and eliminate the compromises required when using other DMFC membrane fabrication techniques, such as those discussed in Section 1.4.

To understand the stretching effect on ionomeric perfluorosulfonic acid (PFSA) membranes, one should first consider the starting morphology. PFSA ionomers often consist of three phases: crystalline, amorphous, and ionic.[54,55] Thus, Nafion® is a semi-crystalline polymer with the degree of crystallinity influenced by the side chain density and length. Increasing the side chain density and/or length creates a more amorphous polymer by decreasing the chain packing efficiency.[12] Ionomers, such as Nafion®, are known to rearrange into a nanophase-separated morphology where the polar, ionic side chains create clusters within the hydrophobic, backbone matrix. The key properties of interest (proton conductivity, methanol permeability, water diffusivity, etc.) all depend on the ionic clusters' size, spatial distribution, connectivity, and organization.[55] This is because the transport of protons, water, and methanol depend on how ionic/hydrophilic percolation pathways develop throughout the membrane.

A wide variety of models have been proposed over the years to describe the ionic domains in Nafion® perfluorosulfonic acid polymer. A well-referenced model considers the ionic domains as swollen inverse micelles of spherical shape.[56] Recently, studies have provided strong support for an elongated inverse micelle morphology for the ionic domains (i.e. water channels).[55,57-61] Some of the finer details (extent of clustering, crystallite shape, and dimensions) of this model are still under investigation, but the hydrophobic polymer backbone creates a cylindrical shell that surrounds the hydrophilic

side chains creating an ionic channel (see Figure 7A). These ionic channels are packed into bundles (as shown in Figure 7B) which result in locally parallel channels.

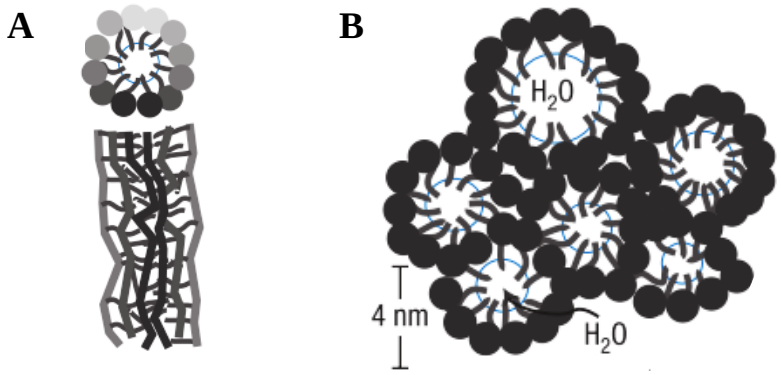

Figure 7: A) Two views of the cylindrical water channels formed in Nafion® by the hydrophobic backbones surrounding the ionic side chains. Shading indicates which chains are in front and in back (darker shaded chains are more in front). B) The clustering (or bundling) of nearby channels which result in locally parallel channels. Images taken from [58].

The bundles of water channels in Nafion® are thought to orient (as shown in Figure 8) via two simultaneously occurring mechanisms upon stretching.[55,59-61] The first mechanism is the rotation of the ionic channel bundles, so that the axial (longitudinal) direction of the individual channels aligns parallel to the stretching direction (Figure 8B).[60] The second mechanism is the better channel alignment within the bundles caused by the continual sliding and disentangling of the individual channels (Figure 8C).[60] At low strain, the first mechanism dominates since the second mechanism occurs typically at higher draw ratios.[60] Crystallites similarly undergo reorientation under stretching and are hypothesized to better align the water channels and reinforce the oriented channel

structure.[58,61] The change in PFSA polymer microstructure caused by stretching is reported to slow water/methanol transport in the through plane direction (perpendicular to the stretching direction) by increasing the tortuosity of the hydrophilic pathways (as shown in Figure 8).[55,61]

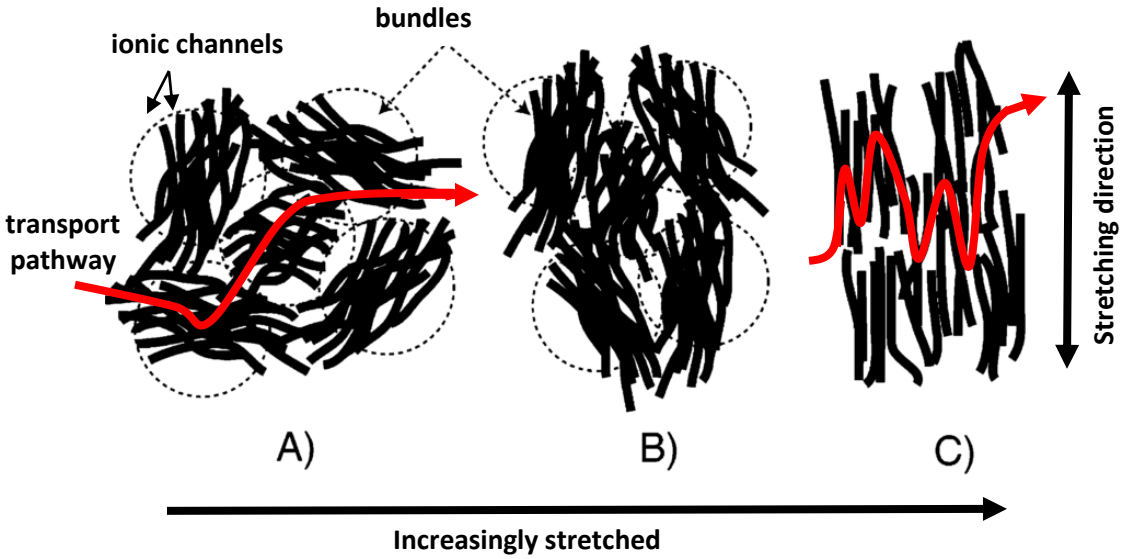

Figure 8: The orientation of the water channel bundles upon uniaxial stretching of a PFSA polymer like Nafion®. A) The initial unordered state of bundles consisting of loosely aligned and ordered channels. B) Bundles rotating to situate the longitudinal direction of the channels parallel to the stretching direction. C) Further channel movement and alignment occurring at higher strains. Image adapted from [60].

1.6 Performance of Stretched Nafion® in DMFCs

Lin et al. in a series of papers demonstrated that one could reduce methanol crossover in a Nafion® membrane without lowering the proton conductivity by uniaxially stretching a Nafion® film in a particular way.[46-49] Pre-stretched recast Nafion® films were prepared by first evaporating the solvent from a commercial alcohol/water Nafion®

solution. The Nafion® powder was then resuspended/dissolved in dimethylacetamide (DMAc) to create a 10 wt% solution. Films were cast into a Teflon® dish at room temperature. Solvent was partially evaporated at 60°C, with the removal of 85-90% of the DMAc. The partially dried membrane was removed from the casting dish and placed into a stretching frame, heated to 125°C, and uniaxially stretched to the desired draw ratio (draw ratio is defined as the final stretched membrane length divided by the initial membrane length). The membrane was kept in the stretching frame at 125°C for one hour to remove residual DMAc solvent, followed by membrane annealing at 150-180ºC for two hours. The resulting membranes were removed from the frame, boiled in 1.0 M H_2SO_4 for one hour, and then boiled in deionized water for one hour to ensure full membrane hydration with all sulfonate ion exchange groups in the H^+ form.

Annealing after stretching and under tension (in the stretching frame) were the key innovative steps that eliminated polymer relaxation, which is usually seen in stretched commercial Nafion® films.[47,49] Pre-stretched recast Nafion® films without annealing or with annealing prior to stretching did not exhibit good DMFC properties. These films would retract to their original dimension when exposed to a hot methanol solution.[46-49] Figure 9 shows the in-plane proton conductivity (in water at 25°C) and methanol permeability (with 1 M methanol at 60°C) for pre-stretched recast Nafion® membranes prepared using the above procedure. The methanol permeability is reduced by 60% to ~$1.5*10^{-6}$ at a draw ratio (final length/initial length) of 4 without a decrease in proton conductivity. The selectivity for this film was 2.6 times higher than unstretched Nafion® under the same conditions (selectivity is defined as proton conductivity divided by methanol permeability).

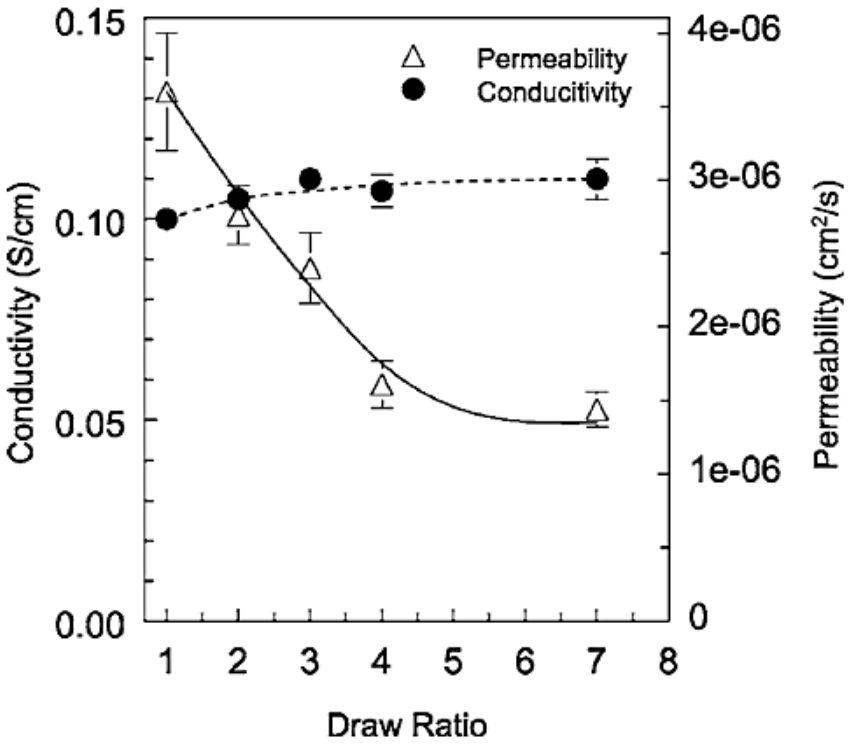

Figure 9: Proton conductivity (in water at 25°C) and methanol permeability (with 1.0 M methanol at 60°C) of pre-stretched recast Nafion® as a function of draw ratio. Plot taken from reference [47].

The improvement in membrane properties caused by stretching led to substantially improved DMFC power outputs. A stretched film (with a draw ratio of 4) produced a 50% higher maximum power density than commercial Nafion® 117 at 60°C with feeds of 1.0 M methanol and ambient pressure air. Table 3 contains reported power densities of pre-stretched recast Nafion® films under different testing conditions by Lin et al.[46] The stretched films improved the fuel cell performance under all testing conditions. To date, these results serve as a benchmark for high performance DMFC membranes.

Table 3: Reported power densities (mW/cm^2) of direct methanol fuel cell tests with pre-stretched recast Nafion® and Nafion® 117. The anode feed was 1.0 M methanol and cathode feed was 500 sccm humidified air. Table lists data from reference [46].

	Pre-stretched recast Nafion®		**Nafion® 117**	
	@ 0.4V	Max	@ 0.4V	Max
4.0 mg/cm^2, 60°C	86	107	56	72
4.0 mg/cm^2, 80°C	170	176	112	137
8.0 mg/cm^2, 60°C	110	117	82	91
8.0 mg/cm^2, 80°C	204	207	144	155
4.0 mg/cm^2, 80°C, 25 psig backpressure	197	202	143	153
8.0 mg/cm^2, 80°C, 25 psig backpressure	240	252	181	203

1.7 Aquivion®

The aim of the present work is to adapt the Nafion® membrane stretching procedure developed by Lin et al.[46-49] for Solvay Solexis, 830 EW Aquivion® polymer (shown in Figure 10).

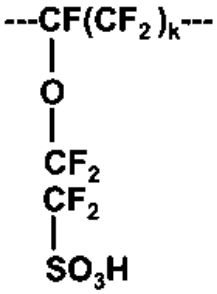

Figure 10: The chemical structure of 830 EW Aquivion® (k=12). Image taken from [63].

The side chain length and polymer equivalent weight (EW) lead to important property differences between 1000 EW Nafion® and 830 EW Aquivion®. Table 4 lists results from Los Alamos National Lab on the two polymers.[62] A higher ion exchange capacity in 830 EW Aquivion® as compared to 1100 EW Nafion® (1.2 mmol/g vs. 0.91 mmol/g) increases the proton conductivity and water swelling in the Aquivion® membranes.

Table 4: Polymer characterization for 1000 EW Nafion® and 830 EW Aquivion® polymers. Table taken from [62].

	1000 EW Nafion®	***830 EW Aquivion®***
Density (g/cm^3)	1.97	2.06
Conductivity (S/cm)*	0.101	0.147
Water uptake (wt%)*	19	30

* in liquid water at room temperature

Shorter sulfonic-acid-terminated side chains means more CF_2 groups between side chains at a given equivalent weight which promote polytetrafluoroethylene segment crystallization. Thus, short side chain ionomers like Aquivion® have a higher crystallinity than Nafion® at the same polymer EW (and ion exchange capacity).[13,16-18,20,63,64] The increase in crystallinity is desirable because an increase in polymer rigidity will control/limit polymer swelling by water and/or methanol. The optimal tradeoff between proton conductivity and acceptable mechanical performance, therefore, occurs at a higher

ion exchange capacity in short side chain perfluorosulfonic acid polymers compared to long side chain PFSAs.[14,19,54]

1.8 Objective of This Master's Thesis

The objective of this thesis is two-fold. First, the stretching procedure used for Nafion® was adapted for Aquivion® films. This entails determining the stretching speed, stretching temperature, and annealing conditions to create properly stretched Aquivion® membranes. Second, the stretched Aquivion® membranes were characterized to determine how stretching affects membrane properties that are key for DMFC applications: crystallinity, water uptake, mechanical strength, proton conductivity, and methanol permeability. The physical property results were compared to those for pre-stretched recast Nafion® to assess the potential use of stretched Aquivion® films in DMFCs.

CHAPTER 2

EXPERIMENTAL

2.1 Membrane preparation

830 EW Aquivion® membranes were prepared using a commercial 10% w/w polymer solution in a propanol/water mixed solvent (36% water, 51% 1-propanol, 13% 2-propanol) which was purchased from Solvay Solexis (D83-10E). The polymer concentration was further diluted to 5% w/w through the addition of dimethylacetamide (DMAc). Sonication for 30 minutes fully mixed the solution. Membranes were cast from this solution at room temperature into a Chemware® PFA (perfluoroalkoxy) tray. A lab oven was used to evaporate >95% of the solvent by heating at 70ºC for ~14 hours. The resulting membrane was removed from the tray. The solvent evaporation was quantified in a separate set of experiments by weighing a polymer film after 14 hours and then placing the film in a lab oven at 60°C under vacuum for 4 hours to remove the remaining solvent. The membrane was then weighed again, and any weight loss was attributed to a loss in residual solvent. All cast membranes were 100-120 μm in dry thickness. Storing the membranes in sealed plastic bags kept any residual DMAc solvent in the membranes; small amounts of DMAc were needed to plasticize the Aquivion® films for stretching. Membranes cast from different D83-10E dispersion batches exhibited identical membrane properties (see Appendix A).

A membrane was loaded into the stretching frame (Figure 11) with the initial distance between clamps dependent on the final draw ratio (draw ratio is defined as the final distance between camps divided by the initial distance); 30 mm for a draw ratio of 2 (DR2), 10 mm for DR4, 6 mm for DR6. All samples were therefore stretched a standard 30 mm distance. For film elongation, the stretching frame and film were placed horizontally into a lab oven set to 190°C and equilibrated for 15 minutes. After thermal equilibration, a rotary motor began turning the shaft which pulled the bottom clamp and uniaxially stretched the membrane at a rate of 0.60 mm/min. After 3 minutes, the stretching rate was increased to 1.25 mm/min. Preparing the membranes by using an initial slow stretching rate followed by a more rapid rate resulted in more uniformly stretched films.

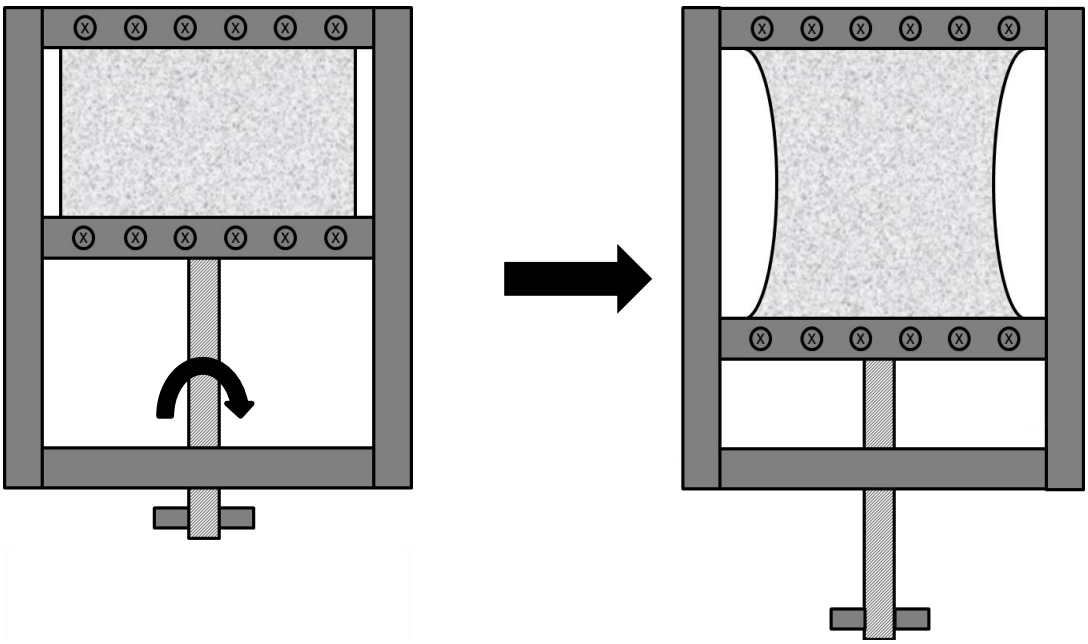

Figure 11: The apparatus used to stretch the Aquivion® membranes. A motor turned the shaft which pulled the lower clamp.

The rotary motor was turned off after reaching the desired stretched distance and the frame/membrane was left in the oven for a specified period of time, such that all membrane samples were kept in the oven at 190°C for a total of 30 minutes (stretching and post-stretch annealing). This total time was chosen because 30 minutes is the time required to fully anneal the Aquivion® (see Section 3.1). Unlike prior studies on Nafion® stretching by Lin,[46-49] stretching and annealing of Aquivion® films were carried out simultaneously. After the completion of the stretching procedure, the fame was taken out of the oven and the membrane temperature was quickly cooled/quenched to maintain the membrane's structure in the stretched conformation. Stretched membranes were boiled for one hour in 1.0 M H_2SO_4 followed by a one hour boiling treatment in deionized (DI) water. All membranes were stored in DI water at room temperature until needed for testing. The resulting water soaked membranes had thicknesses of 140-160 μm, 60-80 μm, 25-35 μm, and 15-20 μm for DR1, DR2, DR4, and DR6, respectively.

2.2 Wide-Angle X-Ray Diffraction

Wide-angle X-ray diffraction (WAXD) measurements were made using a Rigaku diffractometer with nickel filtered CuKα radiation (λ = 1.5418 Å). The incident angle changed from 9º to 25º at a scanning rate of 0.2°/min in the plane perpendicular to the stretching direction.

2.3 Proton Conductivity

In-plane proton conductivity tests were conducted on membranes in a deionized water bath at 25°C. Conductivity was measured in the direction parallel to the stretching direction using a four point Bekktech conductivity cell (shown in Figure 12) and a standard AC impedance technique.[65]

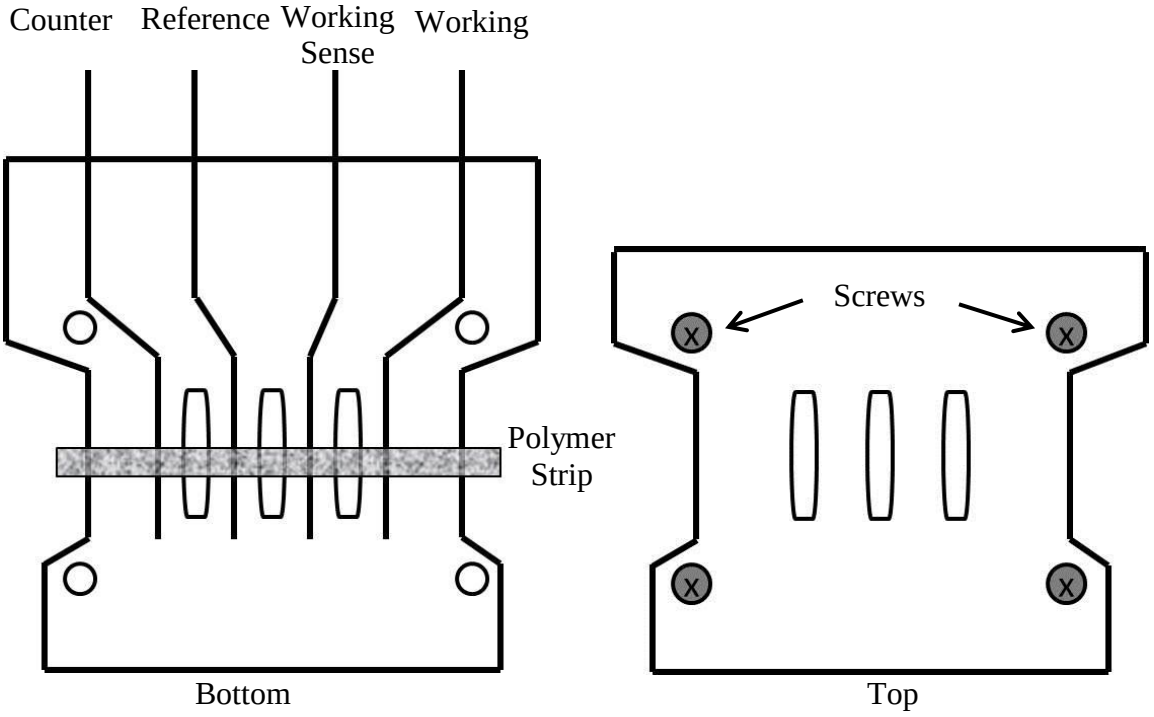

Figure 12: Bekktech conductivity cell used to measure the in-plane resistance of a membrane. All electrodes were Pt wires.

AC impedance data were collected using a Gamry potentiostat over the frequency range of 1 Hz to 300 kHz. The real impedance at $Z_{imaginary}=0$ in a Nyquist plot (as shown in Figure 13) was the membrane's resistance. The conductivity (with units of S/cm) was calculated using the following equation:

$$\sigma = \frac{L}{R*A} \quad [1]$$

where L is the distance between electrodes (cm), R is the membrane resistance from the Nyquist plot (ohm), and A is the water soaked membrane cross-sectional area (thickness times width with units of cm^2).

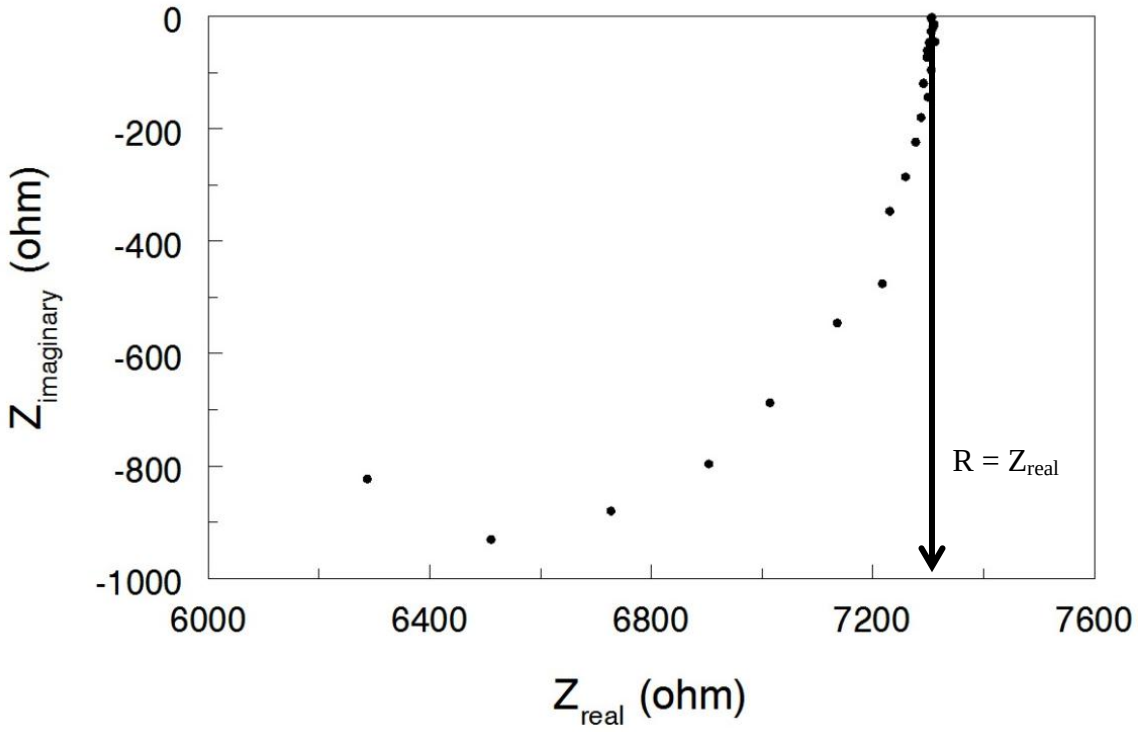

Figure 13: A representative example of an AC impedance Nyquist plot used to determine membrane conductivity. The real impedance (Z_{real}) at $Z_{imaginary}$=0 is the membrane's resistance (R). The resistance is used with Equation 1 to calculate the proton conductivity of the membrane sample.

2.4 Methanol Permeability

Methanol permeability at 25°C and 60°C was measured using a two-compartment diffusion cell (shown in Figure 14).[21,22,32] The membrane was clamped vertically between two solution-filled compartments. One compartment was filled with 1.0 M methanol solution (the feeding chamber) and the other with DI water (the receiving chamber). Stir bars continually mixed the solutions in both compartments to avoid bulk solution concentration gradients. An HPLC pump (Lab Alliance Series I Pump) circulated water from the receiving compartment to a differential refractometer (Waters 2414 Refractive Index Detector). The refractometer recorded methanol concentration vs. time data for the receiving compartment. Data were collected using Personal DaqView software. Figure 15 displays typical concentration vs. time data for membranes of different draw ratio.

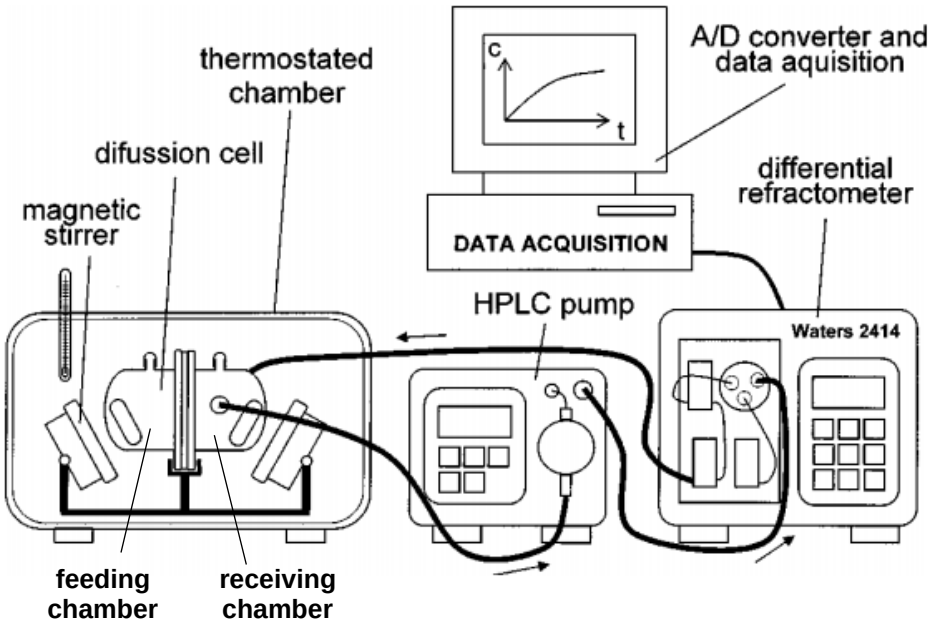

Figure 14: Two compartment diffusion cell apparatus used to determine the methanol permeability in Aquivion® membranes. Figure taken from Wycisk et al. [32]

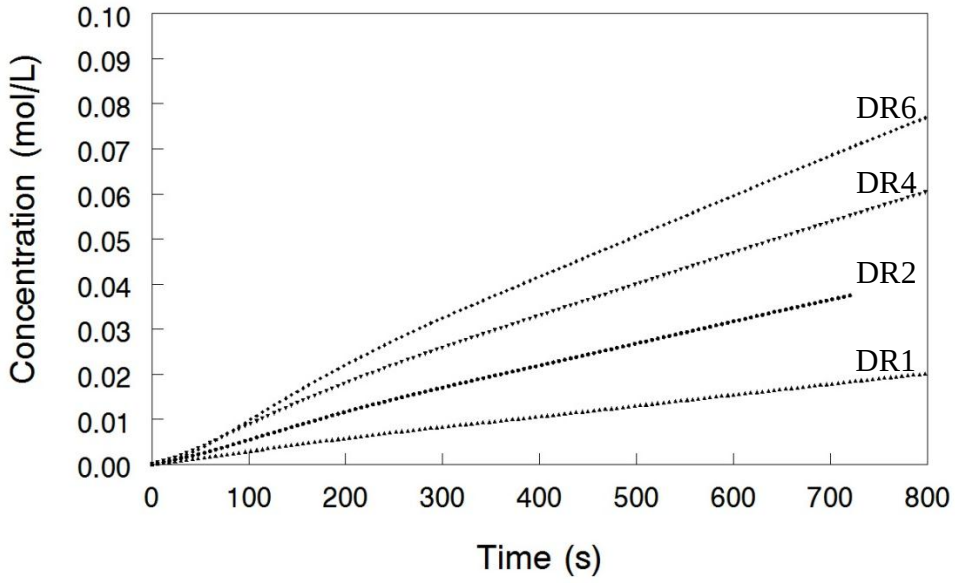

Figure 15: Representative experimental methanol concentration vs. time data (in the receiving chamber) for the determination of methanol permeability in an Aquivion® membrane at different draw ratios (DR1, DR2, DR4, DR6). The slope of the data at t>300 (where the data are linear) was used to calculate the methanol permeability using Equation 3 below.

The slope of a methanol concentration vs. time plot for the receiving chamber was used to calculate the membrane permeability for methanol using Fick's second law.[21,22] When the difference in methanol concentrations between the feeding and receiving compartment is assumed to be constant (setting up pseudo steady-state, 1D diffusion), the slope of such a plot is given by:

$$\text{Slope}=\left(\frac{dC_R(t)}{dt}\right)=\left(\frac{A}{V_R}\right)*\left(\frac{D*K}{L}\right)*C_F \qquad [2]$$

where $C_R(t)$ is the methanol concentration (mol/cm^3) in the receiving compartment at time t (s), A is the area of the exposed membrane (cm^2) , V_R is the volume of the receiving chamber (cm^3), D is the methanol diffusion coefficient in the membrane

(cm^2/s), K is the methanol solubility coefficient in the membrane, L is the wet membrane thickness (cm), and C_F is the initial methanol concentration in the feed compartment (mol/cm^3). Upon rearranging Equation 2, the methanol permeability (P) with units of cm^2/s is given by:

$$P = D*K = \frac{(slope)*V_R*L}{A*C_F} \quad [3]$$

2.5 Water Uptake Measurements

The equilibrium absorption of water vapor in membrane samples was determined by measuring the weight change of dry films using a TA Q5000SA vapor sorption apparatus. The temperature was held constant at 80ºC while the relative humidity was incrementally increased from 0 to 90%. Figure 16 shows typical sorption data for an Aquivion® membrane. The relative humidity was held constant for 2 hours to ensure ample time to reach equilibrium. The number of water molecules per sulfonic acid group (λ) was calculated using the equation below:

$$\lambda\left(\frac{H_2O}{SO_3^-}\right) = \left[\frac{W_{wet}-W_{dry}}{W_{dry}}\right]\frac{1}{[IEC][MW_w]} \quad [4]$$

where W_{wet} and W_{dry} denote wet and dry sample weights (g), IEC is the ion-exchange capacity of the membrane (1.21 mmol/g for 830 EW Aquivion®), and MW_w is the molecular weight of water (18 g/mol).

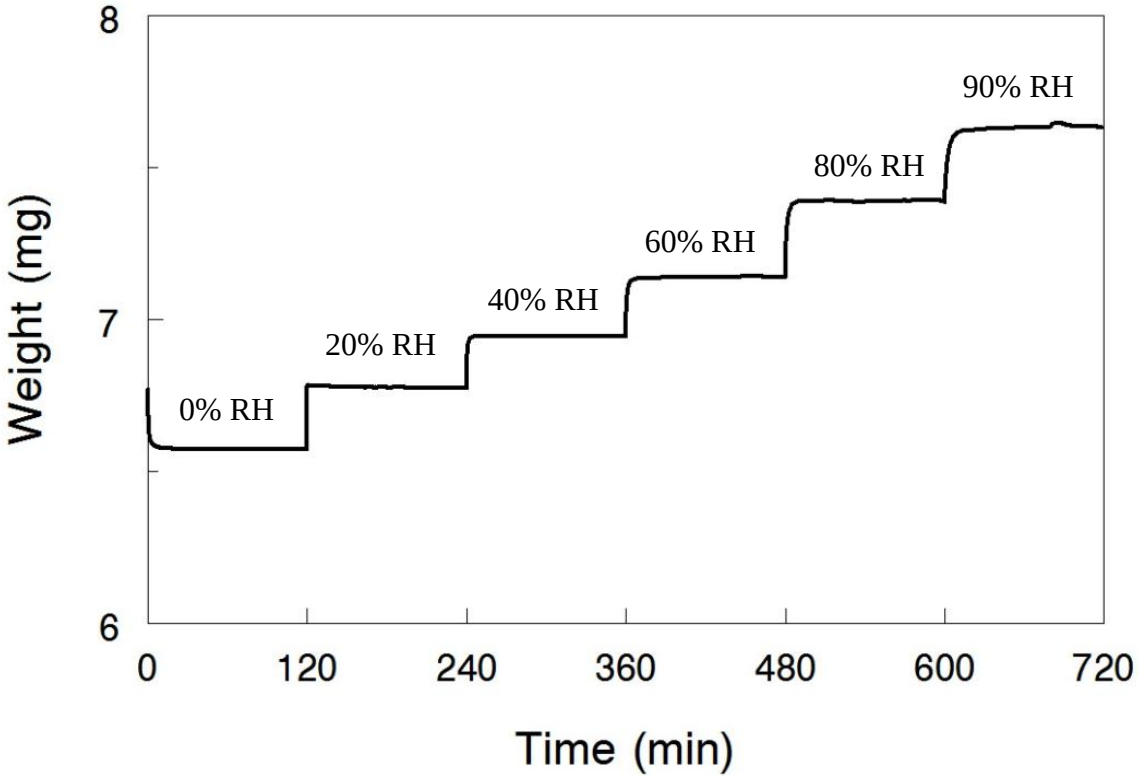

Figure 16: Representative water vapor uptake vs. time data at 80ºC for a stretched Aquivion® film (DR=6). Data were collected using a TA Q5000SA vapor sorption apparatus.

2.6 Mechanical Strength (Stress/Strain Measurements)

Tensile stress vs. strain curves were obtained for stretched and unstretched Aquivion® membranes using a TA Q800 Dynamic Mechanical Analysis apparatus. Prior to testing, samples were cut into 2 mm x 25 mm strips, dried in a lab oven at 60°C under vacuum for one hour, and then equilibrated under atmospheric conditions (20% RH at 30ºC). During testing, the chamber temperature remained constant at 30ºC (with an ambient relative humidity of ~20%). The tensile force was ramped at 0.1 N/min until the sample failed. Samples were stretched parallel to the original stretching direction during

testing. The Young's modulus (elastic modulus in tensile stress tests), plastic modulus, strain at break, and ultimate stress were determined from each set of stress/strain data. Figure 17 shows an experimental stress vs. strain curve property analysis for a stretched Aquivion® membrane (DR4), where each of the four mechanical properties is identified.

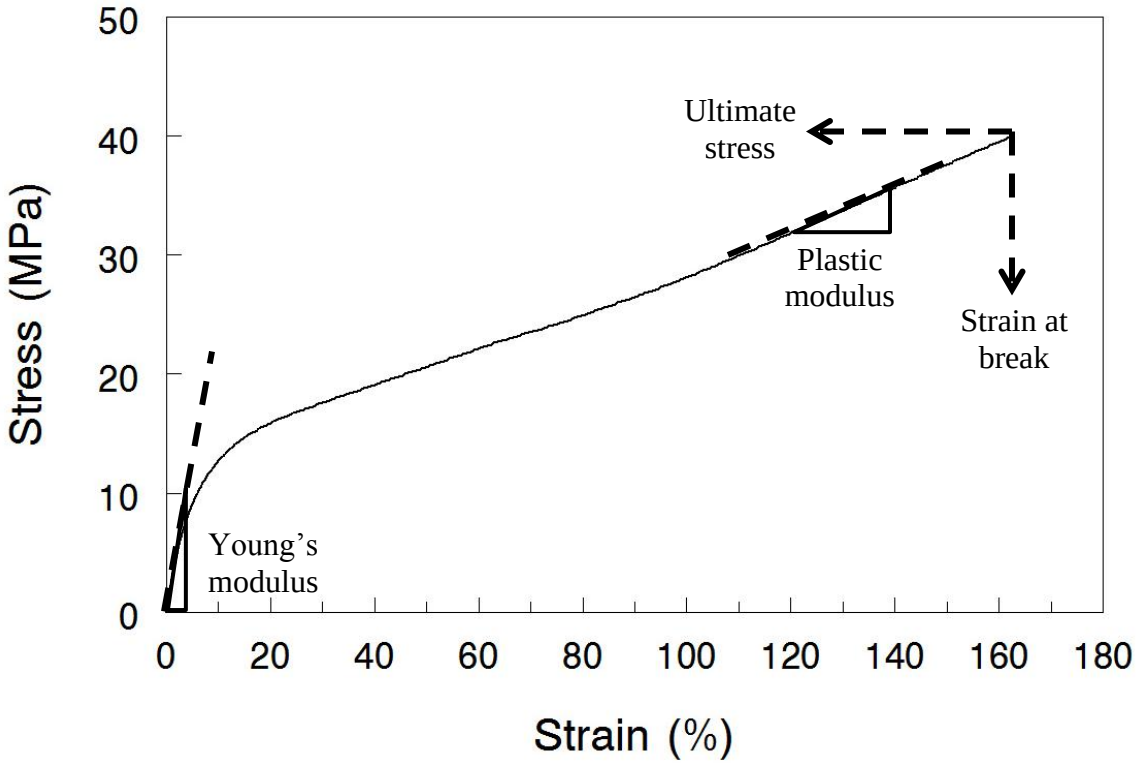

Figure 17: Stress/strain curve for a stretched Aquivion® film (DR=4) at 30ºC and 20% RH illustrating the determination of membrane mechanical properties.

CHAPTER 3

RESULTS AND DISCUSSION

3.1 Annealing Condition

A literature search found no report on the effect of annealing time and temperature on Aquivion® crystallinity, so a proper annealing condition for stretched cast Aquivion® was determined in a set of preliminary experiments. The membrane annealing temperature should be above the α-transition temperature to provide sufficient chain mobility for crystallite formation, yet not so high as to melt the polymer.[66,67] Aquivion® has a reported α-transition temperature of 165ºC,[14,16,18,19] and a complete melting temperature of 235ºC.[19] An annealing temperature 35°C above the glass transition temperature (190°C) was thereby chosen to accelerate the crystallization kinetics.

To determine the required time to fully anneal Aquivion® at 190°C, WAXD (wide angle X-ray diffraction) spectra were collected on cast, unstretched, membrane samples annealed for three different times: 0 minutes (unannealed), 30 minutes, and 60 minutes. All the membrane films were cast following the procedure detailed in Section 2.1. The WAXD spectra of the three Aquivion® films are shown in Figure 18.

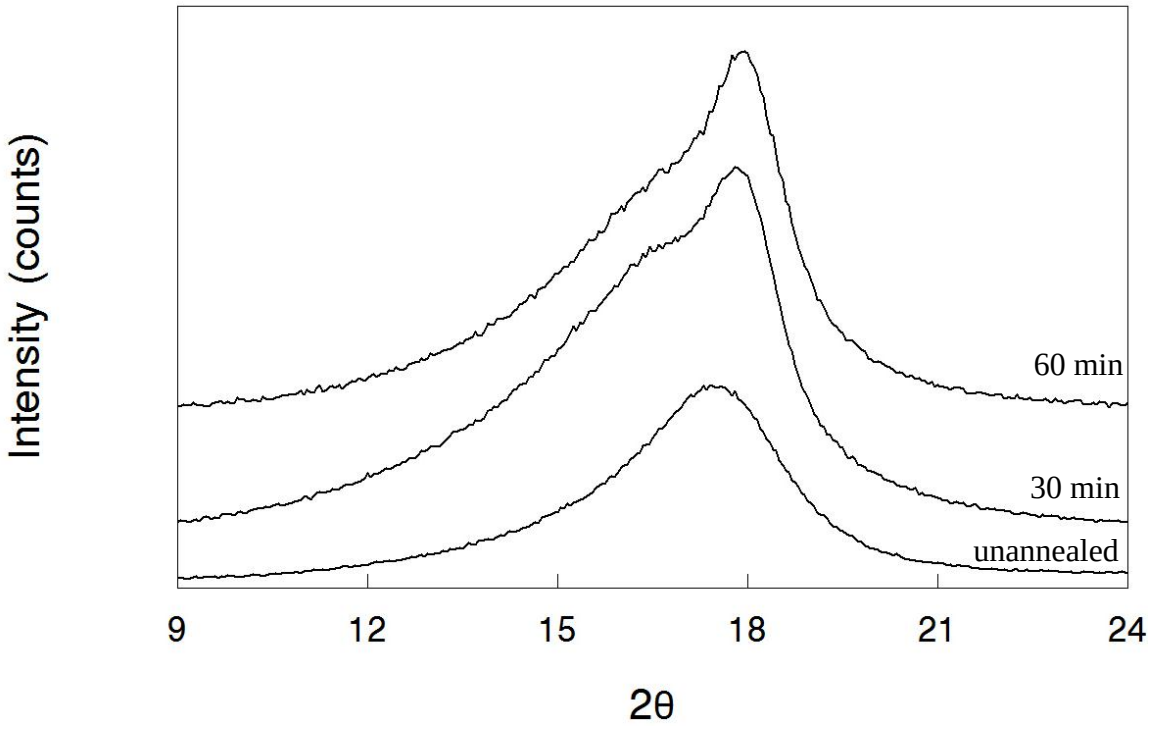

Figure 18: WAXD spectra collected on cast Aquivion® films annealed at 190°C for three different times: 0 min (unannealed), 30 min, or 60 min.

The degree of crystallinity in the membranes was determined by deconvoluting a WAXD spectrum into separate amorphous (at 16.5°) and crystalline (at 18°) peaks using the Pearson VII distribution function.[66]

Figure 19 illustrates the deconvolution of a WAXD spectrum taken on an Aquivion® membrane annealed for 30 min at 190°C.

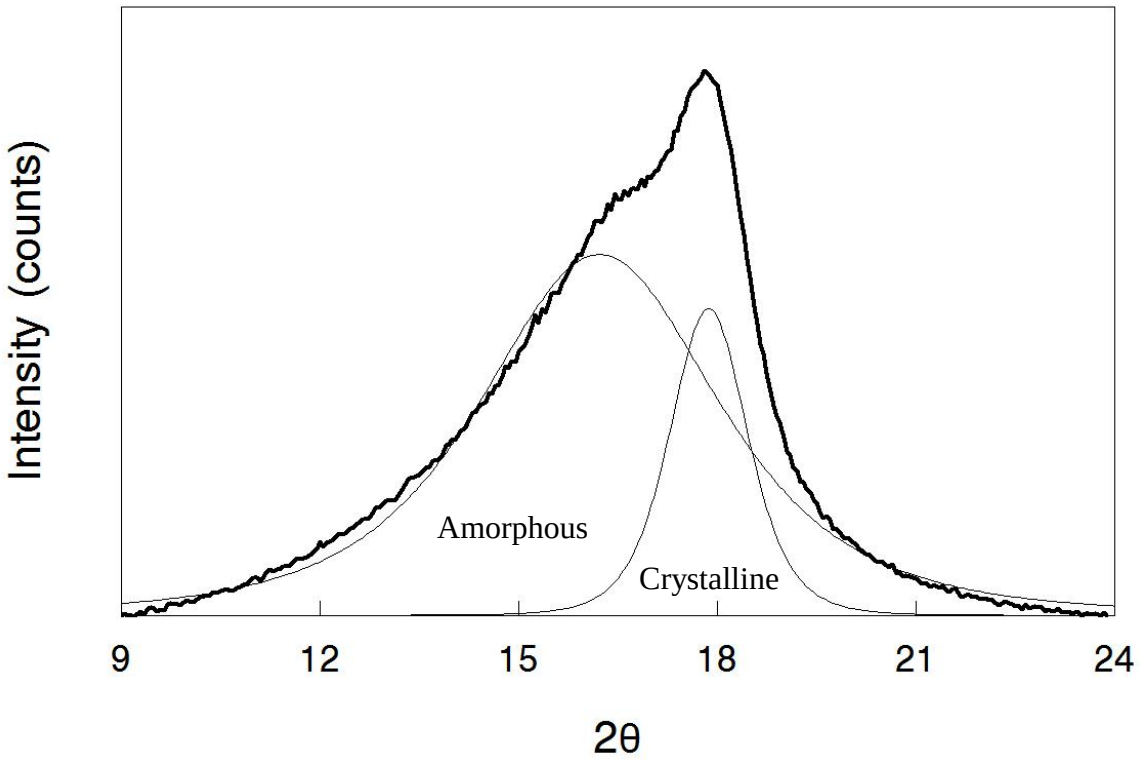

Figure 19: A deconvolution of a WAXD spectrum taken on an Aquivion® film annealed at 190°C for 30 min.

Crystallinity was calculated by integrating the two peak areas, and dividing the area under the sharp crystalline peak (at 18°) by the combined area of the amorphous (at 16.5°) and crystalline peaks.[12] The mathematical equation for the % crystallinity (W_{cr}) is:

$$W_{cr} = \frac{\int_9^{24} I_{cr}(\theta)\theta^2 d\theta}{\int_9^{24} [I_{cr}(\theta)+I_{am}(\theta)]\theta^2 d\theta} * 100\% \quad [5]$$

where $I_{cr}(\theta)$ and $I_{am}(\theta)$ are the intensities of the crystalline and amorphous peaks respectively, and θ is the incident X-ray angle. Peak integration was performed for 2θ incident angles between 9 and 24°. See Appendix B for an in-depth walkthrough of the WAXD deconvolution and integration in Excel®. This procedure was followed on all

WAXD spectra throughout the present work. Table 5 lists the calculated % crystallinity for each of the three membranes.

Table 5: The calculated crystallinity from the WAXD spectra taken during the investigation of the annealing time at 190°C. WAXD spectra are shown in Figure 18.

Annealing Condition	***Crystallinity %***
No annealing	0
190°C, 30 min	21
190°C, 60 min	23

Annealing at 190°C for 30 minutes or 60 minutes successfully crystallized the Aquivion® samples. The annealed samples were >20% crystalline, while the WAXD spectrum of the unannealed Aquivion® had no discernible crystalline peak (see Figure 18). The annealing kinetics of Aquivion® appears rapid at 190°C with full crystallization in 30 minutes. A similar increase in crystallinity has been observed for annealed Nafion®.[66,67] A variety of sources have demonstrated that the chain movement caused by heating the polymer above the glass transition temperature enlarges crystallites, repairs crystallite defects, and develops long-range order.[66-68]

The effect of annealing on proton conductivity and methanol permeability in the Aquivion® membranes was also determined. Prior to annealing, cast Aquivion® has a proton conductivity of 0.065 S/cm (in water at 25°C) and a methanol permeability of $5.12*10^{-6}$ cm^2/s (at 25°C with 1.0 M methanol). The annealed samples show a substantial improvement in both properties with a proton conductivity of ~0.10 S/cm and a methanol permeability of ~$2.85*10^{-6}$ cm^2/s (53% increase and 44% decrease, respectively). After thermal annealing, the cast Aquivion® samples had properties that resembled those of

commercial PFSA membranes. While there were no reported values of methanol permeability or proton conductivity for commercial 830 EW Aquivion® films, the annealed samples exhibited a proton conductivity consistent with similar EW commercial Aquivion® films (~1.1 S/cm for 790 EW in water at 25°C)[18,63] and a methanol permeability comparable to that of Nafion® 117 ($2.5*10^{-6}$ cm^2/s with 1 M methanol at 25°C). In Nafion®, annealing reduces the polymer swelling by increasing crystallinity (crystallites act as physical crosslinks), and enhances the proton conductivity by organizing the ionic domains.[68,69] Aquivion® is likely experiencing similar phenomena upon annealing which explain the observed changes in methanol permeability and proton conductivity. Table 6 provides a summary of the membrane properties for unannealed and annealed cast Aquivion®. Errors reported in the table are standard deviations calculated from the results of repeated experiments. The data in Table 6 support the conclusion that 30 minutes is sufficient time for annealing Aquivion® at 190°C, thus all cast Aquivion® films were annealed at 190°C for 30 minutes (unless otherwise noted).

Table 6: Cast Aquivion® properties before and after annealing at 190°C.

	0 min	***30 min***	***1 h***
Crystallinity (%)	0	21	23
Proton Conductivity (S/cm)*	0.065 ± 0.006	0.100 ± 0.006	0.108 ± 0.015
Methanol Permeability (cm^2/s) x 10^6**	5.12 ± 0.071	2.86 ± 0.096	2.84 ± 0.186

* in deionized water at 25°C
** at 25°C with 1 M methanol

3.2 Determination of Stretching Conditions

Stretching parameters for Aquivion® (stretching rate and temperature) were determined in an attempt to maximize the increase in polymer chain orientation and crystallinity. Recast Nafion® membranes, composed of a long side chain PFSA polymer, have been successfully stretched by Lin.[46-49] Lin's procedure was therefore adapted for the short side chain PFSA polymer, Aquivion®.

A stretching temperature of 190°C (the same as the annealing temperature) was chosen for the cast Aquivion® membranes based largely on the procedure reported for stretching recast Nafion®. Lin et al. stretched Nafion® at a temperature of 125°C followed by annealing at 150°C.[46-49] Stretching above the glass transition temperature is required to provide the polymer chains with added mobility and to ease polymer reorganization.[50] The higher glass transition temperature for Aquivion® compared to Nafion® (165°C vs. 110°C, respectively)[14,19] suggests a stretching temperature approximately 55°C greater for Aquivion® than Nafion® (equaling 180°C). By increasing the stretching temperature to 190°C in the present work, the annealing and stretching steps were performed simultaneously to accelerate and simplify membrane processing. At a stretching temperature greater than 190°C membranes snapped/tore during elongation. This was likely due to excessive rigidity caused by the rapid creation of crystallites and/or evaporation of the residual solvent needed to plasticize the films. Therefore, a stretching temperature of 190°C was used throughout the present study to stretch cast Aquivion® films.

An optimized stretching rate at 190°C was investigated for uniaxially stretched cast Aquivion® membranes by determining the effect of stretching rate (mm/min) on the resulting degree of crystallinity (using WAXD). For this investigation, films with a draw ratio of 4 were created using three different stretching rates: 0.90 mm/min, 1.25 mm/min, and 2.05 mm/min. Prior to stretching, each sample underwent the same casting and membrane preparation procedures outlined in Section 2.1. The timing of the individual stretching/annealing steps however (initial slow stretching, rapid stretching, and annealing with no further stretching) was adjusted to maintain a total annealing time of ~30 min at 190°C. Table 7 lists the time intervals for each of the three different membranes. The membrane that was stretched at the slowest rate (0.90 mm/min) required 36 minutes for processing, 6 minutes longer than the others. However, the additional 6 minutes at 190°C is not expected to affect the membrane's properties since the annealing investigation in Section 3.1 indicated there is no difference in membrane properties for samples annealed between 30 and 60 minutes.

Table 7: Experimental protocols for the Aquivion® stretching rate investigation. For all samples, the total annealing time (including stretching time) was fixed at 30 or 36 minutes and the final draw ratio was 4.

Time spent…	*stretching at initial slow speed* +	*stretching at tested speed* +	*annealing with no further stretching* =	*Total annealing time (including stretching)*
Slow (0.90 mm/min)	3 min	33 min	0 min	36 min
Medium (1.25 mm/min)	3 min	22 min	5 min	30 min
Fast (2.05 mm/min)	3 min	15 min	12 min	30 min

WAXD analysis was used to determine if the polymer crystallinity of stretched cast Aquivion® membranes was dependent on the stretching rate (an in-depth description of the WAXD analysis is described in Section 3.1). Figure 20 and Table 8 show the X-ray spectra and crystallinities for the stretched Aquivion® membranes listed in Table 7. All stretching rates resulted in the same degree of crystallinity (33%). Thus the stretching rate had no effect on the crystallinity over the tested range (0.9-2.05 mm/min). Henceforth, all stretched Aquivion® membranes were prepared with the medium uniaxial stretching rate of 1.25 mm/min (as mentioned in Section 2.1).

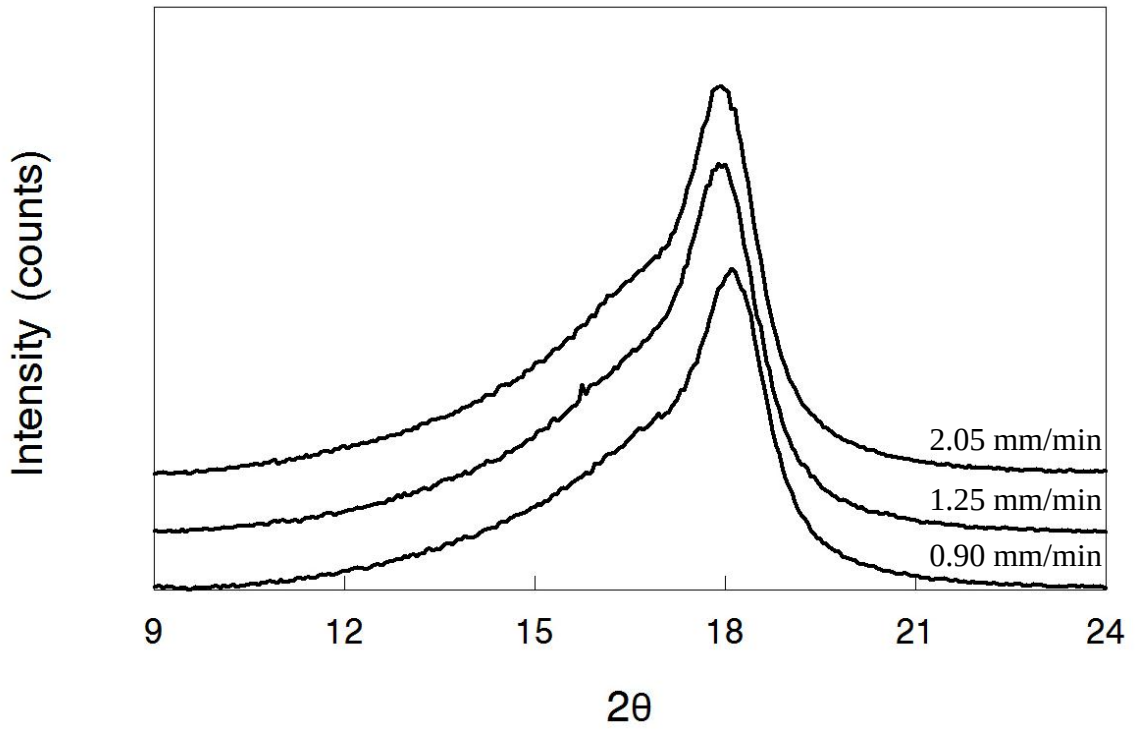

Figure 20: WAXD spectra collected on DR4 uniaxially stretched Aquivion® membranes created using three different stretching rates (slow=0.90 mm/min, medium=1.25 mm/min, and fast=2.05 mm/min) following the protocol outlined in Table 7.

Table 8: Measured crystallinity for three, DR4, uniaxially stretched Aquivion® membranes, where the film stretching rate was varied. Results were calculated using the WAXD spectra in Figure 20.

	***Slow* (0.90 mm/min)**	***Medium* (1.25 mm/min)**	***Fast* (2.05 mm/min)**
Crystallinity (%)	33	33	33

3.3 The Effect of Draw Ratio on Stretched Aquivion® Crystallinity

The effect of draw ratio on crystallinity was investigated by analyzing WAXD spectra of stretched Aquivion® membranes. Previous studies on the stretching of Nafion®,[46-49,55,59] in addition to other stretched polymers (polyethylene,[69] polypropylene,[70] poly(1-butene)[71]), reported an increase in crystallinity with increasing draw ratio. Additionally, enhanced crystallinity was seen in cast Aquivion® membranes stretched to a draw ratio of 4 when compared to an unstretched film during the stretching rate investigation (see Section 3.2). Therefore, increasing crystallinity with draw ratio was expected for stretched Aquivion® membranes. Figure 21 displays WAXD spectra taken on unstretched Aquivion®, both unannealed and annealed (DR1), as well as on stretched/annealed Aquivion® membranes (DR2, DR4, and DR6). The WAXD spectra were decomposed as detailed in Section 3.1 to calculate crystallinity. Figure 22 plots the crystallinity for stretched Aquivion® and stretched Nafion® (obtained from Lin et al.[48]) with respect to draw ratio.

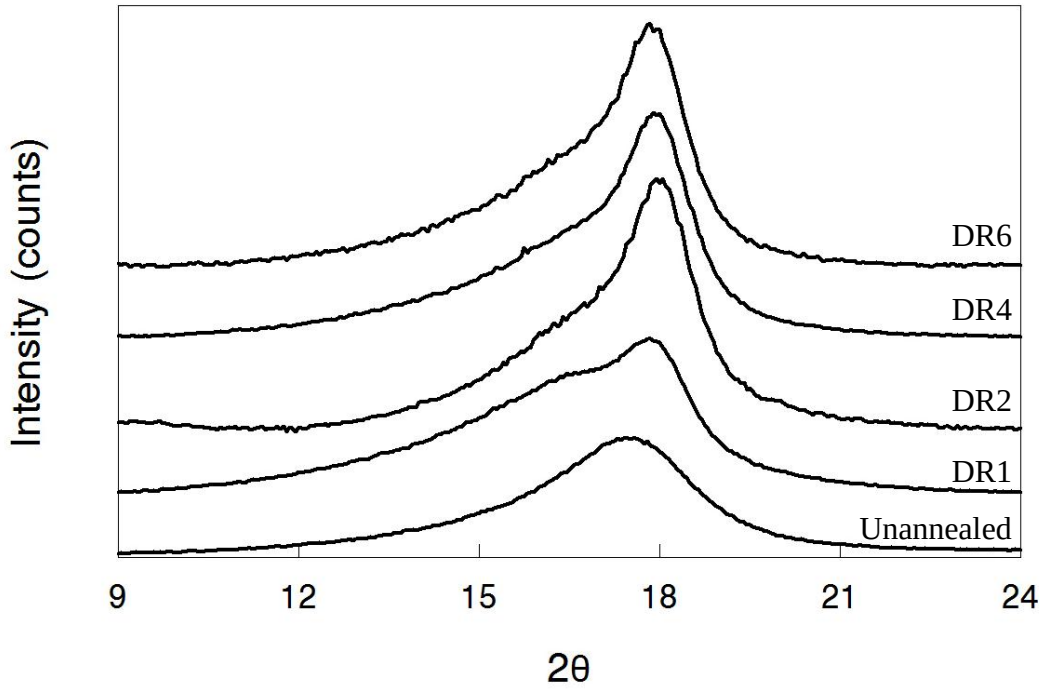

Figure 21: WAXD spectra of cast Aquivion® membranes stretched to different draw ratios (final length/initial length).

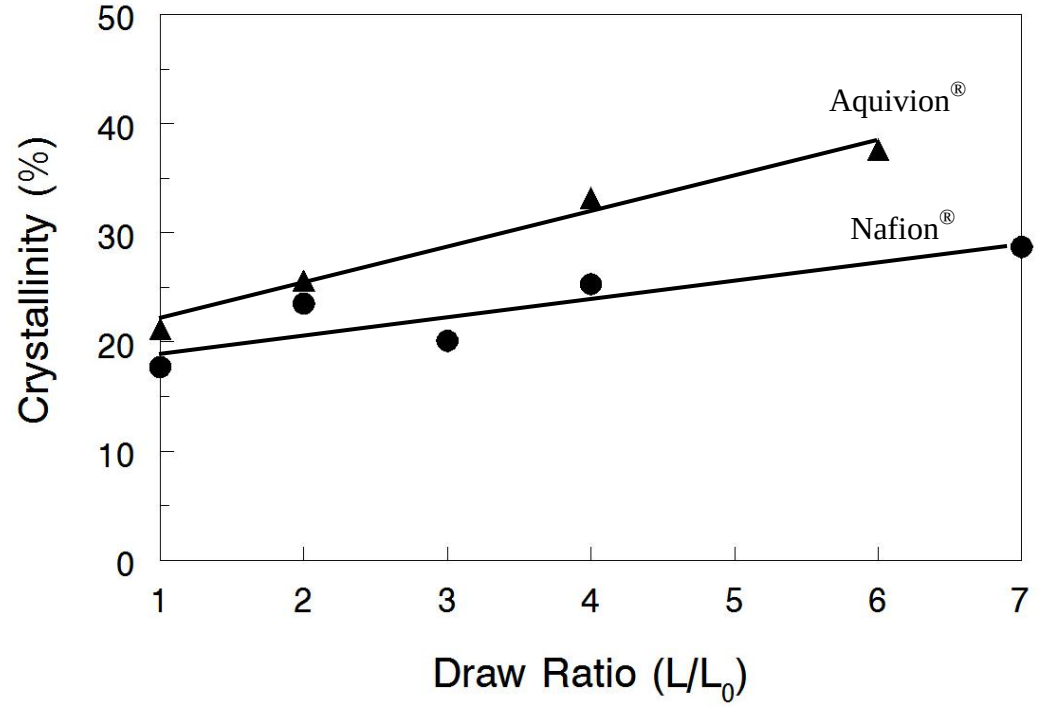

Figure 22: Crystallinity vs. draw ratio for uniaxially stretched Aquivion® (▲) and stretched Nafion® (●). Nafion® data is from reference [48].

The degree of crystallinity is strongly correlated with draw ratio for the uniaxially stretched Aquivion® membranes. Aquivion® and Nafion® originally display similar crystallinity, but 830 EW Aquivion® appears to undergo larger polymer network reorganization than 1100 EW Nafion® upon stretching as evidenced by a larger increase in crystallinity. The cause for this difference is currently unknown, but could be due to the shorter, and therefore less mobile, side chain in Aquivion® which allows the polymer chains to pack more efficiently.[12,54] Additionally, crystallinity in other stretched polymer films (such as polyethylene terephthalate,[72,73] polyethylene,[74] and isotactic polypropylene[75]) has been shown to be a strong function of the stretching temperature. At a constant stretching rate and draw ratio, the crystallinity of these polymers reached a maximum at some stretching temperature between their respective glass transition and melting temperatures. Although there is no investigation on the stretching temperature effect for either ionomeric polymer, based on studies of other stretched polymers the higher stretching temperature for Aquivion® (190°C) compared to Nafion® (125°C) may also contribute to the increase in crystallinity.

The full width at half maximum (FWHM) of the XRD crystalline peak gives insight into the mean size of the crystalline domains (d) through use of the Scherrer equation, which assuming a dimensionless shape factor is:[76]

$$d = \frac{0.9\lambda}{B\cos\theta} \qquad [6]$$

where λ is the x-ray wavelength (in nm), B is the FWHM (in rad), and θ is the Bragg angle = ½ * $2\theta_{\text{crystalline peak}}$(with units of rad).

Table 9 lists the FWHM of the crystalline peak and the corresponding mean crystallite size at various draw ratios for stretched Aquivion® and stretched Nafion® (data from reference [48]). Figure 23 displays the mean crystallite size as a function of draw ratio for the two stretched polymers. In both polymers, the crystallites grow in size after stretching, but appear to reach a critical size at DR≥2 (<5% difference) which means that crystallite nucleation also occurs within the stretched polymers since both polymers show a continued increase in crystallinity at DR≥2. The density of crystallites within the stretched polymers (# of crystallites/μm^3) was calculated from the mean crystallite size (cube root of crystallite volume) and the polymer degree of crystallinity. Figure 24 plots the density of crystallites within the stretched polymers as a function of draw ratio. The crystallite density trends for both stretched Aquivion® and Nafion® suggest that stretching originally disrupts and/or combines a large number of crystallites as their number decreases sharply at DR2 compared to DR1. Further stretching, however, (DR≥2) creates more highly oriented polymer chains which gradually facilitate new crystallite formation. The results for crystallite growth and nucleation reveal that stretched Aquivion® is composed of larger, less numerous crystallites for all DRs, as compared to Nafion®. A full investigation into the cause of the differences in crystallite growth and nucleation is beyond the scope of this work, as reports on other stretched polymers have demonstrated that processing temperatures, stretching rate, chemical structure, and molecular weight all affect the resulting crystallinity.[69,71-73,75] Stretching experiments with Aquivion® at other/additional temperatures may reveal whether the differences in crystallite size and number, compared to Nafion®, are due to different processing temperatures (for annealing and stretching).

Table 9: FWHM of the crystalline peak (in °), and subsequent mean crystallite size, obtained from XRD spectra taken in the plane perpendicular to the stretching direction for stretched Aquivion® and stretched Nafion® (from reference [48]).

	Aquivion® (at 2θ=18°)		*Nafion® (at 2θ=17.5°)*	
	FWHM(°)	d(nm)	FWHM(°)	d(nm)
DR1	1.383	5.81	2.202	3.65
DR2	1.173	6.85	1.727	4.65
DR4	1.200	6.70	1.724	4.66
DR6	1.207	6.66	-	-
DR7	-	-	1.703	4.72

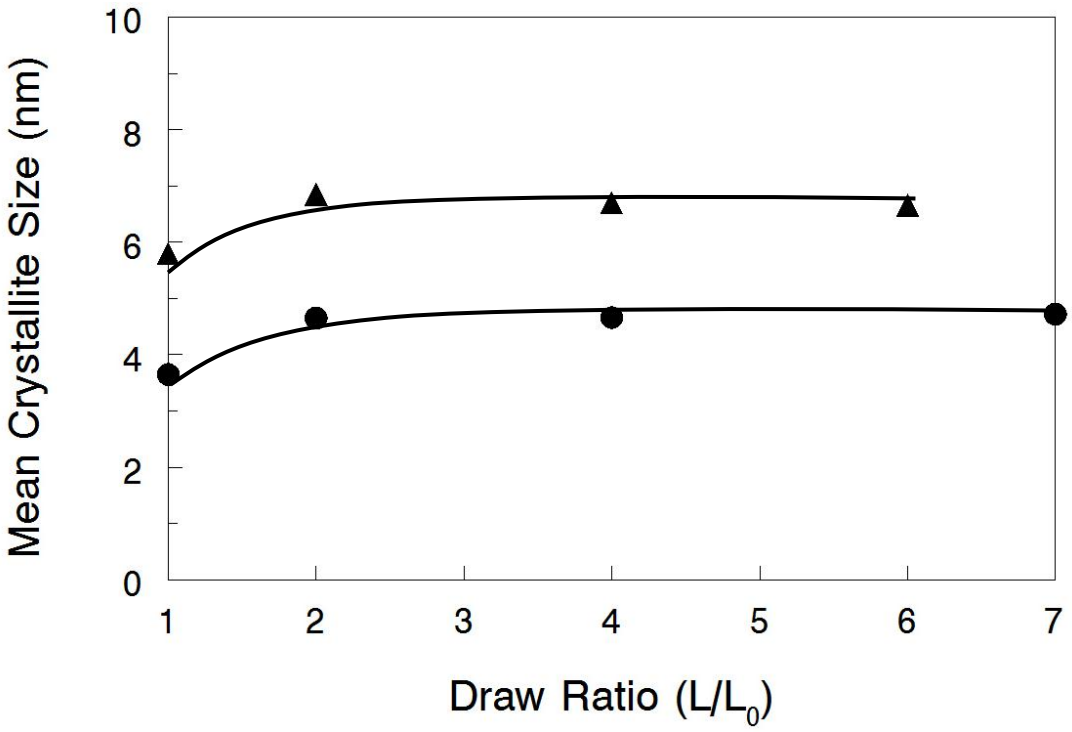

Figure 23: Mean crystallite size as a function of draw ratio for stretched Aquivion® (▲) and stretched Nafion® (●) films.

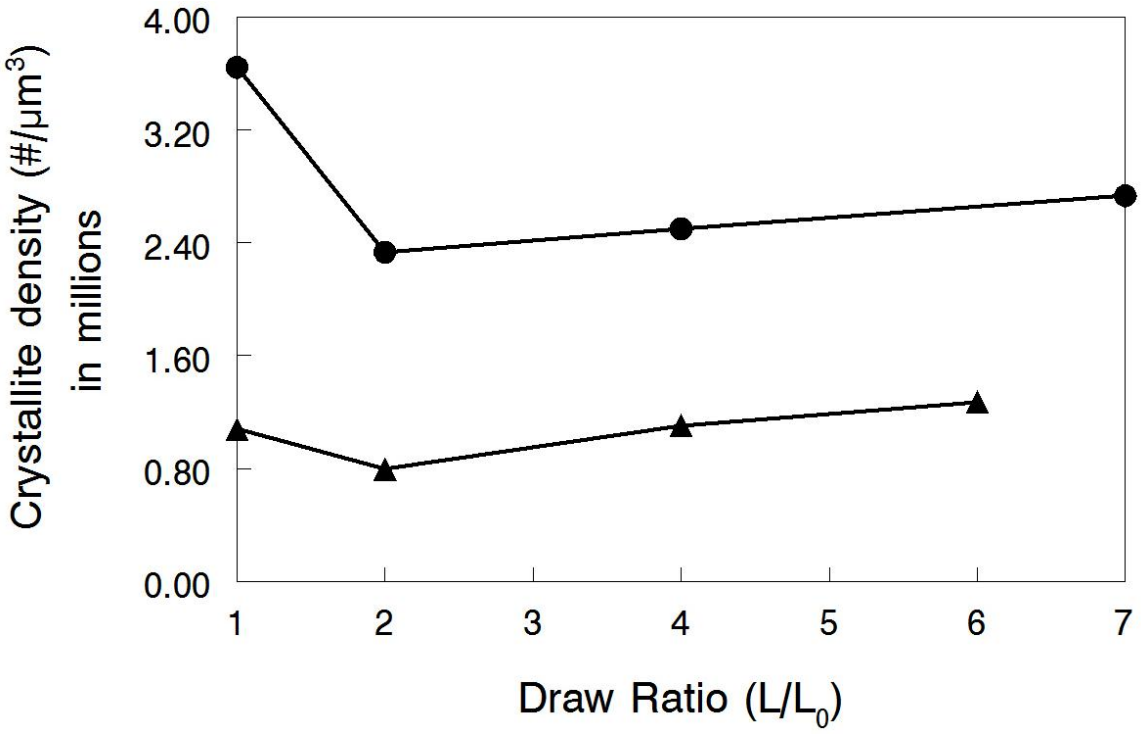

Figure 24: Crystallite density as a function of draw ratio for stretched Aquivion® (▲) and stretched Nafion® (●) calculated from the mean crystallite size and % crystallinity.

Crystallinity has important effects on key DMFC membrane properties. Crystallites in Nafion® have been shown to improve the membrane's mechanical properties by acting as physical crosslinks,[66,67] and they alter water/methanol transport properties by influencing the structure and connectivity of the hydrophilic domains within the polymer.[55,66] The trends in crystallinity for stretched Nafion® and stretched Aquivion® (shown in Figure 22), therefore, suggest progressively altered property differences at higher draw ratios (proton conductivity, methanol permeability, and mechanical strength). These membrane properties of the stretched films are reported in the ensuing sections.

3.4 Equilibrium Water Vapor Uptake

Water is required for proton conductivity, but excessive water uptake causes poor mechanical properties and typically indicates high methanol permeability (methanol and water permeability are often comparable since the solvents are chemically similar).[8,14,77] The property of water (or methanol) uptake in an ionomer results from the competing forces of the polymer's affinity for solvent molecules (osmotic pressure), and the resistance of the polymer network to volumetric swelling.[50,78] To investigate the water uptake properties of stretched Aquivion®, equilibrium water vapor uptake measurements were made on Aquivion® membranes at 80°C as described in Section 2.5. Figure 25 shows plots of the equilibrium water vapor uptake vs. relative humidity in unstretched/annealed (DR1) and stretched/annealed (DR2, DR4, DR6) Aquivion® membranes, along with values reported for commercial Nafion® 117.[78] The equilibrium water vapor uptake is expressed in both wt% (g water/g dry polymer * 100%), and λ (water molecules per sulfonic acid site).

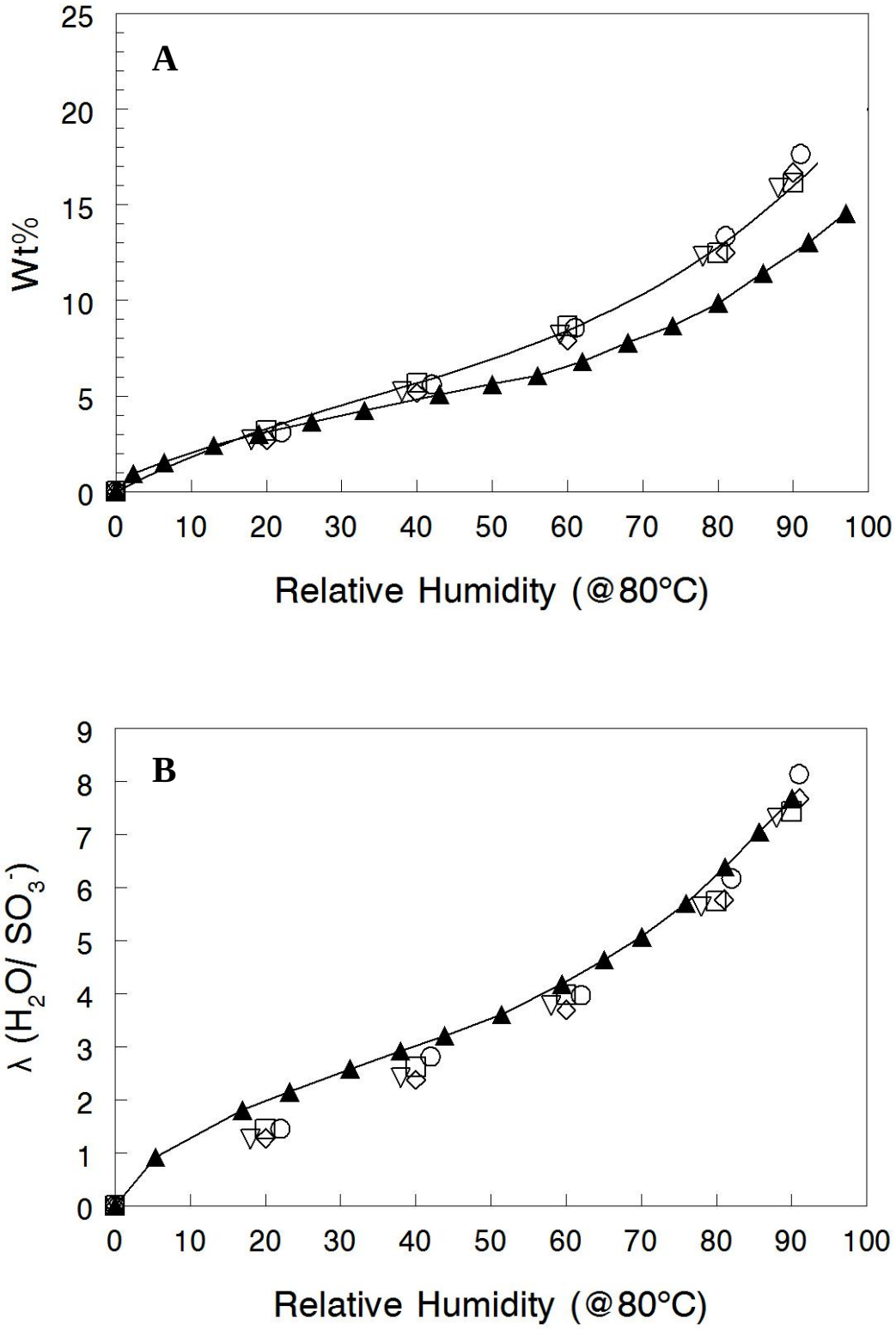

Figure 25: Equilibrium water vapor uptake at 80ºC for Aquivion® films (○,DR1; ▽ ,DR2; ◇,DR4; □ ,DR6) and Nafion® 117 (▲). Nafion® data from reference [78].

830 EW Aquivion®, at all tested draw ratios, absorbed more water (wt%) than Nafion® 117 at relative humidities ≥40%, which agrees with previously reported results.[14,62,64,79] As the concentration of sulfonic acid groups is increased in a polymer (thereby lowering the EW), the osmotic driving force builds as water wants to penetrate into the membrane to dilute the charged side groups. Figure 26 shows the liquid water uptake at 100°C for Nafion® and Hyflon Ion® (a short side chain PFSA polymer of identical chemical structure to Aquivion®) as a function of EW. At equal equivalent weight, the short side chain PFSA demonstrates reduced water uptake compared to Nafion®. This difference is explained by other traits of the ionomeric microstructure such as the width and connectivity of the hydrophilic domains, and/or the degree of crystallinity which also affects the water uptake by influencing the volumetric swelling.[11,14,80] So although Aquivion® demonstrates a better ability to restrict water uptake compared to Nafion® (at equal EW), the significantly lower EW of Aquivion® in this study (830 EW vs. 1100 EW) results in higher water uptake.

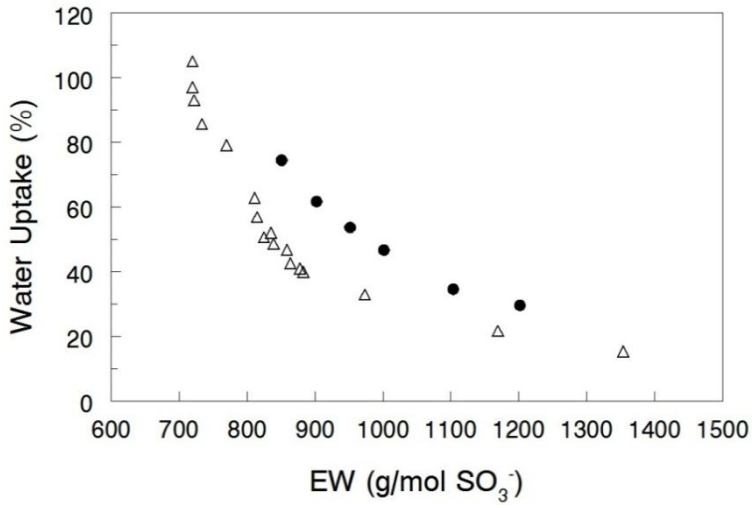

Figure 26: Water uptake for Hyflon Ion® (△) (a polymer of identical chemical structure to Aquivion®) and Nafion® (●) membranes in liquid water at 100°C as a function of EW. Plot taken from [64].

Crystallites act as physical crosslinks which restrict membrane swelling and reduce water uptake,[54] but this effect was not seen for the stretched Aquivion® membranes. WAXD experimental results shown previously (Section 3.3) indicated an increase in crystallinity with stretching, but the equilibrium water vapor uptake (both λ and wt%) was independent of the Aquivion® draw ratio. A similar result was reported for stretched Nafion®,[47,49] and was attributed to the amount of crystallinity induced by stretching (8%) being too small to influence the water uptake property. However, even at a 17% crystallinity increase between DR1 and DR6 in Aquivion®, there is no change in the water uptake so crystallinity does not appear as the dominant factor. Other traits of the ionomeric microstructure mentioned previously that also affect water uptake may supersede or counteract the effect of increased crystallinity to keep the water uptake constant. In any case, the results show that stretching does not change water uptake in Aquivion®.

Although Aquivion® absorbed more water (wt%) than Nafion®, the water uptake measured as λ was essentially equal between the two polymers at 10%<RH<90%. Reports have previously demonstrated that λ is relatively constant across a variety of PFSA ionomers (shown in Figure 27).[78,79] The interaction between water and the sulfonated side chains was therefore identical in Aquivion® and Nafion®. The water vapor equilibrium uptake measurements indicate: 1) The larger wt% water in Aquivion® compared to Nafion® is attributed to the lower EW (higher IEC) and 2) Stretching did not noticeably change the water vapor uptake properties in cast Aquivion® films.

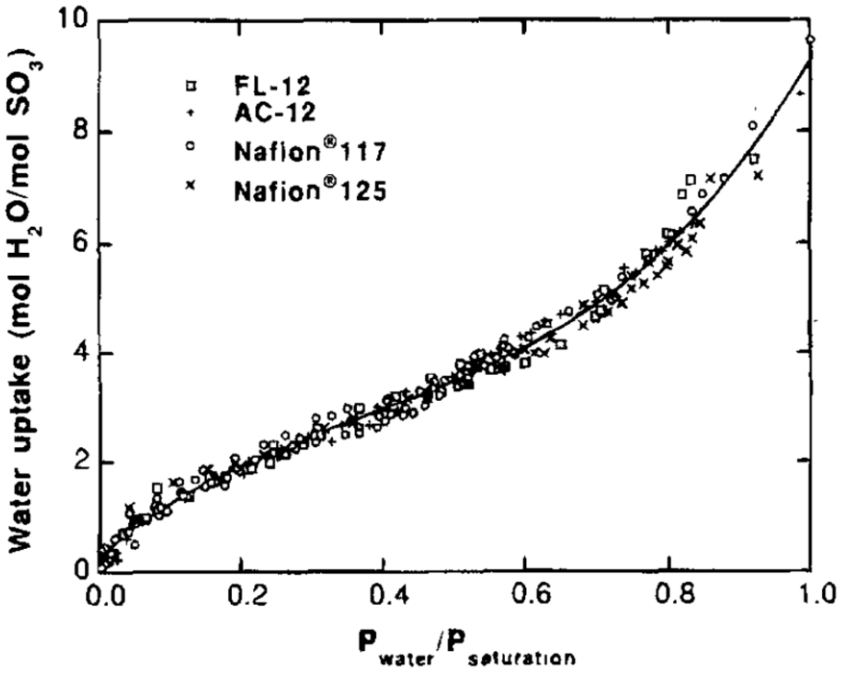

Figure 27: Water uptake as a function of relative humidity for various perfluorosulfonic acid polymers. Fl-12 = 920 EW Flemion®; AC-12 = 1080 EW Aciplex®, Nafion® 117 and 125 = 1100 and 1200 EW, respectively. Graph taken from reference [78].

3.5 Mechanical Properties

A membrane's performance in a DMFC relies heavily on its mechanical properties: (1) The uptake of water (and methanol) is partially controlled by polymer relaxation,[8,81] and (2) tough, durable membranes improve the fuel cell longevity by preventing adverse effects (such as chemical crossover and reduced ionic conductivity) resulting from membrane deformations (caused by membrane swelling and the subsequent stress-buildup).[82,83] Since crystallinity increases with stretching, the stretched Aquivion® samples were expected to show enhanced mechanical strength. Stretched Nafion® [48] in addition to stretched polyethylene,[69] polypropylene,[70] and poly(1-butene)[71] have all been reported to demonstrate superior mechanical performance over their

unstretched counterparts. While relatively few investigations have been devoted towards studying stretched ionomers, these other stretched polymers have demonstrated the complex nature of stress induced strengthening, which has been shown to be a function of the polymer's morphology, molecular orientation, percentage crystallinity, molecular weight, and drawing conditions.[69,71-73,75]

The effects of uniaxial stretching on the mechanical properties of cast Aquivion® membranes were examined by obtaining tensile stress/strain curves for samples of various draw ratios (DR1, DR2, DR4, DR6). Stress/strain curves for unstretched Nafion® and unstretched Aquivion® were first compared to determine the combined effect of the shorter side chain and lower EW of Aquivion® on membrane mechanical properties. The Aquivion® curves were produced in the present work (as detailed in Section 2.6), while the Nafion® curves are those collected by Lin et al.[48] All Aquivion® samples were dried at 60°C under vacuum for 2 hours, then equilibrated and tested at 30ºC and 20% RH (ambient humidity). The stress/strain data were collected in the direction parallel to stretching. Dried Nafion® samples were also tested at 30ºC in the stretching direction, but under a nitrogen atmosphere (0% RH).[48] Figure 28 displays stress/strain curves for unstretched Nafion® and unstretched Aquivion®.

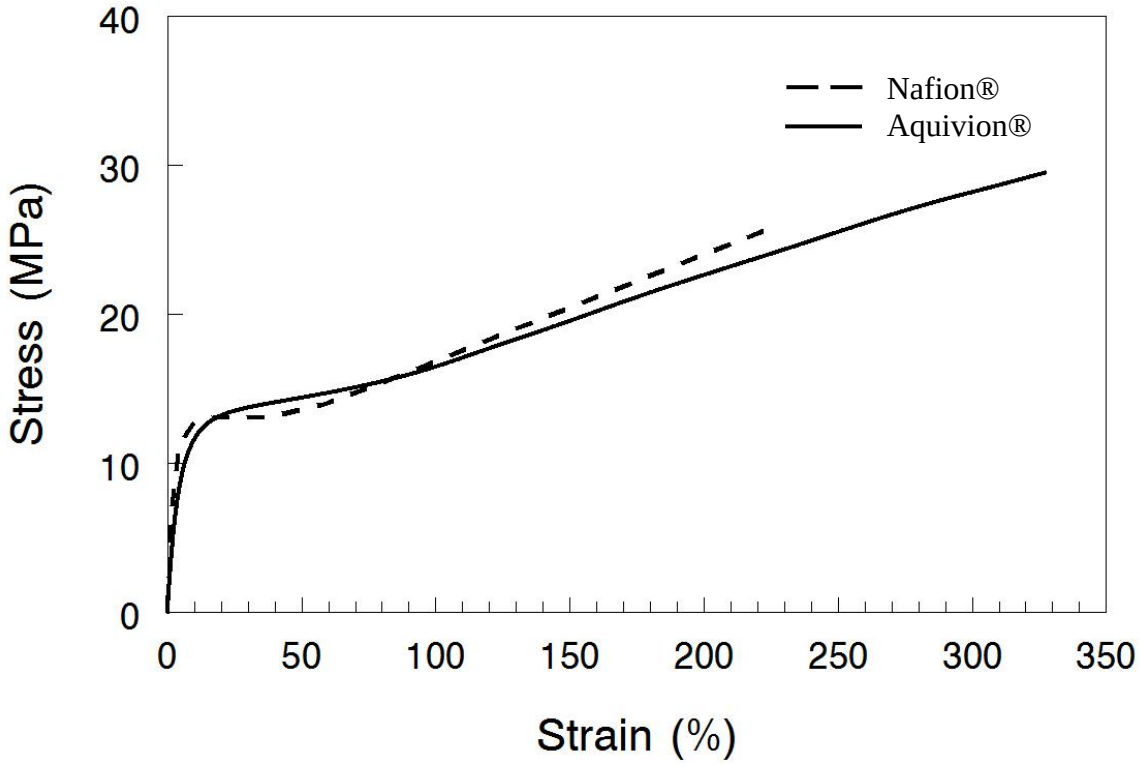

Figure 28: Stress/strain curves for unstretched Aquivion® at 30°C and 20% RH, and unstretched Nafion® at 30°C and 0% RH. Nafion® curve obtained from reference [48].

1100 EW Nafion® and 830 EW Aquivion® demonstrate similar stress/strain curves in both the elastic and plastic regions (low and high strains, respectively). This agrees with previously reported mechanical property results comparing these two polymers,[12,63] as well as the previous finding of similar crystallinity between recast 1100 EW Nafion® and cast 830 EW Aquivion® (see Section 3.3). The results suggest: (1) the difference in PFSA EW between Nafion® and Aquivion® has little effect on membrane mechanical properties (other than strain at break)[12] and (2) for these two polymers, the membrane mechanical properties are not a strong function of RH for 0<RH<20%.

The changes in mechanical properties with draw ratio for stretched/annealed Aquivion® films were examined for $1 \leq DR \leq 6$. The Young's modulus (slope of the

stress/strain curve at a strain <0.5%), the plastic modulus, the ultimate stress, and the strain at break were identified as described in Section 2.6. Four Aquivion® samples were tested at each draw ratio, and data presented in this section are the average of the repeated experiments. The variation in properties from repeated stress/strain experiments is expressed in terms of a standard deviation. Figure 29 shows representative Aquivion® stress/strain curves for unstretched/annealed and stretched/annealed films, while the membrane mechanical properties are listed in Table 10. The same mechanical properties for stretched Nafion® at various draw ratios (from reference [48]) are presented in Table 11 for comparison.

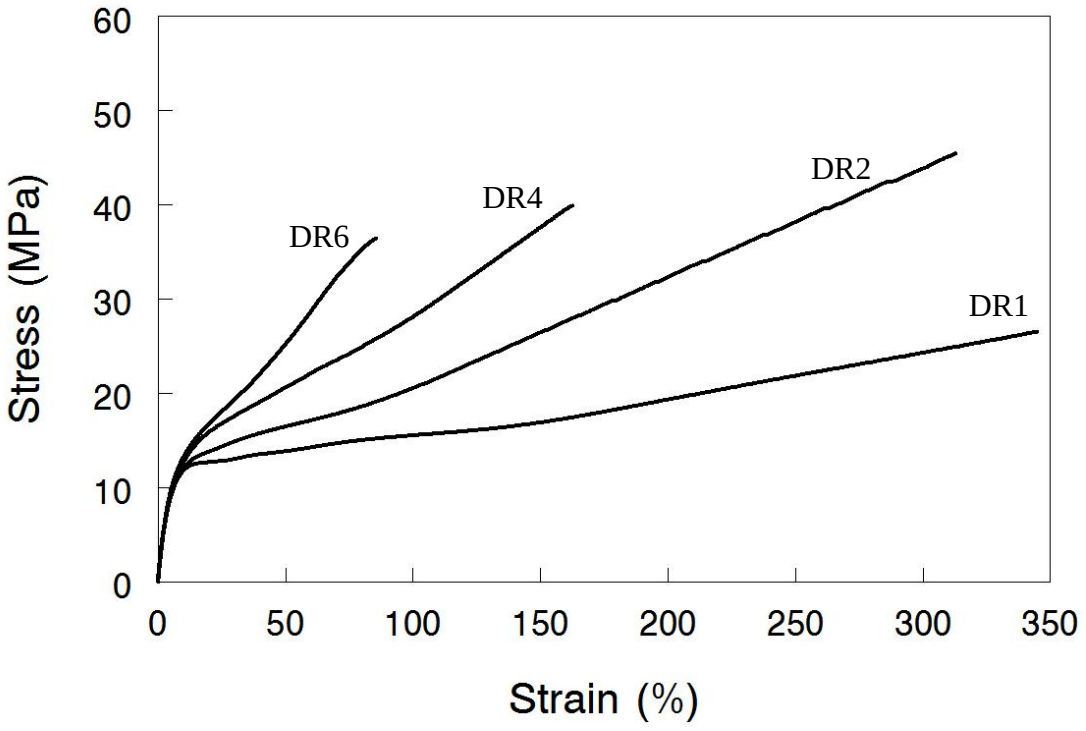

Figure 29: Stress/strain curves for unstretched/annealed and stretched/annealed Aquivion® membranes. Measurements were made at 30°C and 20% RH in the direction parallel to stretching.

Table 10: Mechanical properties of unstretched and stretched Aquivion® films at 30°C and 20% RH for different stretching draw ratios. All membranes were fully annealed at 190°C. The data are the average from four repeated experiments, and the errors depict the standard deviation.

	Young's Modulus (MPa)	***Plastic Modulus (MPa)***	***Ultimate Stress (MPa)***	***Strain at break (%)***
DR1	311 ± 71	5.15 ± 0.7	27 ± 1.8	330 ± 19
DR2	300 ± 31	13.5 ± 1.5	46 ± 6.2	285 ± 29
DR4	318 ± 61	25.8 ± 6.8	41 ± 3.7	148 ± 35
DR6	386 ± 14	36.3 ± 4.7	38 ± 9.6	80 ± 23

Table 11: Mechanical properties of unstretched annealed and pre-stretched annealed Nafion® films at 30°C and 0% RH [48].

	Young's Modulus (MPa)	***Plastic Modulus (MPa)***	***Ultimate Stress (MPa)***	***Strain at break (%)***
DR1	305	7.4	26	227
DR2	412	9.2	30	189
DR4	590	14.4	35	162
DR7	595	14.2	31	139

As expected, higher draw ratios resulted in an increase in Young's modulus; a trend that was also observed in stretched Nafion® (Young's modulus vs. DR for both polymers is shown in Figure 30). Stretching increases the degree of crystallinity in both polymers (see Section 3.3), and the resulting crystallites act as physical crosslinks. Although both unstretched Aquivion® and unstretched Nafion® exhibit a Young's modulus of ~300 MPa, the increase in this property induced by stretching Nafion® is significantly larger (35% vs. 95%). This finding was unexpected and is currently unexplained since the Aquivion® membranes showed a greater increase in crystallinity with draw ratio. The trends in Young's modulus, however, do reflect those of crystallinity

as the property improvement for stretched Nafion® levels off at DR4, while it continues to improve in stretched Aquivion® beyond DR4. This was attributed to the significantly lower change in crystallinity for Nafion® at high draw ratios (≥4) compared to Aquivion® (see Section 3.3). While a higher Young's modulus typically results in reduced membrane swelling, and therefore lower solvent uptake, this was not seen in either polymer for water sorption (see Section 3.4).[51] This may be explained by other morphological changes occurring during stretching, which can increase the water uptake such as changes in the width, connectivity, and/or alignment of the hydrophilic domains.[14,80] Currently, the exact reason why there is no correlation between Young's modulus and water uptake is unknown.

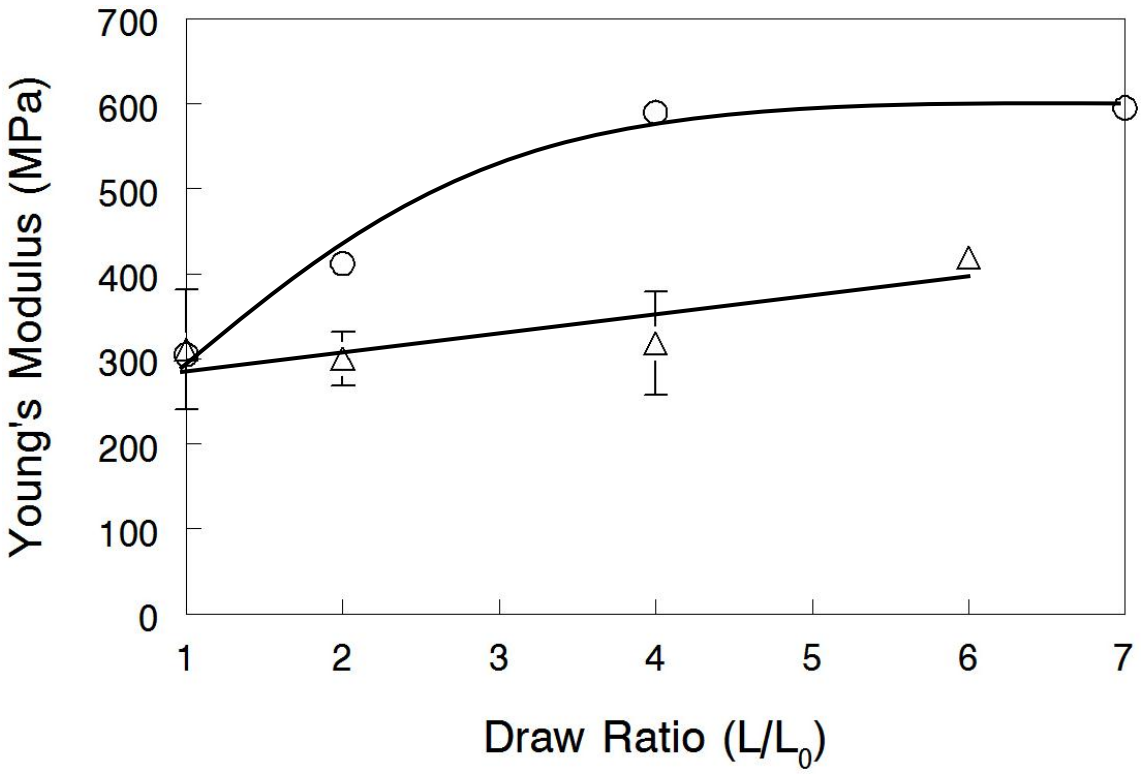

Figure 30: Young's modulus as a function of draw ratio for stretched Aquivion® (△) and stretched Nafion® (○) membranes. The stretched Nafion® values are reported by Lin et al. [48] Error bars show the standard deviation between repeated experiments.

The plastic modulus in both Nafion® and Aquivion® similarly shows an improvement in rigidity (resistance to physical deformation) following the increase in crystallinity, as a plateau is again present in Nafion® yet absent in Aquivion®. Figure 31 plots plastic modulus as a function of draw ratio for both polymers. The Aquivion® films show a more drastic increase in plastic modulus with DR compared to Nafion®. This is in contrast with the Young's modulus results which showed greater improvement for stretched Nafion®, but the result can be explained by the higher degree of crystallinity in the stretched Aquivion® films. Analyses on the remaining mechanical properties (ultimate stress and strain at break) result in similar conclusions. Figure 32 and Figure 33 show plots of ultimate stress and strain at break, respectively, as a function of draw ratio for both polymers. Although ultimate stress shows no trend with draw ratio, all stretched Aquivion® films exhibited a higher ultimate stress (thereby expressing enhanced strength) as compared to both unstretched Aquivion® and stretched Nafion®. Additionally, the Aquivion® samples show a greater loss in elasticity compared to Nafion® as the strain at break decreases with increasing draw ratio. This result can also be explained by the presence of more impliable crystalline regions.

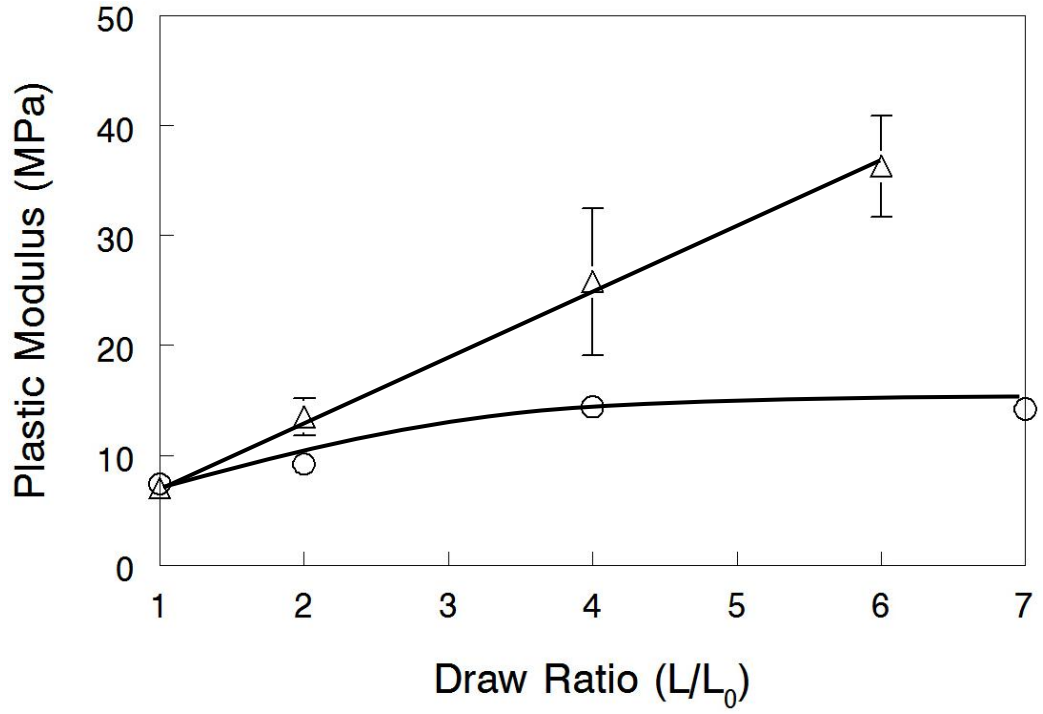

Figure 31: Plastic modulus as a function of draw ratio for stretched Aquivion® (△) and Nafion® (○) membranes. The stretched Nafion® values are reported by Lin et al. [48]

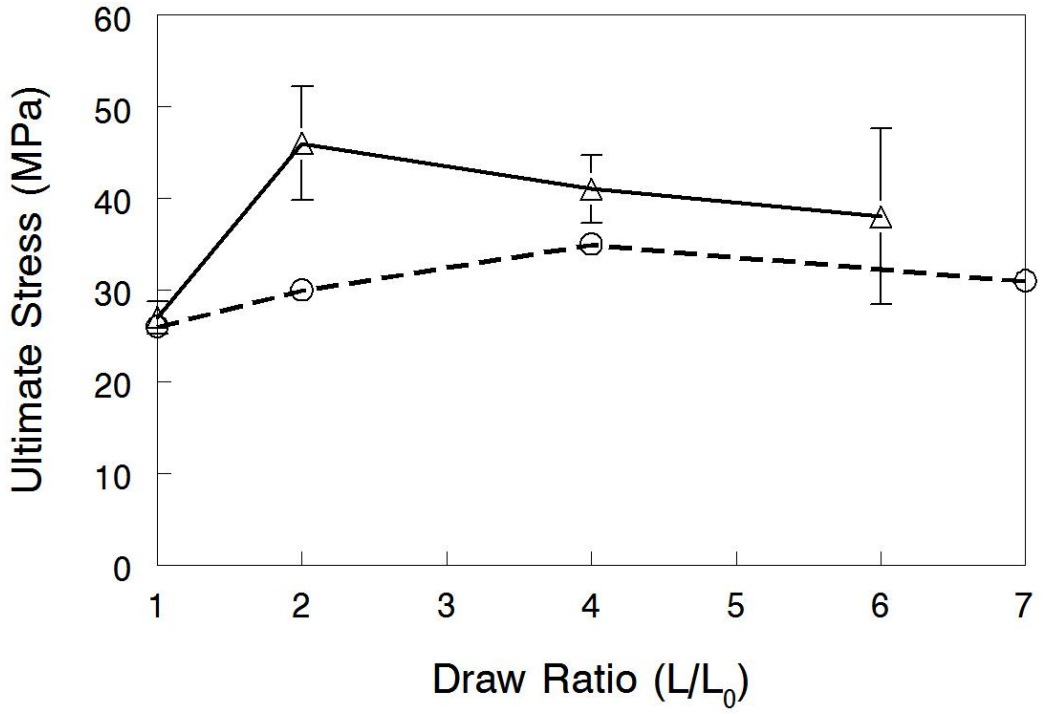

Figure 32: Ultimate stress as a function of DR for stretched Aquivion® (△) and stretched Nafion® (○)

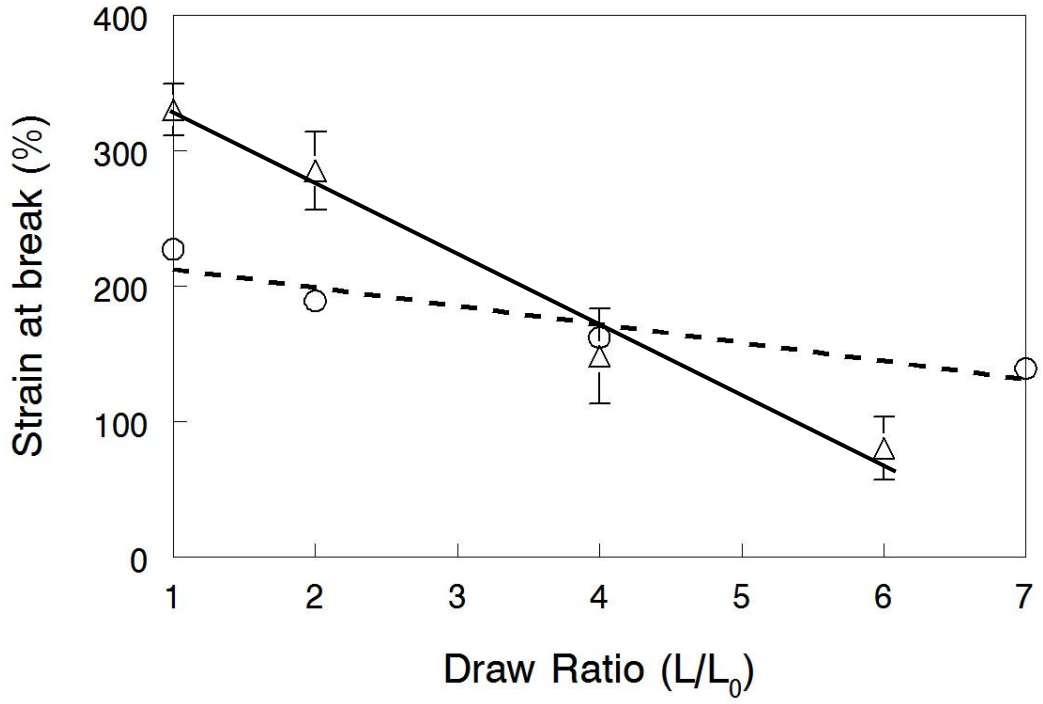

Figure 33: Strain at break as a function of DR for stretched Aquivion® (△) and stretched Nafion® (○).

Figure 34 shows a direct comparison between stress/strain curves for stretched Aquivion® and stretched Nafion® at an equivalent draw ratio (DR4). The results for higher DRs (DR6 Aquivion®, and DR7 Nafion®) are also shown. DR6 Aquivion® shows the continued change in mechanical properties for high DRs (>4) with this PFSA polymer, while stretched Nafion® shows essentially no change in stress/strain curves for DR>4 (other than a lower ultimate stress). The mechanical property analyses lead to two conclusions: 1) that both Nafion® and Aquivion® exhibit an increase in rigidity (resistance to physical deformation) and strength (the ability to withstand a greater load) with draw ratio in the stretching direction, and 2) Aquivion® films continue to exhibit changing mechanical properties at high draw ratios (≥4) while Nafion® mechanical properties level off at DR≥4. Whether these improvements in mechanical properties lead

to a more durable, longer lasting membrane in a fuel cell is yet to be determined, but should be investigated once the membranes are converted into a membrane-electrode-assembly.

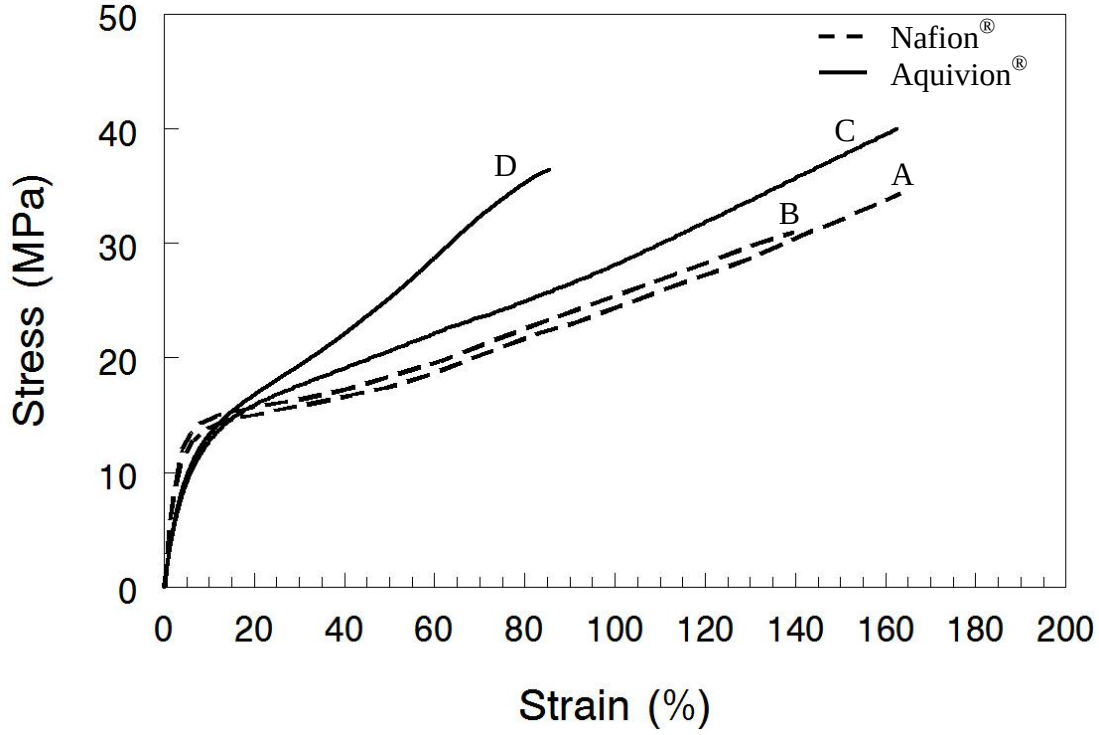

Figure 34: Stress/strain curves for stretched Nafion® (A=DR4; B=DR7) and stretched Aquivion® (C=DR4, D=DR6). Nafion® data obtained from [48].

3.6 Proton Conductivity

The proton conductivity of an ionomer is a function of the coupled effects of equivalent weight (due to the concentration of charged side-groups) and subsequent water uptake.[8] Due to a lower EW, 830 EW Aquivion® films absorb more water than Nafion® 117 and exhibit higher proton conductivity.[14,16,17,62,63] Figure 35 displays the proton conductivity for 800 EW Dow Ionomer (a polymer of identical chemical structure to

Aquivion®) and Nafion® 117 as a function of the membrane hydration (λ).[79] Equilibrium water vapor uptake measurements shown in Section 3.4 proved equal λ between the two polymers at all tested relative humidities. Therefore, due to the higher ion exchange capacity (IEC), 830 EW Aquivion® has a higher proton conductivity than Nafion® 117 under any given state of hydration.

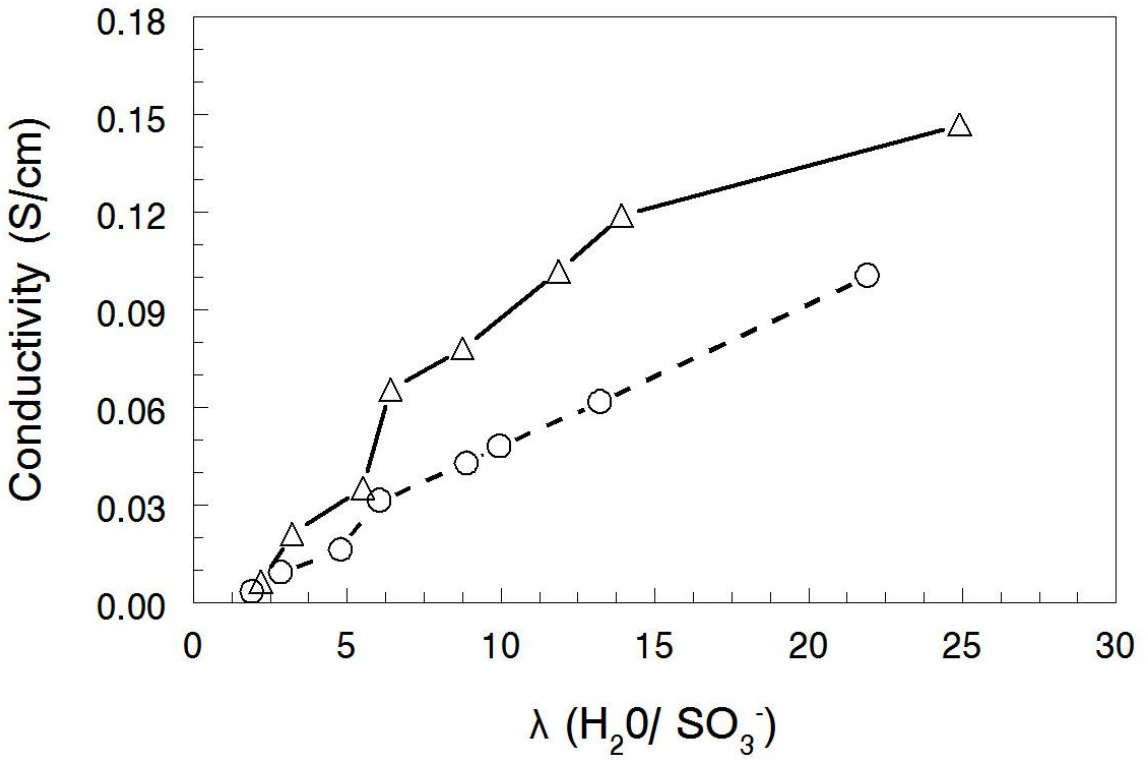

Figure 35: Conductivity as a function of water uptake (λ) at 30°C for 800 EW Dow Ionomer (△) (a polymer of identical chemical structure to Aquivion®) and 1100 EW Nafion® (○). Plot taken from [79].

In the present study, in-plane proton conductivity was measured on water-equilibrated unstretched and stretched Aquivion® films to determine the effect of uniaxial stretching on H^+ movement in the polymer under the influence of a voltage gradient

during current flow (a representative Nyquist plot at each Aquivion® draw ratio is shown in Appendix C). Figure 36 shows the effect of uniaxial stretching on in-plane proton conductivity (at 25°C in water) for Aquivion® and Nafion®[46] films in the stretched direction. Each Aquivion® data point is an average of four repeated experiments. For comparison, the proton conductivity of commercial Nafion® 117 under identical conditions was 0.090 ± 0.004 S/cm as determined in the present work.

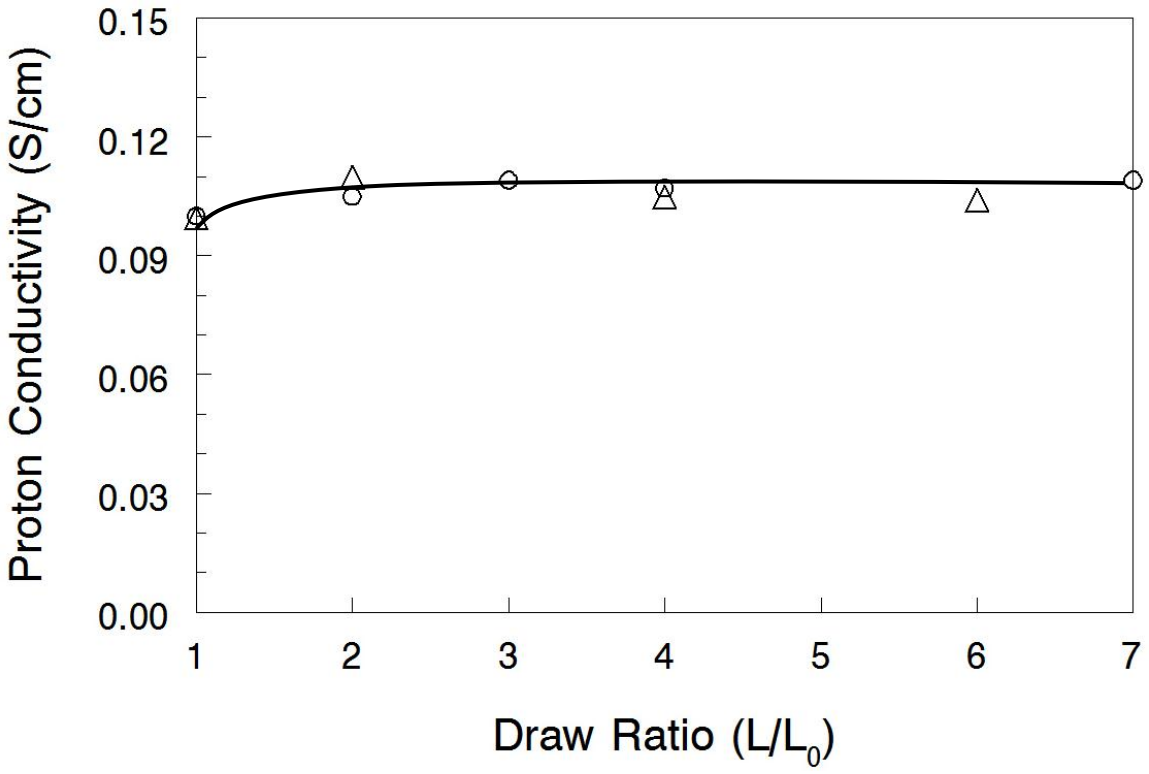

Figure 36: In-plane proton conductivity (in water at 25°C) as a function of draw ratio in Aquivion® (△) and Nafion® (○) films.

The in-plane proton conductivity for the DR1 Aquivion® membrane was 0.100 S/cm, which is consistent with similar EW commercial Aquivion® films (~1.1 S/cm for

790 EW in water at 25°C).[18,63] As expected, the Aquivion® proton conductivity was higher than that of commercial Nafion® 117 (as tested in the present work) due to its lower EW. However, the reported conductivity for unstretched recast Nafion®, which Lin reports as identical to that of Nafion® 117, was approximately equal to Aquivion®. This inconsistency was therefore attributed to differences in the experimenter and testing apparatus. There was a modest increase in proton conductivity for both Nafion® and Aquivion® after stretching, but conductivity was independent of draw ratio above DR2 (a conductivity of 0.107 S/cm at DR ≥2). Previously shown water uptake measurements (see Section 3.4) concluded that stretching did not change the amount of absorbed water in Aquivion® and a similar result was reported for stretched Nafion® by Lin.[49] The increase in proton conductivity along the stretched direction of Nafion® has been attributed by Park [55] and Li [61] to the greater alignment of the hydrophilic channels which enhance the proton transport. Therefore it is reasonable to assume a similar conclusion in stretched Aquivion® due to the comparable chemical structure.

In a fuel cell, protons permeate across the membrane in the through-plane direction. Through-plane conductivity measurements however were not taken as they are time intensive, prone to significant experimental errors, and require expensive equipment compared to in-plane conductivity tests.[84] Additionally, through-plane conductivity measurements taken on stretched Nafion® showed no change with stretching and were equal to the in-plane measurements.[47,48] Therefore, through-plane and in-plane proton conductivity were assumed to be comparable to one another in stretched Aquivion®. The validity of this assumption will be determined once the through-plane proton conductivity of stretched Aquivion® films can be measured in a membrane electrode assembly.

3.7 Methanol Permeability

Methanol permeability tests were carried out on stretched Aquivion® films to determine whether uniaxial stretching decreased the methanol permeability as was the case for stretched Nafion®. Figure 37 is a plot of the methanol permeability for stretched Aquivion® films at 25°C and 60°C with 1.0 M methanol. Each data point is an average of two repeated experiments. The methanol permeability of commercial Nafion® 117 under identical conditions was $2.4*10^{-6}$ cm^2/s at 25°C and $4.63*10^{-6}$ cm^2/s at 60°C (both were determined in the present work).

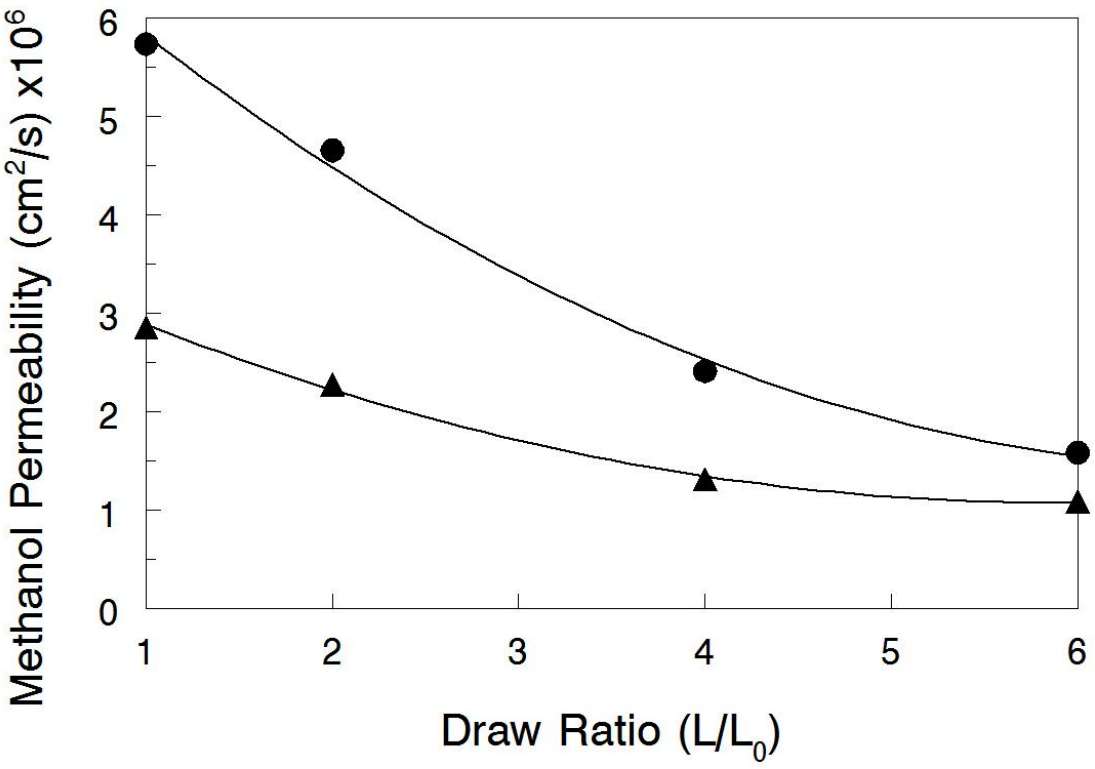

Figure 37: Effect of draw ratio on methanol permeability in Aquivion® membranes at 25°C (▲) and 60°C (●) with 1.0 M methanol. The data points are the average of two experimental measurements and the measured permeability between repeated measurements differed by less than 5%.

The methanol permeability results confirm an expected decrease in permeability with increasing draw ratio. Unstretched Aquivion® exhibits a slightly higher methanol permeability than Nafion® 117 due to an increase in solvent swelling caused by its higher IEC. Equilibrium water vapor uptake measurements shown in Section 3.4 led to the same conclusion of greater solvent uptake in 830 EW Aquivion®, as compared to 1100 EW Nafion®. As opposed to water uptake however, stretching causes a substantial reduction in methanol permeability with draw ratio. The ability to decrease the methanol permeability without lowering the water uptake is unique to the stretching technique and is discussed later in this section. Compared to DR1, a DR6 stretched Aquivion® membrane shows significant reduction in methanol permeability at both 25°C and 60ºC respectively. These trends resemble the previously reported drop in methanol permeability for stretched Nafion® films.[46-49] Figure 38 displays the methanol permeability at 60°C with 1 M methanol for stretched Aquivion® and stretched Nafion®[46] as a function of draw ratio. Figure 39 is a plot of the relative methanol permeability (permeability/permeability of DR1) for each polymer under the same conditions as Figure 38.

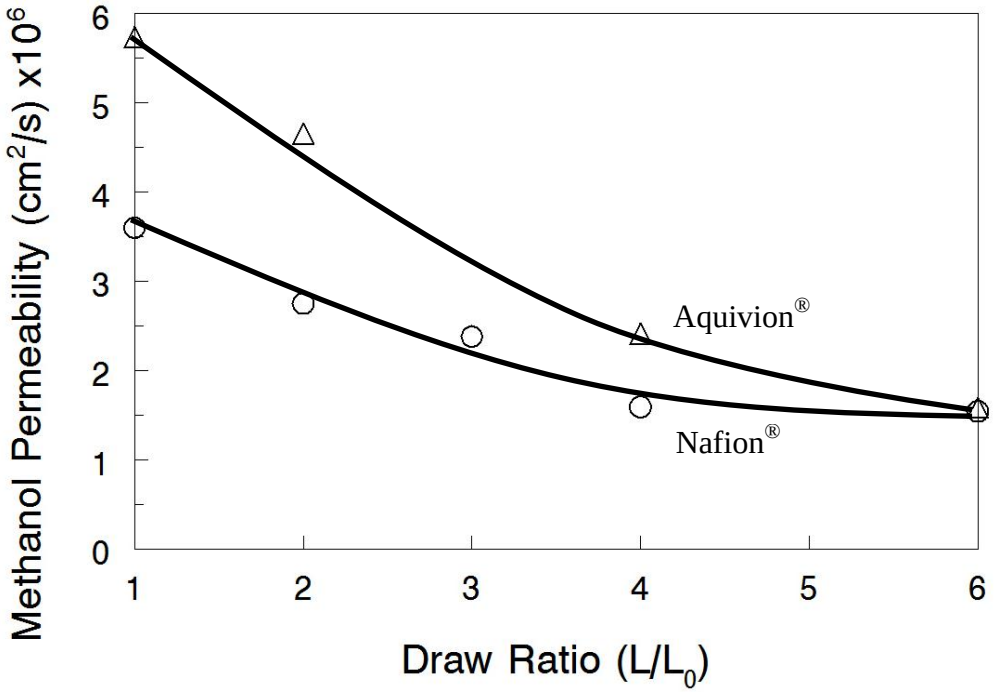

Figure 38: Methanol permeability at 60°C with 1.0 M methanol for stretched Aquivion® (△) and stretched Nafion® (○) films. Nafion® data obtained from reference [47].

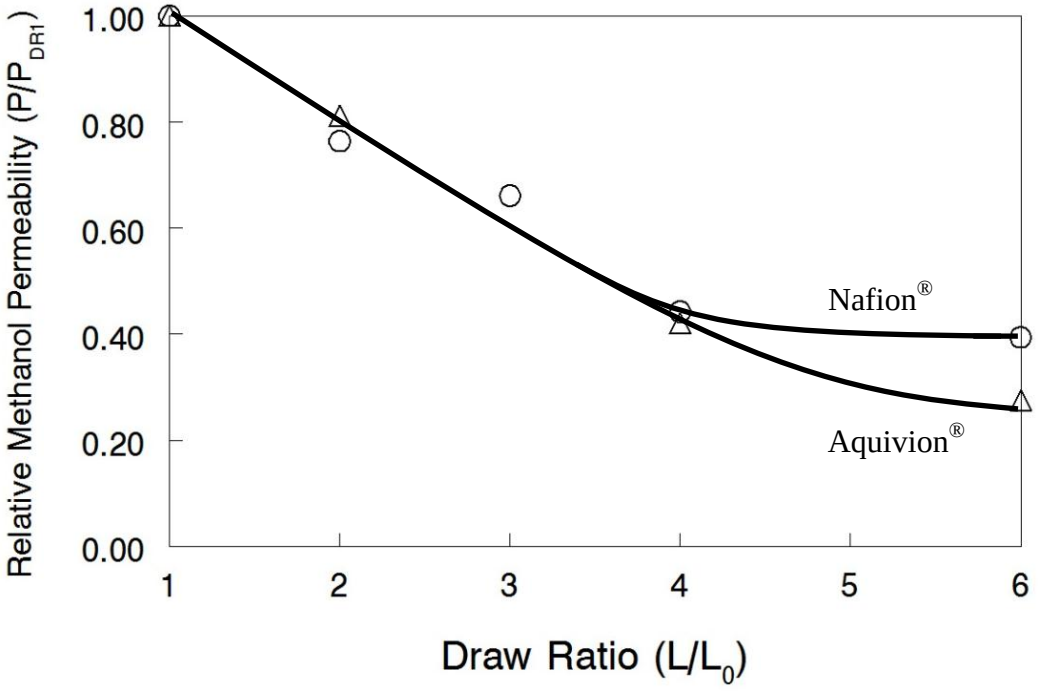

Figure 39: Relative methanol permeability (permeability/permeability at DR1) as a function of draw ratio for Aquivion® (△) and Nafion® (○) membranes. Permeability was measured at 60ºC with 1.0 M methanol. Nafion® data obtained from reference [47].

Aquivion® exhibits a higher methanol permeability than Nafion® at all draw ratios until DR6. At this point, the permeability of stretched Aquivion® becomes equal to stretched Nafion® as the greater reduction in permeability caused by stretching nullifies the effect of the lower EW and greater solvent swelling. The relative decrease in permeability for both Nafion® and Aquivion® with stretching is the same up to a draw ratio of 4 (see Figure 39). Aquivion® however shows a reduction at DR6 that appears to continue declining, while the Nafion® permeability remains constant for DR >4. This is similar to the crystallinity and mechanical property data which showed greater property differences between the two stretched polymers at higher draw ratios. Crystallinity is not the only factor that controls methanol permeability (much like the water uptake detailed in Section 3.4) as Aquivion® has a higher crystallinity at all draw ratios. However, the greater increase in crystallinity for Aquivion® may lower the methanol permeability by generating more tortuous diffusional pathways, creating a larger number of dead end pathways, and/or restricting the width of the hydrophilic domains.[8,11,30,31] These are properties of the membrane microstructure that have been demonstrated previously to successfully reduce methanol permeability.

Previous work has investigated the cause of the reduced methanol permeability in Nafion® upon uniaxial stretching. Lin et al. reported a decrease of the methanol solubility in the polymer with draw ratio (shown in Figure 40).[46,49] This was explained by a reduction in the freezable water content within the membrane (water that interacts weakly or not at all with the sulfonic acid side groups), which appeared coupled to the decline in methanol permeability. The total water content, however, stayed relatively constant since the amount of nonfreezable water increased (water that is strongly bound to the ionic

groups of the polymer). This change in ratio between freezable and nonfreezable water was theorized to give the stretching technique the unique ability to decrease the methanol permeability without lowering water uptake since the sulfonic acid groups preferentially bound with water. Water content (total, freezable, and nonfreezable) as a function of draw ratio in stretched Nafion® films is plotted in Figure 41 as reported by Lin.[49] Additionally, Park[55] and Li[61] reported an increasing degree of anisotropic transport at higher draw ratios in stretched Nafion®. Transport in the plane perpendicular to the stretched direction was slowed, while transport increased in the stretched direction (shown in Figure 42).[55] The diffusional pathways were thought to become more tortuous in the through-plane direction as the hydrophilic pathways were directionally oriented in the stretched direction (as described in Section 1.5). Since Aquivion® and Nafion® have similar chemical structures, it is reasonable to assume similar effects in stretched Aquivion® films. Further investigation is required however to determine the exact cause behind the greater reduction in methanol permeability for Aquivion® compared to Nafion®.

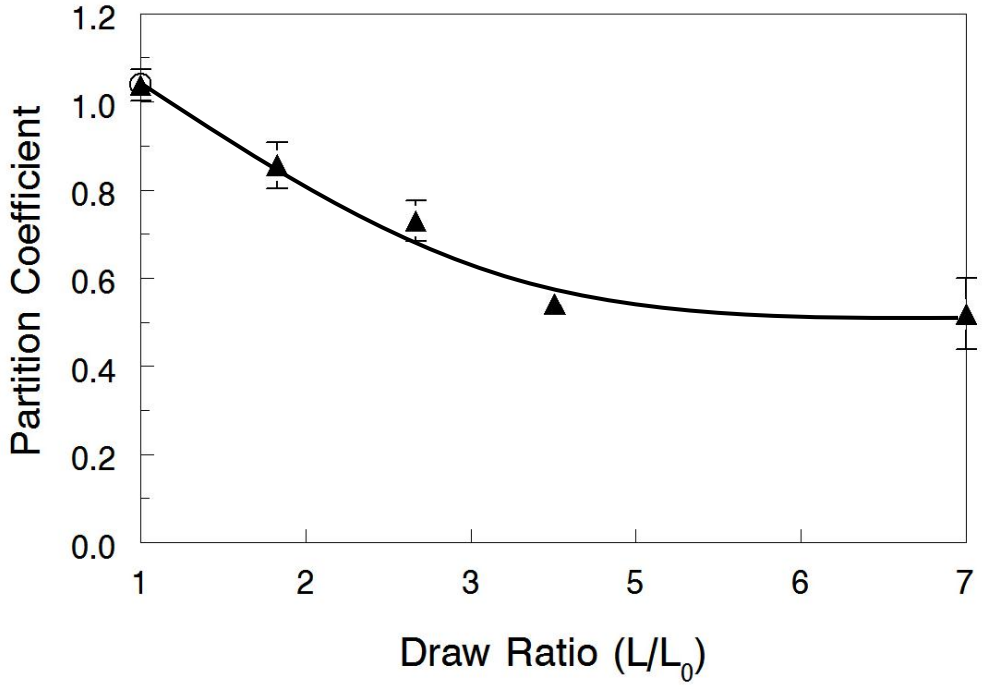

Figure 40: Methanol partition coefficient (methanol in polymer/methanol in solution) as a function of draw ratio for stretched Nafion® films (▲), and commercial Nafion® (○). Data from reference [46].

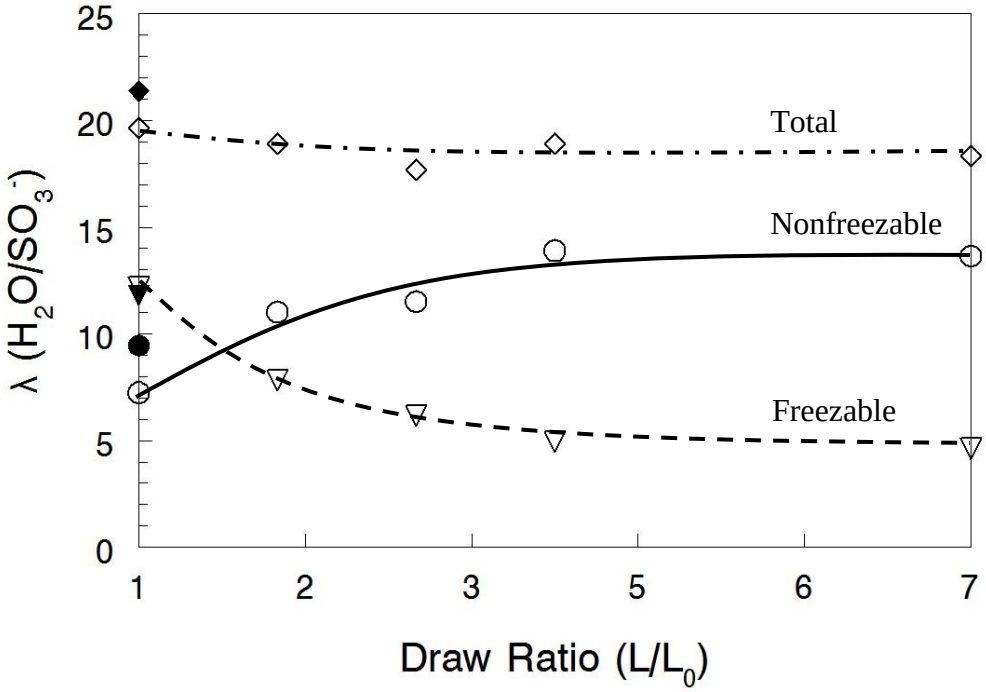

Figure 41: Total (◆), freezable (▼), and nonfreezable (●) water content in Nafion® 117 (closed symbols) and recast Nafion (open symbols) at various draw ratios. Data from reference [49].

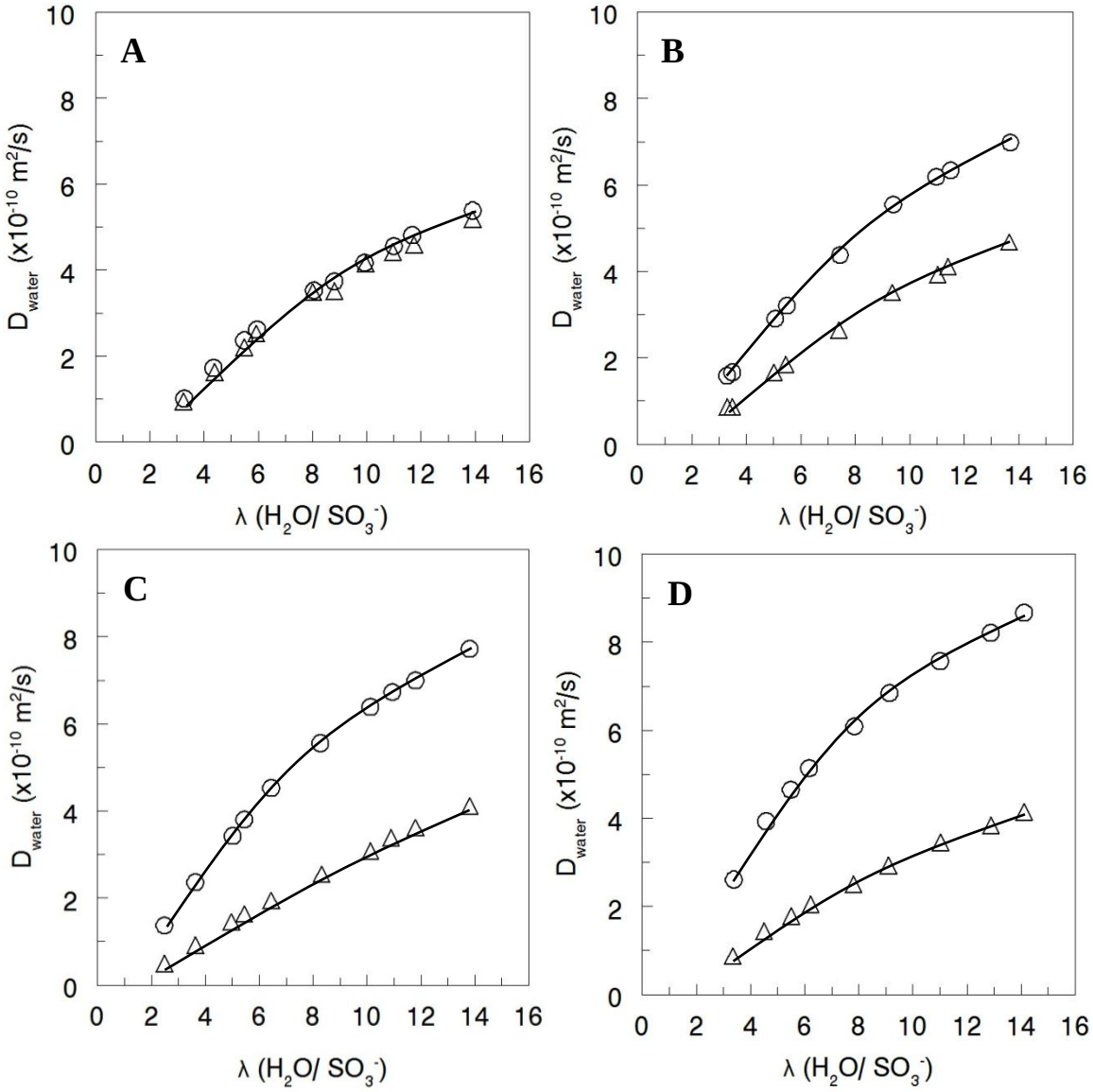

Figure 42: Water diffusion coefficient (D_{water}) in the stretched direction (○) and through-plane direction (△) as a function of water content (λ) in stretched Nafion® (A=DR1; B=DR2; C=DR3; D=DR4). Data from reference [55].

3.8 Relative Selectivity in Stretched Aquivion® and Stretched Nafion®

The selectivity (the ratio of proton conductivity and methanol permeability) of commercial Nafion® 117 is a widely used benchmark in comparing direct methanol fuel

cell (DMFC) membranes. Therefore, the selectivity of stretched Nafion® and stretched Aquivion® membranes were related to that of commercial Nafion® 117 to determine their relative selectivities (defined as the selectivity of a given membrane divided by the selectivity of Nafion® 117). The values of conductivity (in water at 25°C), methanol permeability (at 60ºC, measured with 1 M methanol), and relative selectivity for stretched Aquivion®, stretched Nafion®, and commercial Nafion® 117 are listed in Table 12

.

Table 12: Tabulated data used in the calculation of the relative selectivities (selectivity of stretched membrane/selectivity of commercial Nafion® 117) at different draw ratios. Values for stretched Nafion® were collected from [47].

		Cond @ 25°C (S/cm)	Perm @ 60°C (cm2/s)	Relative Selectivity
	Nafion 117*	0.100	3.60 e-06	1
	Nafion 117**	0.090	4.63 e-06	1
Stretched Nafion®*	**DR1**	0.100	3.60 e-06	0.95
	DR2	0.105	2.75 e-06	1.31
	DR3	0.109	2.38 e-06	1.57
	DR4	0.107	1.59 e-06	2.31
	DR7	0.109	1.42 e-06	2.63
Stretched Aquivion®**	**DR1**	0.100	5.74 e-06	0.90
	DR2	0.110	4.66 e-06	1.21
	DR4	0.105	2.41 e-06	2.24
	DR6	0.104	1.58 e-06	3.38

* Data in Lin et al. [47]
** Data collected in the present study

Upon membrane elongation, the observed decrease in methanol permeability without an accompanying drop in proton conductivity leads to an increase in relative selectivity for both Aquivion® and Nafion®. The relative selectivity for stretched Aquivion® and stretched Nafion® is plotted against membrane draw ratio in Figure 43. The relative selectivity for the stretched polymers is essentially identical for DR <4. At high DR (>4) however, Aquivion® demonstrates a higher selectivity due to the larger reduction in methanol permeability (see Section 3.6 for in-depth methanol permeability discussion).

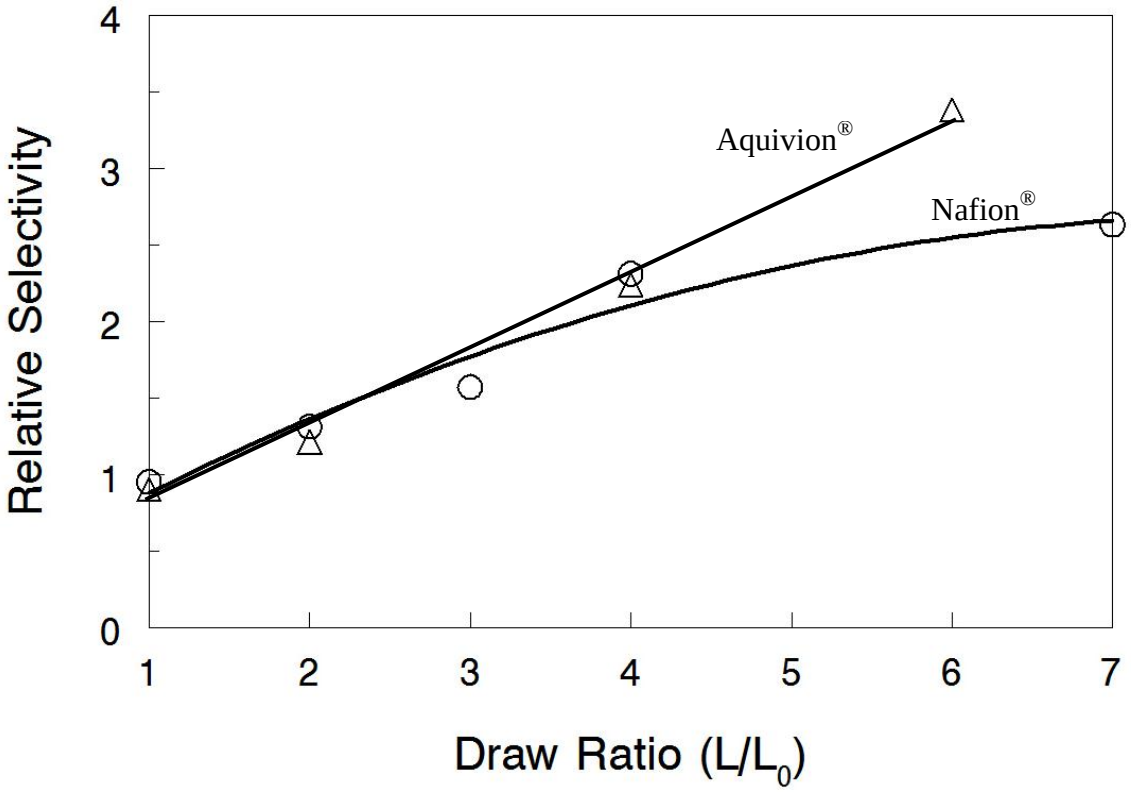

Figure 43: The relative selectivity (selectivity of membrane divided by selectivity of Nafion® 117) for stretched Aquivion® (△), and stretched Nafion® (○) as a function of draw ratio. The stretched Nafion® values are reported in [47].

Although the gain in relative selectivity is smaller than that seen in SPEEK, blended Teflon®/Nafion®, and some other membranes referenced in Section 1.4, the improvement comes without the unwanted cost of increased proton transfer resistance. Therefore, the compromise between decreased methanol crossover and increased proton transfer resistance, which limits many DMFC membranes, is not an issue for stretched Aquivion®. Lin et al. previously demonstrated the value of stretched membranes by setting a benchmark for high performance direct methanol fuel cell testing with stretched Nafion® (DMFC test results are detailed in Section 1.6).[46-49] The improvement in relative selectivity of DR6 Aquivion® over stretched Nafion® (~30% improvement) suggests that the stretched Aquivion® membranes will perform well in a DMFC. Such experiments were not performed in the present study.

CHAPTER 4

CONCLUSIONS

Uniaxial stretching of recast 1100 EW Nafion® was described in a series of papers by Lin et al.[46-49] In the present study, the method was adapted for use on 830 EW Aquivion® (a short side chain PFSA). Stretched Aquivion® membranes exhibited increased crystallinity with draw ratio (DR), up to 38% crystallinity at DR6. The increased crystallinity and polymer chain orientation led to substantial improvements in key direct methanol fuel cell membrane properties: better mechanical strength and a lower methanol permeability, without a loss in proton conductivity. Stretching caused the in-plane proton conductivity to increase slightly (7% to 0.107 S/cm in water @ 25°C), while reducing the methanol permeability substantially (72% in a DR6 film at 60°C and 1 M methanol), as compared to unstretched Aquivion®. The conductivity improvement seen in stretched Aquivion® and Nafion® polymers was similar, but stretching caused a larger reduction in methanol permeability for Aquivion® at higher values of DR which resulted in a 30% improvement in relative selectivity (2.6 for DR4 Nafion® vs. 3.4 for DR6 Aquivion®). Although no direct methanol fuel cell tests were performed during this study, the measured membrane properties appear well suited for use in direct methanol fuel cells. The Aquivion® stretching results presented in this work are encouraging. The use of stretched Aquivion® in a direct methanol fuel cell may yield high power outputs, as compared to commercial Nafion® films and pre-stretched recast Nafion® membranes.

CHAPTER 5

SUGGESTIONS FOR FUTURE WORK

i. Whether the membrane properties (crystallinity, methanol permeability reduction, mechanical moduli, etc.) reach a maximum with draw ratio in Aquivion® has not been determined. Aquivion® membranes appear to continue improving beyond DR6, but this was not investigated in the present work. A study on higher DR Aquivion® membranes (>6) may reveal further improved membrane properties.

ii. Study the operational temperature effect on the methanol permeability reduction. The methanol permeability reduction is greater at 60ºC than 25ºC in the present work. A higher glass transition temperature and added crystallinity may help the Aquivion® performance compared to Nafion® 117 at the desired high operation temperatures (>80°C). More testing temperatures are required however before reaching any definitive conclusion.

iii. Determine the methanol concentration effect on the methanol permeability of stretched Aquivion® membranes. A higher methanol concentration in the fuel provides greater energy density, but increases methanol crossover. No concentration other than 1.0 M methanol was utilized throughout this work.

iv. Lin et al. theorized that a reduction in free water (water not bound to the sulfonate ions) causes the decrease in methanol permeability.[49] A study on the bound/unbound water in stretched Aquivion® films may help explain the greater permeability reduction in Aquivion® compared to Nafion®.

v. Determine the lifetime for the stretched Aquivion® films. The stretched Aquivion® films showed no retraction after boiling in 1 M H_2SO_4, boiling in water, or exposure to 1 M methanol at 60°C. However, stretching/annealing simultaneously may affect the long term rate at which the films relax.

vi. Place the DR6 Aquivion® membranes into an MEA and test whether the membranes improve the DMFC power output over commercial Nafion® 117 and pre-stretched recast Nafion®. The membranes will have to be stacked to determine an optimal ionomer thickness.

vii. Place the DR6 Aquivion® membranes into a hydrogen fuel cell. The added mechanical strength and organization of the proton conducting channels induced by stretching may improve the fuel cell power output compared to Nafion® 117.

APPENDIX A

CHECKING THE CONSISTENCY BETWEEN DIFFERENT BATCHES OF COMMERCIAL AQUIVION® D83-10E

Two commercial D83-10E Aquivion® dispersions were used throughout the present work to cast membranes. Methanol permeability and proton conductivity tests were run on annealed solution cast films to examine any property differences between the polymer dispersions. Table A.1 displays the measured membrane properties. The error is reported as the standard deviation between repeated experiments. The tests concluded that the dispersions created membranes with identical properties.

Table A.1: Properties of membranes cast from different batches of D83-10E Aquivion® dispersion from Solvay Solexis.

	1st Polymer dispersion	*2nd Polymer dispersion*
Methanol Permeability (cm^2/s)	2.84 ± 0.24	2.83 ± 0.14
Proton Conductivity (S/cm)	0.105 ± 0.009	0.104 ± 0.003

APPENDIX B

IN-DEPTH WALKTHROUGH OF THE DECONVOLUTION AND INTEGRATION OF WAXD SPECTRA IN EXCEL®

The crystallinity was calculated from WAXD spectra in this work by using the Pearson VII distribution function for the deconvolution, and the trapezoidal rule for the integration. Table B.1 displays the abbreviations that are used throughout this section.

Table B.1: List of abbreviations used during the discussion of the WAXD deconvolution and integration.

Abbreviation	***Meaning***
X	2θ from data (independent variable)
Y	Intensity from data
HL	Height of left peak
CL	Center of left peak
WL	Full width at half maximum of left peak
EL	Exponent of left peak
HR	Height of right peak
CR	Center of right peak
WR	Full width at half maximum of right peak
ER	Exponent of right peak
PearL	Calculated intensity of left Pearson peak
PearR	Calculated intensity of right Pearson peak
R	Residual
N	Index of data point
N	Total number of data points
SSR	Sum of squared residuals

The data was loaded into Excel®, and then deconvoluted into two separate peaks using Pearson VII distribution functions:[66] Equation B.1=left (amorphous), and Equation B.2=right (crystalline). The solver function in Excel® was used to find the minimum SSR (Equation B.5) by varying HL, CL, WL, EL, HR, CR, WR, and ER.

$$\text{PearL}(X) = \frac{HL}{\left[1+4\left(\frac{X-CL}{WL}\right)^2\left(2^{1/EL}-1\right)\right]^{EL}} \quad \text{[B.1]}$$

$$\text{PearR}(X) = \frac{HL}{\left[1+4\left(\frac{X-CL}{WL}\right)^2\left(2^{1/EL}-1\right)\right]^{EL}} \quad \text{[B.2]}$$

$$\text{Combined intensity}(X) = \text{PearL}(X) + \text{PearR}(X) \quad \text{[B.3]}$$

$$R^2(X) = \text{Combined intensity}(X) - Y(X) \quad \text{[B.4]}$$

$$\text{SSR} = \sum_{n=1}^{n=N} R^2(X_n) \quad \text{[B.5]}$$

After deconvolution, the fit functions were integrated using the trapezoidal rule for each peak (Equation B.6 and Equation B.7). Finally, the crystallinity was calculated by calculating the ratio between the area of the right (crystalline) peak to the total integrated area of both peaks.

$$\text{Area of left peak} = \sum_{n=1}^{n=N-1} \frac{PearL(X_n)+PearL(X_{n+1})}{X_{n+1}-X_n} \quad \text{[B.6]}$$

$$\text{Area of right peak} = \sum_{n=1}^{n=N-1} \frac{PearR(X_n)+PearR(X_{n+1})}{X_{n+1}-X_n} \quad \text{[B.7]}$$

$$\%\ \text{Crystallinity} = \frac{Area\ of\ right\ peak}{Area\ of\ left\ peak + Area\ of\ right\ peak} \times 100\% \quad \text{[B.8]}$$

APPENDIX C

REPRESENTATIVE NYQUIST PLOT FOR AQUIVION® AT EACH DRAW RATIO (DR1, DR2, DR4, DR6)

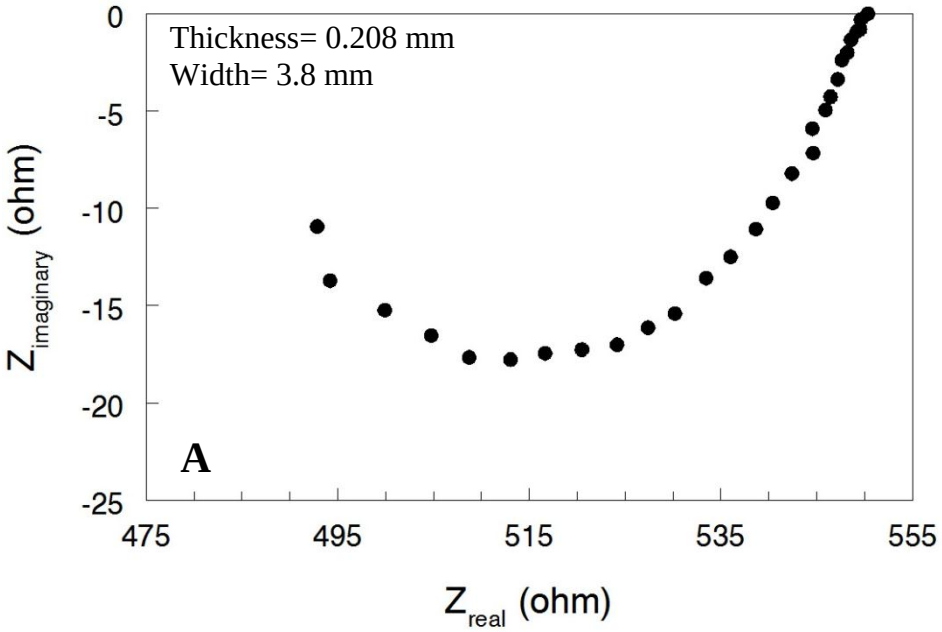

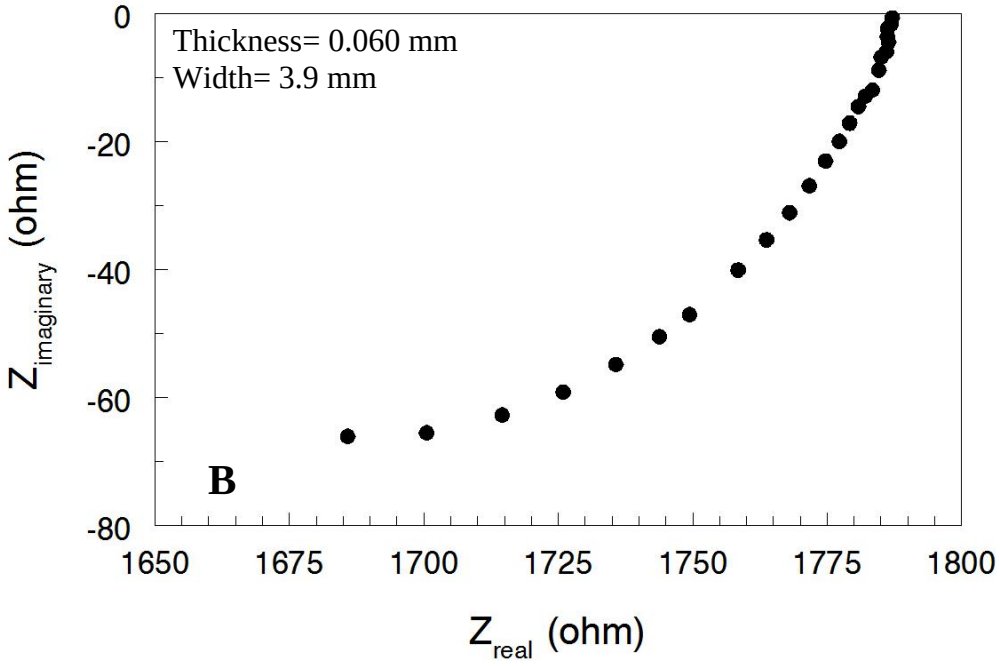

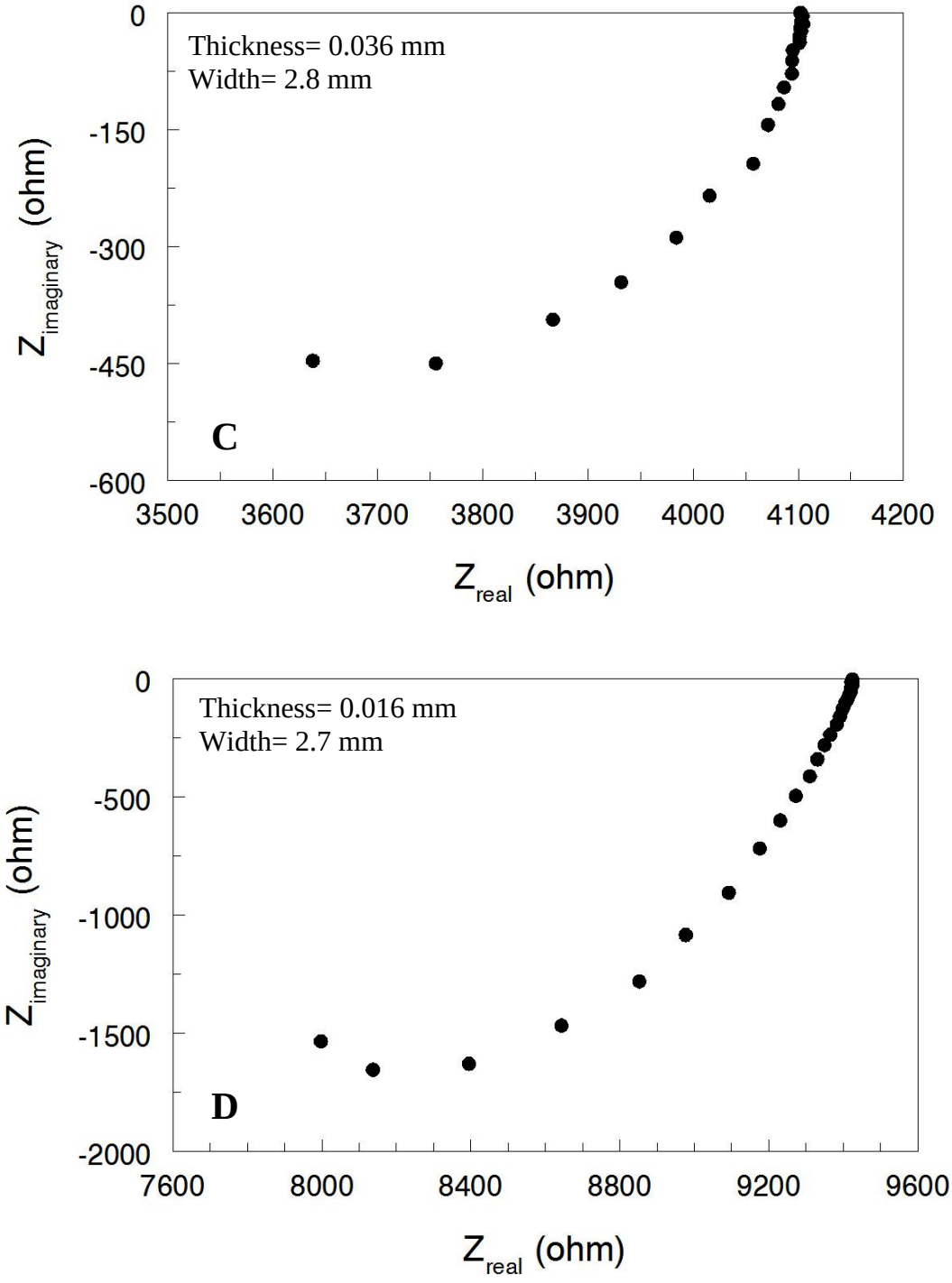

Figure C.1: Representative Nyquist plots for Aquivion® at each draw ratio (A=DR1, B=DR2, C=DR4, D=DR6) which were used to calculate the membrane proton conductivity with Equation 1. The wet membrane cross-sectional dimensions for each sample are displayed on their respective plot, and the distance between electrodes (L in Equation 1) for all samples was 44 mm.

REFERENCES

[1] International Energy Agency, "World Energy Outlook," 2011.

[2] Exxon Mobil, "The Outlook for Energy: A View to 2040," 2012. [Online]. Available: http://www.exxonmobil.com. [Accessed 31 January 2012].

[3] U.S. Energy Information Administration, "International Energy Outlook 2011," 2011.

[4] S. Zaidi and M. Rauf, "Fuel Cell Fundamentals," in *Polymer Membranes for Fuel Cells*, S. Zaidi and T. Matsuura, Eds., 2009, pp. 1-5.

[5] N. Brandon and D. Thompsett, Fuel Cells Compendium, 2005.

[6] International Partnership for Hydrogen and Fuel Cells In the Economy, "2010 Hydrogen and Fuel Cell Global Commercialization & Development Update," 2010.

[7] A. Ismail, R. Naim and N. Zubir, "Fuel Cell Technology Review," in *Polymer Membranes for Fuel Cells*, S. Zaidi and T. Matsuura, Eds., 2009, pp. 27-49.

[8] P. Kundu, V. Sharma and Y. Shul, "Composites of Proton Conducting Polymer Electrolyte Membrane in Direct Methanol Fuel Cells," *Critical Reviews in Solid State and Materials Sciences,* vol. 32, no. 1, pp. 51-66, 2007.

[9] U.S. Department of Energy: Energy Efficiency and Renewable Energy, "Comparison of Fuel Cell Technologies," February 2011. [Online]. Available: http://www1.eere.energy.gov/hydrogenandfuelcells/fuelcells/pdfs/fc_comparison_chart.pdf. [Accessed March 2012].

[10] S. Zaidi, "Research Trends in Polymer Electrolyte Membranes for PEMFC," in *Polymer Membranes for Fuel Cells*, S. Zaidi and T. Matsuura, Eds., 2009, pp. 7-25.

[11] K. Kreuer, "On the development of proton conducting polymer membranes for hydrogen and methanol fuel cells," *Journal of Membrane Science,* vol. 185, pp. 29-39, 2001.

[12] M. Tant, K. Darst, K. Lee and C. Martine, "Structure and Properties of Short-Side-Chain Perfluorosulfonate Ionomers," in *Multiphase Polymers: Blends and Ionomers*, L. Utracki and R. Weiss, Eds., 1989, pp. 370-400.

[13] V. Arcella, A. Ghielmi and L. Merlo, "Membrane electrode assemblies based on perfluorosulfonic ionomers for an evolving fuel cell technology," *Desalination,* vol. 199, pp. 6-8, 2006.

[14] K. Kreuer, M. Schuster, B. Obliers, O. Diat, U. Traub, A. Fuchs, U. Kock, S. Paddison and J. Maier, "Short-side-chain proton conducting perfluorosulfonic acid ionomers: Why they perform better in PEM fuel cells," *Journal of Power Sources,* vol. 178, pp. 499-509, 2008.

[15] D. Lee, T. Saito, A. J. Benesi, M. A. Hickner and H. R. Allcock, "Characterization of Water in Proton-Conducting Membranes by Deuterium NMR T1 Relaxation," *The Journal of Physical Chemistry,* vol. 115, pp. 776-783, 2011.

[16] V. Arcella, A. Ghielmi and G. Tommasi, "High Performance Perfluoropolymer Films and Membranes," *Annals of the New York Academy of Sciences,* vol. 984, no. 1, pp. 226-244, 2003.

[17] V. Arcella, C. Troglia and A. Ghielmi, "Hyflon Ion Membranes for Fuel Cells," *Industrial & Engineering Chemistry Research,* vol. 44, no. 20, pp. 7646-7651, 2005.

[18] A. S. Arico, A. D. Blasi, G. Brunaccini and e. al, "High Temperature Operation of a Solid Polymer Electrolyte Fuel Cell Stack Based on a New Ionomer Membrane," *Fuel Cells,* vol. 10, no. 6, pp. 1013-1023, 2010.

[19] A. Arico, V. Baglio, A. Blasi, V. Antonucci, L. Cirillo, A. Ghielmi and V. Arcella, "Proton exchange membranes based on the short-side-shain perfluorinated ionomer for high temperature direct methanol fuel cells," *Desalination,* vol. 199, pp. 271-273, 2006.

[20] A. Stassi, I. Gatto, E. Passalacqua and e. al., "Performance Comparison of Long and Short-Side Chain Perfluorosulfonic Membranes for High Temperature Polymer Electrolyte Membrane Fuel Cell Operation," *Journal of Power Sources,* 2011.

[21] L. Li, J. Zhang and Y. Wang, "Sulfonated poly(ether ether ketone) membranes for direct methanol fuel cell," *Journal of Membrane Science,* vol. 226, pp. 159-167, 2003.

[22] Y. Woo, S. Y. Oh, Y. S. Kang and B. Jung, "Synthesis and characterization of sulfonated polyimide membranes for direct methanol fuel cell," *Journal of Membrane Science,* vol. 220, no. 1-2, pp. 31-45, 2003.

[23] Q. Guo, P. Pintauro, H. Tang and S. O'Connor, "Sulfonated and crosslinked polyphosphazene-based proton-exchange membranes," *Journal of Membrane Science,* vol. 154, no. 2, pp. 175-181, 1999.

[24] D. Kim, B. Liu and M. Guiver, "Influence of silica content in sulfonated poly(arylene ether ether ketone ketone) hybrid membranes on properties for fuel cell application," *Polymer,* vol. 47, pp. 7871-7880, 2006.

[25] M. Rodgers, Z. Shi and S. Holdcroft, "Transport properties of composite membranes containing silicon dioxide and Nafion," *Journal of Membrane Science,* vol. 325, pp. 3346-356, 2008.

[26] B. Holmberg, X. Wang and Y. Yan, "Nanocomposite fuel cell membranes based on Nafion and acid functionalized zeolite beta nanocrystals," *Journal of Membrane Science,* vol. 320, pp. 86-92, 2008.

[27] J. Lin, J. Lee, M. Kellner, R. Wycisk and P. Pintauro, "Nafion-fluorinated ethylene-propylene resin membrane blends for direct methanol fuel cells," *Journal of Electrochemical Society,* vol. 153, 2006.

[28] J. Lin, R. Wycisk and P. P.N., "Modified Nafion as the Membrane Material for Direct Methanol Fuel Cells," in *Polymer Membranes for Fuel Cells*, 2009, pp. 341-359.

[29] M. Song, Y. Kim, J. Fenton, H. Kunz and H. Rhee, "Chemically-modified Nafion/poly(vinylidene fluoride) blend ionomers for proton exchange membrane fuel cells," *Journal of Power Sources,* vol. 117, no. 1-2, pp. 14-21, 2003.

[30] N. Deluca and Y. Elabd, "Polymer Electrolyte Membranes for the Direct Methanol Fuel Cell: A Review," *Journal of Polymer Science: Part B: Polymer Physics,* vol. 44, pp. 2201-2225, 2006.

[31] V. Neburchilov, J. Martin, H. Wang and J. Zhang, "A review of polymer electrolyte membranes for direct methanol fuel cells," *Journal of Power Sources,* vol. 169, pp. 221-238, 2007.

[32] R. Wycisk, J. Lee and P. Pintauro, "Sulfonated Polyphosphazene-Polybenzimidazole Membranes for DMFCs," *Journal of the Electrochemical Society,* vol. 152, no. 5, pp. A892-A898, 2005.

[33] D. Kim, H. Park, J. Rhim and Y. Lee, "Proton conductivity and methanol transport behavior of cross-linked PVA/PAA/silica hybrid membranes," *Solid State Ionics,* vol. 176, pp. 117-126, 2005.

[34] M. Sumner, W. Harrison, R. Weyers, Y. Kim, J. McGrath, J. Riffle, A. Brink and M. Brink, "Novel proton conducting sulfonated poly(arylene ether) copolymers containing aromatic nitriles," *Journal of Membrane Science,* vol. 239, pp. 199-211, 2004.

[35] J. Shin, B. Chang, J. Kim, S. Lee and D. Suh, "Sulfonated polystyrene/PTFE composite membranes," *Journal of Membrane Science,* vol. 251, pp. 247-254, 2005.

[36] K. Okamoto, Y. Yin, O. Yamada, M. Islam, T. Honda, T. Mishima, Y. Suto, K. Tanaka and H. Kita, "Methanol permeability and proton conductivity of sulfonated co-polyimide membranes," *Journal of Membrane Science,* vol. 258, pp. 115-122, 2005.

[37] R. Thangamuthu and C. Lin, "DBSA-doped PEG/SiO2 proton-conducting hybrid membranes for low-temperature fuel cell applications," *Solid State Ionics,* vol. 176, pp. 531-538, 2005.

[38] L. Li and Y. Wang, "Sulfonated polyethersulfone Cardo membranes for direct methanol fuel cell," *Journal of Membrane Science,* vol. 246, pp. 167-172, 2005.

[39] N. Carretta, V. Tricoli and F. Picchioni, "Ionomeric membranes based on partially sulfonated poly(styrene): synthesis, proton conduction and methanol permeation," *Journal of Membrane Science,* vol. 166, pp. 189-197, 2000.

[40] V. Tricoli, N. Caretta and Bartolozzi, "A Comparative Investigation of Proton and Methanol Transport in Fluorinated Ionomeric Membranes," *Journal of the Electrochemical Society,* vol. 147, no. 4, pp. 1286-1290, 2000.

[41] Y. Yin, J. Fang, Y. Cui, K. Tanaka, H. Kita and K. Okamoto, "Synthesis, proton conductivity and methanol permeability of a novel sulfonated polyimide from 3-(2',4'-diaminophenoxy)propane sulfonic acid," *Polymer,* vol. 44, pp. 4509-4518, 2003.

[42] M. Gil, X. Ji, X. Li, H. Na, J. Hampsey and Y. Lu, "Direct synthesis of sulfonated aromatic poly(ether ether ketone) proton exchange membranes for fuel cell applications," *Journal of Membrane Science,* vol. 234, pp. 75-81, 2004.

[43] M. Shen, S. Roy, J. Kuhlmann, K. Scott, K. Lovell and J. Horsfall, "Grafted polymer electrolyte membrane for direct methanol fuel cells," *Journal of Membrane Science,* vol. 251, pp. 121-130, 2005.

[44] Y. Elabd, E. Napadensky, J. Sload, D. Crawford and C. Walker, "Triblock coopolymer ionomer membranes Part I. Methanol and proton transport," *Journal of Membrane Science,* vol. 217, pp. 227-242, 2003.

[45] M. Kang, J. Kim, J. Won, S. Moon and Y. Kang, "Highly charged proton exchange membranes prepared by using water soluble polymer blends for fuel cells," *Journal of Membrane Science,* vol. 247, pp. 127-135, 2005.

[46] J. Lin, P. Wu, R. Wycisk, A. Trivisonno and P. Pintauro, "Direct methanol fuel cell operation with pre-stretched recast Nafion," *Journal of Power Sources,* vol. 183, no. 2, pp. 491-497, 2008.

[47] J. Lin, R. Wycisk, P. Pintauro and e. al., "Stretched Recast Nafion for Direct Methanol Fuel Cells," *Electrochemical and Solid-State Letters,* vol. 10, no. 1, pp. 819-822, 2007.

[48] J. Lin, W. R. Wu Pin-Han and P. Pintauro, "PEM Fuel Cell Properties of Pre-Stretched Recast Nafion®," *ECS Transactions,* vol. 16, no. 2, pp. 1195-1204, 2008.

[49] J. Lin, P. Wu, R. Wycisk, P. Pintauro and Z. Shi, "Properties of Water in Prestretched Recast Nafion," *Macromolcules,* vol. 41, no. 12, pp. 4284-4289, 2008.

[50] W. Zhang, D. Kish and P. Pintauro, "Morphology and Performance of Stretched PFSA for Direct Methanol Fuel Cells," *ECS Transations,* vol. 33, no. 1, pp. 635-645, 2010.

[51] L. H. Sperling, Introduction to Physical Polymer Science, 2006.

[52] A. Peterlin, "Crystalline Character in Polymers," *Journal of Polymer Science,* vol. 9, pp. 61-89, 1965.

[53] V. A. Marikhin and L. P. Myasnikova, "Structural bases of high-strength high-modulus polymers," in *Oriented Polymer Materials,* 2002, pp. 38-92.

[54] R. B. Moore and C. Martin, "Morphology and Chemical Properties of the Dow Perfluorosulfonate Ionomers," *Macromolecules,* vol. 22, no. 9, pp. 3594-3599, 1989.

[55] J. Park, J. Li, D. Gilles, L. Madsen and R. Moore, "Oriented Morphology and Anisotropic Transport in Uniaxially Stretched Perfluorosulfonate Ionomer Membranes," *Macromolecules,* vol. 44, pp. 5701-5710, 2011.

[56] T. Gierke, G. Munn and F. Wilson, *Journal of Polymer Science, Polymer Physics Edition,* vol. 19, pp. 1687-1704, 1981.

[57] K. Mauritz and R. Moore, *Chemical Reviews,* vol. 104, pp. 4535-4585, 2004.

[58] K. Schmidt-Rohr and Q. Chen, "Parallel cylindrical water nanochannels in Nafion fuel-cell membranes," *Nature Materials,* vol. 7, pp. 75-83, 2008.

[59] L. Rubatat and O. Diat, "Stretching Effect on Nafion Fibrillar Nanostructure," *Macromolecules,* vol. 40, pp. 9455-9462, 2007.

[60] P. van der Heijden, L. Rubatat and O. Diat, "Orientation of Drawn Nafion at Molecular and Mesoscopic Scales," *Macromolecules,* vol. 37, pp. 5327-5336, 2004.

[61] J. Li, J. Park, R. Moore and L. Madsen, "Linear coupling of alignment with transport in a polymer electrolyte membrane," *Nature Materials,* vol. 10, pp. 507-511, 2011.

[62] T. Rockward, R. Borup, J. Chlistunoff, J. Davey, F. Garzon, Y. Kim, R. Mukundan, C. Quesada, K. Rau and M. Wilson, "2011 DOE Hydrogen and Fuel Cells Program and Vehicle Technologies Program Annual Meric Review and Peer Evaluation Meeting," 9-13 May 2011. [Online]. Available: http://www.hydrogen.energy.gov/pdfs/review11/fc052_rockward_2011_p.pdf. [Accessed 17 March 2012].

[63] M. Gebert, A. Ghielmi, L. Merlo, M. Corasaniti and V. Arcella, "Aquivion The short-side-chain and low-EW PFSA for next-generation PEFCs expands production and utilization," in *Fuel Cell Seminar 2009,* 2009.

[64] A. Ghielmi, P. Vaccarono, C. Troglia and V. Arcella, "Proton exchange membranes based on the short-side-chain perfluorinated ionomer," *Journal of Power Sources,* vol. 145, no. 2, pp. 108-115, 2005.

[65] B. Cahan and J. Wainright, "AC Impedance Investigations of Proton Conduction in Nafion," *Journal of The Electrochemical Society,* vol. 140, no. 12, pp. L185-L186, 1993.

[66] J. Hensley, J. Way, S. Dec and K. Abney, "The effects of thermal annealing on commercial Nafion® membranes," *Journal of Membrane Science,* vol. 298, no. 1-2, pp. 190-201, 2007.

[67] J. Li, X. Yang, H. Tang and M. Pan, "Durable and high performance Nafion membrane prepared through high-temperature annealing methodology," *Journal of Membrane Science,* vol. 361, no. 1-2, pp. 38-42, 2010.

[68] G. Gebel, M. Aldebert and M. Pineri, "Structure and related properties of solution-cast perfluorosulfonated ionomer films," *Macromolecules,* vol. 20, no. 6, pp. 1425-1428, 1987.

[69] T. Crompton, "Ultrahigh Modulus Polyethylene by High-Temperature Drawing," *Polymer,* vol. 17, no. 7, pp. 644-645, 1976.

[70] K. Yamada, M. Kamezawa and M. Takayanagi, "Relationship between Orientation of Amorphous Chains and Modulus in Highly Oriented Polypropylene," *Journal of Applied Polymer Science,* vol. 26, pp. 49-60, 1981.

[71] M. Al-Hussein and G. Strobl, "Strain-Controlled Tensile Deformation Behavior of Isotactic Poly(1-butene) and Its Ethylene Copolymers," *Macromolecules,* vol. 35, pp. 8515-8520, 2002.

[72] A. Mahendrasingam, C. Martin, W. Fuller, D. Blundell, R. Oldman, J. Harvie, D. MacKerron, C. Riekel and P. Engstrom, "Effect of draw ratio and temperature on the strain-induced crystallization of poly (ethylene terephthalate) at fast draw ratio," *Polymer,* vol. 40, no. 20, pp. 5553-5565, 1999.

[73] R. Stein, "Stress-Induced Crystallization of Poly(ethylene-terephthalate)," *Journal of Polymer Science. Part B, Polymer Physics,* vol. 17, no. 2, pp. 235-257, 1979.

[74] A. Peterlin and R. Corneliussen, "Small-Angle X-Ray Diffraction Studies of Plastically Deformed Polyehylene. II. Influence of Draw Temperature, Draw Ratio, Annealing Temperature, and Time," *Journal of Polymer Science: Part A-2,* vol. 6, pp. 1273-1282, 1968.

[75] F. Zuo, J. Keum, X. Chen, B. Hsiao, H. Chen, S. Lai, R. Wevers and J. Li, "The role of interlamellar chain entanglement in deformation-induced structure changes during uniaxial stretching of isotactic polypropylene," *Polymer,* vol. 48, pp. 6867-6880, 2007.

[76] J. Langford and J. Wilson, "Scherrer after Sixty Years: A Survey and Some New Results in the Determination of Crystallite Size," *Journal of applied crystallography,* vol. 11, pp. 102-113, 1977.

[77] M. A. Hickner, H. Ghassemi, Y. S. Kim, B. R. Einsala and J. E. McGrath, "Alternative Polymer Systems for Proton Exchange Membranes," *Chemical Reviews,* pp. 4587-4612, 2004.

[78] J. Hinatsu, M. Mizuhata and H. Takenaka, "Water Uptake of Perfluorosulfonic Acid Membranes from Liquid Water and Water Vapor," *Journal of The Electrochemical Society,* vol. 141, no. 6, pp. 1493-1498, 1994.

[79] T. Zawodzinski, T. Springer, J. Davey, R. Jestel, C. Lopez, J. Valerio and S. Gottesfeld, "A Comparitive Study of Water Uptake By and Transport Through Ionomeric Fuel Cell Membranes," *Journal of the Electrochemical Society,* vol. 170, no. 7, pp. 1981-1985, 1993.

[80] K. Kreuer, S. Paddison, E. Spohr and M. Schuster, "Transport in Proton Conductors for Fuel-Cell Applications: Simulations, Elementary Reactions, and Phenomenology," *Chemical Reviews,* vol. 104, pp. 4637-4678, 2004.

[81] P. Majsztrik, M. Satterfield, A. Bocarsly and J. Benziger, "Water Sorption, Desorption and Transport in Nafion Membranes," *Journal of Membrane Science,* vol. 301, pp. 93-106, 2007.

[82] F. Bauer, S. Denneler and M. Willert-Porada, "Influence of temperature and humidity on the mechanical properties of Nafion 117 polymer electrolyte membrane," *Journal of Polymer Science Part B-Polymer Physics,* vol. 43, no. 7, pp. 786-795, 2005.

[83] G. Alberti, M. Casciola, L. Massinelli and B. Bauer, "Polymeric proton conducting membranes for medium temperature fuel cells (110-160 degrees C)," *Journal of Membrane Science,* vol. 185, no. 1, pp. 73-81, 2001.

[84] BekkTech LLC, "In-Plane Conductivity vs. Through Plane Conductivity Measurements," [Online]. Available: http://www.bekktech.com/dwnlds/InPlaneVsThroughPlaneRevC.pdf. [Accessed 9 5 2012].